Voltage-Dependent Calcium Channels

Ľ. Lacinová

Institute of Molecular Physiology and Genetics
Slovak Academy of Sciences
Vlárska 5, 833 34 Bratislava 37, Slovakia
E-mail: lubica.lacinova@savba.sk

This Supplement represents abbreviated version of thesis
submitted by Ľubica Lacinová for obtaining Doctor of Science degree.

Contents

Introduction 4
Classification of voltage-gated calcium channels 4
Subunit composition of the calcium channel complex 7
α_1 subunit 7
β subunit 10
Cloning of β subunits family 10
Interaction of β subunits with α_1 subunits 11
Modulation of interactions of α_1 subunit with calcium channel inhibitors by β subunits 14
$\alpha_2\delta$ subunit 16
Cloning of the $\alpha_2\delta$ subunit family 16
Modulatory role of $\alpha_2\delta$ subunits 17
Tissue distribution of $\alpha_2\delta$ subunits 19
Regulation of high-voltage-activated calcium channels by the $\alpha_2\delta$-1, -2 and -3 subunits 19
Regulation of low-voltage-activated calcium channels by $\alpha_2\delta$-1, -2 and -3 subunits 22
Interaction of $\alpha_2\delta$ subunit with gabapentin 24
γ subunit 25
L-type calcium channel 30
Subunit composition of the calcium channel 30
Regulation by calcium channel blockers and activators 30
Dihydropyridines 30
Phenylalkylamines and benzothiazepines 40
Inactivation of L-type calcium channels 42
Calcium-dependent inactivation 43
Voltage-dependent inactivation 44
Neuronal calcium channels 44
The $Ca_v2.1$ channel 44
The $Ca_v2.2$ channel 44
The $Ca_v2.3$ channel 45
Low-voltage-activated calcium channels 45
Cloning of low-voltage-activated calcium channels 45
Subunit composition of T-type calcium channels 47
Permeability properties of T-type calcium channels 48
Voltage-dependent activation and inactivation of T-type calcium channels 48
Pharmacology of recombinant T-type calcium channels 51
Block by inorganic cations 52
Organic blockers 53
Gating of T-type calcium channels 54
Acknowledgement 61
References 61

Abstract. Voltage-activated calcium channels can be divided into two subgroups based on their activation threshold, low-voltage-activated (LVA) and high-voltage-activated (HVA). Auxiliary subunits of the HVA calcium channels contribute significantly to biophysical properties of the channels. We have cloned and characterized members of two families of auxiliary subunits: $\alpha_2\delta$ and γ. Two new $\alpha_2\delta$ subunits, $\alpha_2\delta$-2 and $\alpha_2\delta$-3, regulate all classes of HVA calcium channels. While the ubiquitous $\alpha_2\delta$-2 modulates both neuronal and non-neuronal channels with similar efficiency, the $\alpha_2\delta$-3 subunit regulates $Ca_v2.3$ channels more effectively. Furthermore, $\alpha_2\delta$-2 may modulate the LVA $Ca_v3.1$ channel. Four new γ subunits, γ-2, γ-3, γ-4 and γ-5, were characterized. The γ-2 subunit modulated both the non-neuronal $Ca_v1.2$ channel and the neuronal $Ca_v2.1$ channel. The γ-4 subunit affected only the $Ca_v2.1$ channel. The γ-5 subunit may be a regulatory subunit of the LVA $Ca_v3.1$ channel.

The $Ca_v1.2$ channel is a major target for treatment of cardiovascular diseases. We have mapped the interaction site for clinically important channel blockers – dihydropyridines (DHPs) – and analysed the underlying inhibition mechanism. High-affinity inhibition is characterized by interaction with inactivated state of the channel. Its structural determinants are amino acids of the IVS6 segment, with smaller contribution of the IS6 segment, which contributes to voltage-dependence of DHP inhibition. Removal of amino acids responsible for the high-affinity inhibition revealed a low-affinity open channel block, in which amino acids of the IIIS5 and IIIS6 segments take part. Experiments with a permanently charged DHP suggested that there is another low-affinity interaction site on the α_1 subunit.

We have cloned and characterized murine neuronal LVA $Ca_v3.1$ channel. The channel has high sensitivity to the organic blocker mibefradil, moderate sensitivity to phenytoin, and low sensitivity to ethosuximide, amiloride and valproat. The channel is insensitive to tetrodotoxin and DHPs. The inorganic blockers Ni^{2+} and Cd^{2+} are moderately effective compared to La^{3+}. The current through the $Ca_v3.1$ channel inactivates faster with Ba^{2+} compared to Ca^{2+}. Molecular determinants of fast inactivation are located in amino side of the intracellular carboxy terminus. The voltage dependence of charge movement is very shallow compared to the voltage dependence of current activation. Transfer of 30 % of charge correlates with activation of 70 % of measurable macroscopic current. Prolonged depolarization does not immobilize charge movement of the $Ca_v3.1$ channel.

Key words: Calcium channel — α_1 subunit — Auxiliary subunits — Low-voltage-activated — High-voltage-activated — Dihydropyridines

Abbreviations: AID, α interaction domain; BID, β interaction domain; BTZ, benzothiazepine; CaM, calmodulin; DHP, dihydropyridine; GBP, gabapentin; HEK, human embryonic kidney; HP, holding potential; HVA, high-voltage-activated; IC_{50}, concentration for 50 % inhibition; LVA, low-voltage-activated; MPS, α-methyl-α-phenylsuccinimide; PAA, phenylalkylamine; TTX, tetrodotoxin; VDCC, voltage-dependent calcium channels; VACC, voltage-activated calcium channel.

Introduction

Living cells are surrounded by impermeable membranes containing specialized proteins providing for exchange of various atoms and molecules between the extracellular and intracellular spaces. Traditionally, two basic mechanisms of transmembrane transport have been recognized: carriers and channels. Carriers, such as the Ca^{2+} pump, Na^{+}-Ca^{2+} exchanger, or Na^{+}-K^{+} pump, transport ions against concentration and/or electrical gradients and are coupled to metabolic energy consumption. Membrane channels are viewed as pores, which, when opened, allow passive transport downhill the electric and/or concentration gradients. Opening of a channel can be accomplished in two ways: i) by binding of a specific ligand either directly to the channel or to another membrane protein coupled to the channel, and ii) by a change in transmembrane voltage. The first pathway is characteristic for ligand-gated channels, such as the glutamate or acetylcholine receptors. The second pathway activates the so-called voltage-gated channels. The foundation of biophysical analyses of voltage-gated ion channels was laid in the pioneering works of Hodgkin and Huxley in the 1930's and culminated in the 1950's by formulating the Hodgkin-Huxley model of action potential (Hodgkin and Huxley 1952a,b,c,d). Initially, the Na^{+} and K^{+} selective voltage-gated channels and a leakage channel were recognized. Later, the family of voltage-gated ion channels was extended to include Ca^{2+} and Cl^{-} channels.

Voltage-gated calcium channels were first identified by Fatt and Katz (1953). Later it was discovered that there are different channel subtypes in excitable cells and, consequently, voltage-gated calcium channels were classified and named according to various schemes.

In the 1980's, the calcium channel protein was purified and shown to consist of several subunits (Borsotto et al. 1985; Flockerzi et al. 1986; Sieber et al. 1987; Takahashi et al. 1987; Vaghy et al. 1987; Leung et al. 1988). The principal subunit of the voltage-dependent calcium channel (VDCC) was named α_1, and auxiliary subunits were named β, α_2, δ, and γ. Cloning of the genes encoding individual subunits followed soon. So far, ten genes for α_1 subunits, four for β subunits, four for the $\alpha_2\delta$ complex and eight for γ subunits were identified (for review, see Hofmann et al. 1999).

Mutation analyses during the 1990's allowed a precise identification of interaction sites for major calcium channel ligands like dihydropyridines (DHPs), phenylalkylamines (PAAs) and benzothiazepines (BTZs), of phosphorylation sites, and of the molecular structures responsible for voltage- and calcium-dependent regulation of channel activation and inactivation. Most recently, investigation of transgenic mouse models has allowed analysis of the physiological role of calcium channels in an organism at large.

Classification of voltage-gated calcium channels

The very first channel classification was based on basic electrophysiological and pharmacological properties. An observation was made that some calcium channels

need only a small depolarization to be activated, while other require a relatively high step in membrane voltage to open (Hagiwara et al. 1975; Llinás and Yarom 1981). According to this criterion, calcium channels were divided into low-voltage-activated (LVA) and high-voltage-activated (HVA). LVA calcium channels activate at a membrane voltage positive to −70 mV. Because of the small amplitude of single channel conductance and its fast decay, these channels were also called T-type calcium channels (T for tiny and transient). HVA channels have an activation threshold at membrane voltages positive to −20 mV. The first generally known representative of the HVA channel family was found abundantly in skeletal, smooth and cardiac muscles as well as in neurons. Because of its large-single channel conductance amplitude and slow kinetics of current decay, it was named L-type calcium channel (L for large and long-lasting) in contrast to the T-type. A pharmacological hallmark of all L-type channels is their sensitivity to 1,4-DHPs – a wide class of drugs with either inhibitory (nifedipine, nisoldipine, isradipine) or activatory (Bay K 8644) action on the channel.

In the 1980's, experiments with neuronal cells revealed novel calcium channels, insensitive to DHPs and with single-channel conductances between those of T-type and L-type channels (Nowycky et al. 1985; Fox et al. 1987). These channels were named N-type calcium channels (N for neuronal). Later, it was shown that neuronal non-L-type channels could be further classified into subtypes according to their sensitivity to peptide toxins isolated from cone snails and spiders. The channel sensitive to ω-conotoxin GVIA, kept the name N-type channel, while the channel sensitive to ω-Aga IVA toxin was named P/Q-type calcium channel (P for Purkinje cells, where this channel was characterized by Llinás and co-authors in 1989). The channels resistant to these toxins were named R-type calcium channel (R for resistant).

The second classification of voltage-gated calcium channels was developed in the 1980's and was based on cloning of cDNAs encoding individual channel types. The cloning experiments revealed that calcium channels consist of the principal α_1 subunit and several auxiliary subunits β, $\alpha_2\delta$, and γ, which have regulatory functions and each of them has several subtypes. The α_1 subunit is responsible for basic electrophysiological and pharmacological properties that formed the basis of early channel classifications. Therefore, investigators tried to establish links between the newly cloned subunits and channel complexes identified earlier by traditional electrophysiological experiments in native tissues. Several α_1 subunits representing class L calcium channels were identified. As the first one, the α_1 subunit from skeletal muscle was purified (Curtis and Catterall 1984), cloned and named α_{1S} (Tanabe et al. 1987). Later, α_1 subunit was cloned from cardiac ($\alpha_{1C\text{-}a}$, Mikami et al. 1989) and smooth ($\alpha_{1C\text{-}b}$, Biel et al. 1990) muscle. Both splice variants of the α_{1C} subunit are structurally closely related and share 95 % of identical amino acids. Two further representatives of the L-type subfamily were identified later: α_{1D} (Seino et al. 1992; Williams et al. 1992a) and α_{1F} (Bech-Hansen et al. 1998; Strom et al. 1998).

Three α_1 subunits, representing the three neuronal types of calcium channels,

were cloned. α_{1A} subunit (Mori et al. 1991; Starr et al. 1991) corresponds to the P/Q-type channel. The properties of α_{1B} subunit (Williams et al. 1992b; Dubel et al. 1992) match those of the N-type channel. α_{1E} subunit (Niidome et al. 1992; Soong et al. 1993) was initially characterized as an LVA T-type channel; however, later studies demonstrated that it has the properties of R-type channel.

Three members of the LVA T-type subfamily were identified so far: α_{1G} (Perez-Reyes et al. 1998), α_{1H} (Cribbs et al. 1998), and α_{1I} (Lee et al. 1999a).

As the number of cloned calcium channel α_1 subunits has been increasing, a need has arisen for a systemic nomenclature. It was agreed that individual α_1 subunits will be named according to the Ca_vx.y scheme (Ertel et al. 2000), where Ca_v stands for voltage-activated calcium channel (VACC), x is a number designating the channel subfamily (i.e., L-type, neuronal, and T-type in the initial classification), and y is a number designating individual members of subfamilies. An overview of VACC known to-date is given in Table 1.

Table 1. Historical development of VACCs

	Nomenclature according to [1]		Nomenclature according to [2,3]	Structural nomenclature [4]
HVA channels		L-type	α_{1S}	$Ca_v1.1$
			α_{1C}	$Ca_v1.2$
			α_{1D}	$Ca_v1.3$
			α_{1F}	$Ca_v1.4$
	Neuronal	P/Q-type	α_{1A}	$Ca_v2.1$
		N-type	α_{1B}	$Ca_v2.2$
		R-type	α_{1E}	$Ca_v2.3$
LVA channels		T-type	α_{1G}	$Ca_v3.1$
			α_{1H}	$Ca_v3.2$
			α_{1I}	$Ca_v3.3$

[1] Tsien et al. (1988); [2] Snutch et al. (1990); [3] Birnbaumer et al. (1994); [4] Ertel et al. (2000).

Comparison of amino acid sequences of individual calcium channels revealed an evolutionary relationship between channel classes. An early evolutionary event separated the α_1 subunits into LVA and HVA channels, with less than 30 % of sequence homology. A later evolutionary event divided HVA channels into two subfamilies: L-type and neuronal types, with about 50 % sequence homology. Individual members of both subfamilies share more than 80 % of sequence homology (Figure 1). Virtually all known α_1 subunits have more splice variants. These share usually more than 95 % sequence homology and will be described in chapters devoted to individual channels.

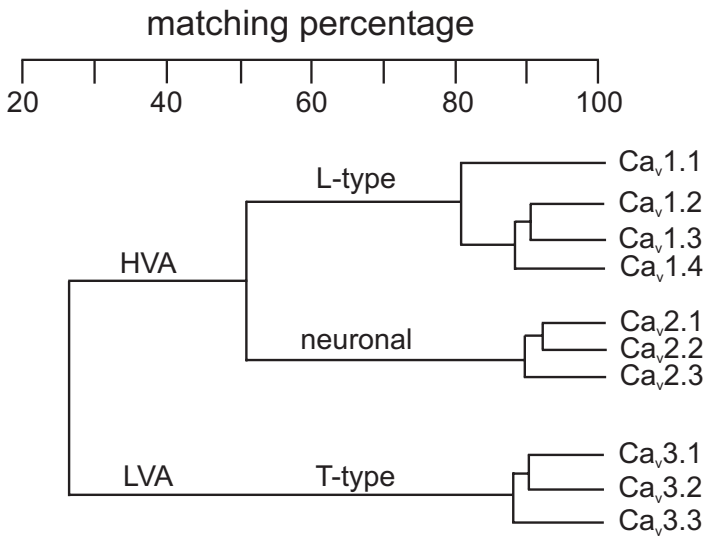

Figure 1. Phylogenetic comparison of all known VACCs. The amino-acid alignment was constructed using the CLUSTAL program. Only the membrane-spanning regions of α_1 sequences were included into analysis.

Subunit composition of the calcium channel complex

HVA channels are heterooligomeric complexes, consisting of up to five proteins from four genes (Figure 2). α_1 subunit is a principal subunit, localized in the cell membrane and forming a conductive pore. β, α_2, δ, and γ are auxiliary subunits. Not all four modulatory proteins are necessarily present in each channel complex. Regulation by γ subunit is undoubtedly proven only for the $Ca_v1.1$ channel. While all α_1 subunits of HVA channels are most probably associated with β and $\alpha_2\delta$ subunits (Hofmann et al. 1999), the subunit composition of LVA channels is not known yet (Lacinová et al. 2000a). β, $\alpha_2\delta$, and γ subunits create gene families with 4, 4 and 8 members, respectively. For many subunits, splice variants are known which may differ dramatically in functional characteristics.

α_1 *subunit*

α_1 subunits VACCs of are large proteins with molecular weight between 212 and 273 kDa. They belong to the same multigene family as voltage-activated sodium and potassium channels. Hydrophobicity analysis predicted transmembrane topology with four homologous transmembrane domains, each containing six membrane-spanning putative α-helices, creating six transmembrane segments and a pore region between segments S5 a S6 (Figure 3). The length of α_1 subunit ranges approximately between 1870 and 2420 amino acids. Sizes of several cloned α_1 subunits are given in Table 2. Individual transmembrane segments contain approximately

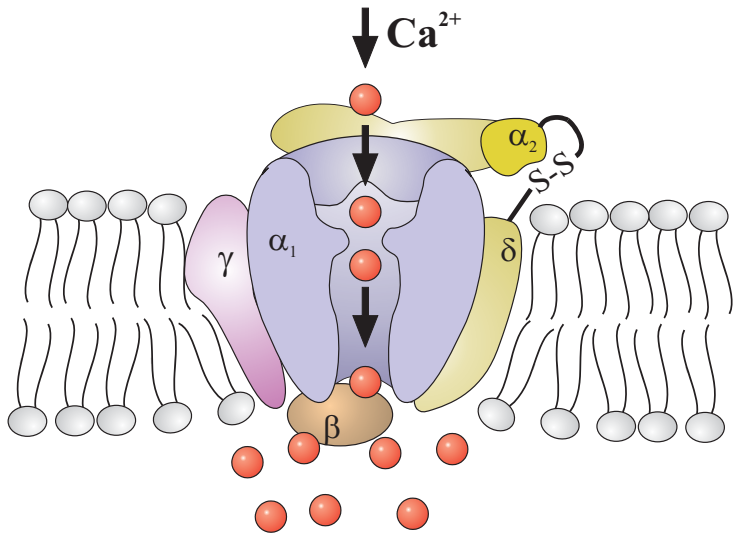

Figure 2. A proposed schematic structure of VACC. The principal α_1 subunit is a transmembrane protein containing a conducting pore, through which calcium ions can pass upon opening. α_1 subunit is further regulated by auxiliary subunits: intracellular β subunit, transmembrane γ subunit and a complex of extracellular α_2 subunit and transmembrane δ subunit, connected by a disulphide bridge.

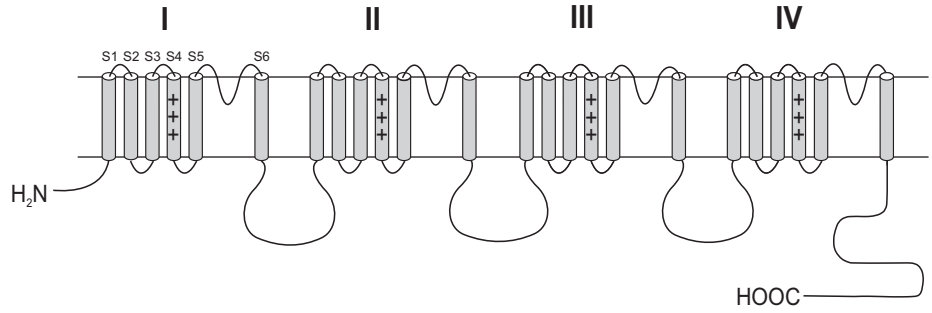

Figure 3. Suggested membrane topology of α_1 subunit of the VACC. The subunit consists of four homologous domains I–IV, each containing six transmembrane segments S1–S6 and a pore region between segments S5 and S6. Putative α-helices are shown as cylinders. The fourth transmembrane segment S4 in each domain bears a net positive charge.

20 amino acids. S4 segments contain five to six positively charged arginins and lysines (Figure 4), so that these segments bear a net positive charge and can act as voltage sensors controlling VDCC gating. Movement of the S4 segment during

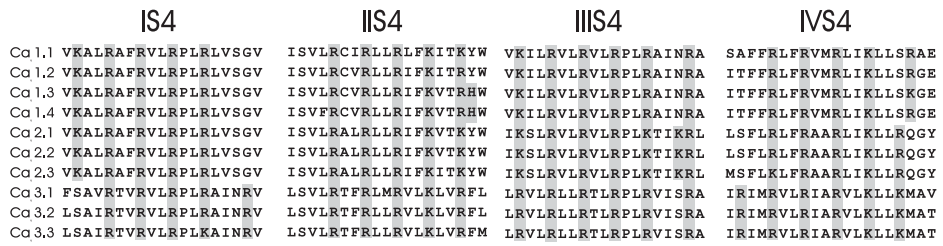

Figure 4. Alignment of S4 segments of VACC. Charged amino acids are highlighted by grey boxes.

Table 2. Sizes of individual cloned α_1 subunits of the VACC

Subunit / origin	Molecular weight (kDa)	Number of amino acids	Reference
$Ca_v1.1$ / rabbit skeletal muscle	212	1873	Tanabe et al. 1987
$Ca_v1.2$ / rabbit heart	242.8	2171	Mikami et al. 1989
$Ca_v1.2$ / rabbit lung	242.5	2166	Biel et al. 1990
$Ca_v1.2$ / rat aorta	243.6	2169	Koch et al. 1990
$Ca_v1.3$ / human pancreas	247.6	2181	Seino et al. 1992
$Ca_v1.3$ / human brain	245.2	2161	Williams et al. 1992a
$Ca_v1.4$ / human retina		1912	Bech-Hansen et al. 1998
$Ca_v1.4$ / human retina	219.5	1966	Strom et al. 1998
$Ca_v2.1$ / rabbit brain	257.3 273.2	2273 2424	Mori et al. 1991
$Ca_v2.2$ / ray	264.5	2326	Horne et al. 1993
$Ca_v2.2$ / human brain	262.5 251.8	2339 2237	Williams et al. 1992b
$Ca_v2.3$ / ray	251.8	2223	Horne et al. 1993
$Ca_v2.3$ / rat brain	252	2222	Soong et al. 1993
$Ca_v3.1$ / mouse brain		2295	Klugbauer et al. 1999a
$Ca_v3.2$ / human heart		2387	Cribbs et al. 1998
$Ca_v3.3$ / rat brain	205.2	1835	Lee et al. 1999a

channel activation was directly proved for the K^+ channel (Logothetis et al. 1992; Glauner et al. 1999). Based on structural homology of all voltage-gated channels, we can hypothesize that the S4 segments of the VACC play a similar role. The pore region contains a putative selectivity filter, which ensures high selectivity of the channel pore for calcium ions. Furthermore, the α_1 subunit sequence contains sites of interaction with auxiliary subunits, binding sites for various activators and

blockers, including G-proteins, as well as several putative phosphorylation sites. Some of these interaction sites are common, e.g., the site of the interaction with β subunit, while others are channel type specific, e.g., the binding sites for specific channel ligands.

When expressed in heterologous expression system, either in *Xenopus* oocytes or in a mammalian cell line (Chinese hamster ovary, tsa201, and HEK 293 are the most commonly used mammalian expression systems), α_1 subunit undergoes voltage-dependent activation and inactivation and is subject to regulation by various blockers and activators. However, quantitative characteristics of voltage- and drug-dependent regulation of expressed α_1 subunits of HVA channels differ from those described for the corresponding calcium channel types in native tissues. To mimic the behaviour of native channels, coexpression of auxiliary subunits and other regulatory proteins was necessary. LVA channels are an exception. No remarkable difference between current regulations observed in native tissue and from $Ca_v3.x$ channels expressed in a mammalian cell line has been reported so far. The subunit composition of the LVA channel remains an open and controversial issue (Lacinová et al. 2000a).

β subunit

β subunit is an intracellular auxiliary subunit coexpressed with α_1 subunit of all HVA channels (Figure 5). Coexpression of β subunit with α_1 subunit of the LVA channel has not been demonstrated (for review, see Lacinová et al. 2000a). So far, four β subunit isoforms (β_1–β_4), coded by distinct genes, have been identified (for review, see Hofmann et al. 1999). Each isoform has multiple splice variants. Primary structure alignment of ß subunits revealed that all share a common central core, whereas their amino (N)- and carboxy (C)-termini and a part of the central region differ significantly.

Cloning of β subunits family

The first cloned β_1 subunit was that from rabbit skeletal muscle containing 524 amino acids, with calculated molecular weight of 57.9 kD (Ruth et al. 1989). Hydropathicity analysis revealed absence of a typical membrane-spanning region. Its splice variants β_{1a}, β_{1b} and β_{1c} were identified in skeletal, cardiac and neuronal tissues (for review, see Birnbaumer et al. 1998). Two splice variants of β_2 subunits, β_{2a} and β_{2b}, containing 606 and 632 amino acids, respectively, as well as a 477 amino acids long β_3 subunit were cloned from rabbit heart by Hullin and co-workers (1992). Perez-Reyes and co-workers (1992) isolated β_2 subunit from rat brain (604 amino acids, 68.2 kD). Castellano and co-workers (1993a) cloned a homologue of β_3 subunit from rat brain (484 amino acids, 54.6 kD). β_4 subunit was first cloned from rat brain (Castellano et al. 1993b). It encodes a protein with 519 amino acids and molecular weight of 58.0 kD.

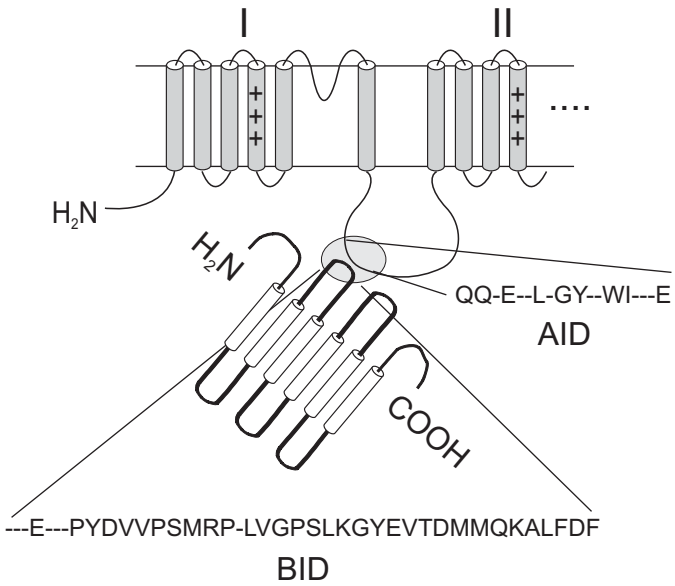

Figure 5. Suggested structure of the $\alpha-\beta$ interaction site. Putative α-helices are depicted as barrels. AID is the sequence alignment of the α interaction site, BID represents sequence alignment of the β interaction site.

Interaction of β subunits with α_1 subunits

Purification of the calcium channel protein demonstrated the association of the transmembrane α_1 subunit with the intracellular β subunit (Borsotto et al. 1985; Flockerzi et al. 1986; Sieber et al. 1987; Takahashi et al. 1987; Vaghy et al. 1987; Leung et al. 1988). Individual α_1 subunits associate with various β subunits or their splice variants in a tissue-dependent manner. Interaction between the subunits was tested by analyzing changes in current properties caused by coexpression of a β subunit with a particular α_1 subunits in *Xenopus* oocytes or in a mammalian cell line. Table 3 summarizes combinations of subunits tested positively for modulatory effects of β subunit on calcium current through a given α_1 subunit. Modulation of the current through expressed $Ca_v3.x$ subunits was not detected. Several facts seems to exclude this interaction: i) the amino acid sequence of all three $Ca_v3.x$ subunits lacks the α interaction domain (AID) identified in α_1 subunits of HVA channels (for review, see Hofmann et al. 1999); ii) elimination of the four known ß subunits by transfection of nodus ganglion neurons (Lambert et al. 1997) or mammalian neuronal NG108-15 cells (Leuranguer et al. 1998) with antisense oligonucleotides did not affect the size or voltage-dependence of native T-type current; iii) overexpression of the neuronal $ß_{2a}$ subunit (Wyatt et al. 1998) did not alter the characteristics of T-type current in undifferentiated mammalian NG108-15 cells.

Table 3. Original papers describing interactions between particular α_1 and β subunits in a recombinant expression system. Only initial studies are included. For more recent citations, see Birnbaumer et al. (1998) and Hofmann et al. (1999)

α_1	β_1	β_2	β_3	β_4
$Ca_v1.1$	Varadi et al. 1991 Lacerda et al. 1991			
$Ca_v1.2$	Wei et al. 1991 Singer et al. 1991	Hullin et al. 1992 Perez-Reyes et al. 1992	Hullin et al. 1992 Castellano et al. 1993a	Castellano et al. 1993b
$Ca_v1.3$		Williams et al. 1992a Ihara et al. 1995	Koschak et al. 2001 Scholze et al. 2001	
$Ca_v1.4$	not investigated			
$Ca_v2.1$	Stea et al. 1994 De Waard et al. 1994	Stea et al. 1994 De Waard et al. 1994	Stea et al. 1994 De Waard et al. 1994	Stea et al. 1994 De Waard et al. 1994
$Ca_v2.2$	Canti et al. 2000 Stephens et al. 2000	Stephens et al. 2000 Canti et al. 2000	Stephens et al. 2000 Canti et al. 2000	Stephens et al. 2000 Canti et al. 2000
$Ca_v2.3$	Olcese et al. 1994 Parent et al. 1997	Olcese et al. 1994 Parent et al. 1997	Parent et al. 1997 Nakashima et al. 1998	Parent et al. 1997

The skeletal muscle α_1 subunit is most probably regulated exclusively by the skeletal β_1 subunit. Coexpression of the α_1 subunit of the $Ca_v1.4$ channel with auxiliary subunits has not been studied yet. All other HVA α_1 subunits can interact in heterologous expression systems with all four β_1 subunits. However, this does not prove that such regulation takes place also *in situ*. Other authors used antisense depletion of β subunits in cell culture as a functional test for the interaction between α_1 and β subunits (Berrow et al. 1995; Lambert et al. 1997; Leuranguer et al. 1998). This analysis showed lack of modulation of T-type channels by β subunits and participation of all β subunits in regulation of neuronal HVA channels. Immunohistological studies (Biel et al. 1991; Hullin et al. 1992; Ludwig et al. 1997;

Volsen et al. 1997) revealed complex tissue distributions of β subunits. The β_{1a} subunit is expressed in skeletal muscles. The β_2 gene is expressed abundantly in the heart and, to a lower degree, in aorta, trachea, lungs and brain, whereas the β_3 specific mRNA is detectable in the brain and a variety of smooth muscle tissues.

The interaction site of α_1 and β subunits was identified on the connector between the first and second homologous domains of α_1 subunit (Pragnell et al. 1994). The consensus sequence of this AID is 428QQ-E–L-GY–WI—E445, in terms of amino acid numbering according to the $\alpha_{1C\text{-}b}$ sequence (Biel et al. 1990). The corresponding β interaction domain (BID) is located between the second and third predicted α-helices of β subunit (Figure 5). The amino acid sequence of the BID is —E—PYDVVPSMRP-LVGPSLKGYEVTDMMQKALFDF (De Waard et al. 1994, 1996). However, the most recent studies describing crystal structure of β_{2a} subunit (Van Petegem et al. 2004) and β_3 and β_4 subunits (Chen et al. 2004) suggested that BID is buried in the core of crystallized protein and is unavailable for protein-protein interaction. Instead, AID interacts with a hydrophobic groove in a guanylate kinaze domain.

The stoichiometry of α_1/β interaction is supposedly 1 : 1. However, identification of low-affinity α_1/β interaction site at the carboxy terminus of α_1 subunit of the $Ca_v2.3$ (Qin et al. 1996; Tareilus et al. 1997) or $Ca_v2.1$ channel (Walker et al. 1998), and at the amino terminus of α_1 subunit of the $Ca_v2.1$ channel (Walker et al. 1999) and $Ca_v2.2$ channel (Stephens et al. 2000) raised the possibility that more than one β subunit may interact with a single α_1 subunit. Hümmer and collaborators (2003) demonstrated that β_{1b} subunit interacts with the C terminus of $Ca_v2.1$ channel α_1 subunit. Nevertheless, deletion of the C terminus of $Ca_v2.2$ channel α_1 subunit did not affect its interaction with the β_3 subunit (Stotz et al. 2004). García and co-authors (2002) injected purified β_1 a subunits into vesicles derived from frog and mouse adult skeletal myocytes and observed enhanced current amplitude and altered tail current. Time courses of current activation and inactivation and parameters characterizing charge movement were not altered. Authors concluded that these effects were true modulatory effects of the β subunit mediated by interaction with the second interaction site distinct from the site that mediates chaperoning effect of β subunits.

There may be complex modulatory effects of β subunits on α_1 subunits. Coexpression of a β subunit with various α_1 subunits increases peak current (Singer et al. 1991), most likely by increasing the number of functional surface membrane channels and by facilitating channel pore opening (Neely et al. 1993; Josephson and Varadi 1996; Kamp et al. 1996). With the exception of the rat brain β_{2a}, all other β subunits accelerate channel activation and inactivation and shift the steady state inactivation curve to hyperpolarized membrane voltages (Singer et al. 1991; Wei et al. 1991; Hullin et al. 1992; Castellano et al. 1993a). The rat brain β_{2a}, when coexpressed with the $Ca_v2.3$ channel, slowed down inactivation rate and caused a right shift in the steady-state inactivation curve (Olcese et al. 1994; Qin et al. 1998). The role of β subunits is not restricted to modulatory effects on α_1 subunits. The β_{4c} subunit is a multifunctional protein that not only regulates α_1 subunit of

Table 4. I_{max} for each cell was calculated from the peak current of individual current-voltage relations and was normalized to the cell capacity. The inactivation time constants τ_1 and τ_2 were calculated from double exponential fits to the current traces measured during 800 ms depolarizing pulses from HP −80 mV to +30 mV. $V_{0.5}$ represents the half-maximal inactivation voltage calculated from a Boltzmann fit of the current-voltage relation

Channel	I_{max} (pA/pF)	Inactivation time constants τ_1 (ms)	τ_2 (s)	$V_{0.5}$ (mV)
$Ca_v1.2$-a	-11.3 ± 1.3 (11)	$254 \pm 20^{*}$ (11)	$2.8 \pm 0.4^{***}$	-3.2 ± 1.3 (9)
$Ca_v1.2$-aβ_3	-13.8 ± 1.7 (16)	$166 \pm 14^{*}$ (16)	$0.90 \pm 0.07^{***}$	-8.4 ± 0.8 (13)

* and *** indicate a significant difference between the two cell lines at $p < 0.05$ and $p < 0.001$, respectively. Numbers of cells measured are given in brackets.

a calcium channel but also regulates gene transcription in cochlear cells (Hibino et al. 2003).

Modulation of interactions of α_1 subunit with calcium channel inhibitors by β subunits

Coexpression of a β subunit may also affect the interaction of a calcium channel with its blockers (Lacinová et al. 1995; Welling et al. 1995). We have shown that coexpression of the β_3 subunit with a heart-specific splice variant of the $Ca_v1.2$-a channel shifted the average current-voltage relation by −3.2 mV in the hyperpolarizing direction, significantly accelerated the kinetics of current inactivation and shifted the half-maximal inactivation voltage by −5.2 mV toward hyperpolarizing potentials (Lacinová et al. 1995 and Table 4).

In addition to its effects on the basic electrophysiological properties of the $Ca_v1.2$ channel, the β_3 subunit significantly increased the channel affinity for the PAAs verapamil and gallopamil. The inhibitory potency of the DHP isradipine and of mibefradil, an organic calcium channel blocker, which does not belong to the above two classes of channel blockers, was not affected by the presence of the β_3 subunit (Figure 6). Because the action of all tested channel blockers is known to be voltage-dependent, we have tested all of them at a hyperpolarized membrane potential of −80 mV and at a relatively depolarized membrane potential of −40 mV. Current inhibition was measured at five different concentrations of each drug at each holding potential (HP). The data measured on 5 to 10 cells for each compound and channel type were averaged and fitted by the Hill equation. The resulting values of concentration for 50 % inhibition (IC_{50}) are summarized in Table 5.

Furthermore, we have investigated the effect of mibefradil on the $Ca_v1.2$-b, smooth muscle splice variant of the $Ca_v1.2$ channel alone or coexpressed either with the skeletal muscle β_1 or the neuronal β_3 subunits (Welling et al. 1995). Consistent with our observation on the $Ca_v1.2$-a, the cardiac splice variant of the

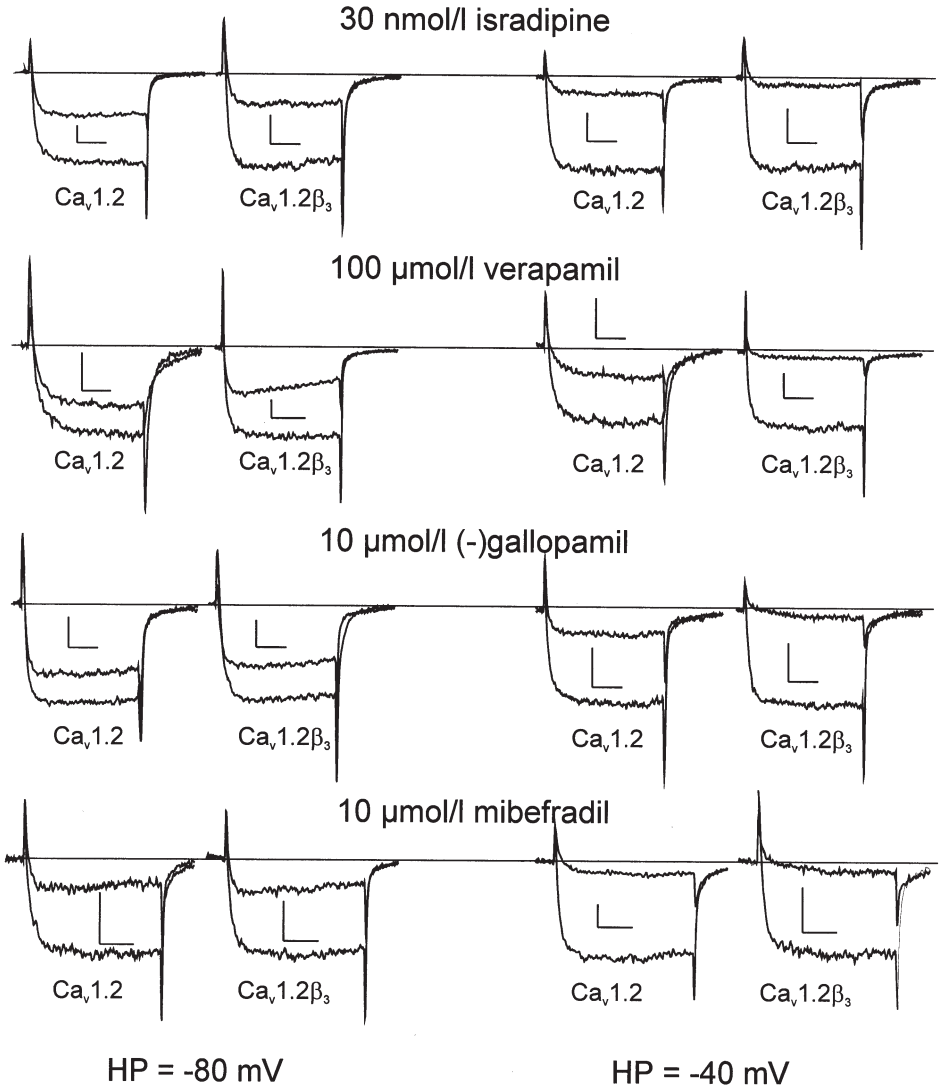

Figure 6. In each pair of traces, the control trace was recorded just before the indicated drug concentration was added to the bath solution. The second trace shows I_{Ba} three min after drug application, when a new stable current amplitude was reached. The I_{Ba} was activated by a 40 ms long pulse from the HP −80 mV to +30 mV, or from the HP −40 mV to +30 mV with frequency of 0.2 Hz. Calibration bars represent 10 ms (horizontal) and 100 pA (vertical). Modified from Lacinová et al. (1995).

$Ca_v1.2$ channel β_3 subunit did not significantly affect the current inhibition by mibefradil. When β_1 subunit was coexpressed together with the $Ca_v1.2$-b channel, the interaction between the channel and the drug was altered in a complex man-

Table 5. IC_{50} values were calculated according to the Hill equation. Significance of differences between the two channels was evaluated using non-paired Student's *t*-test

Compound	HP (mV)	IC_{50} [μmol/l]		$p \leq$
		$Ca_v1.2$	$Ca_v1.2\beta_3$	
Isradipine	−80	0.025 ± 0.002	0.020 ± 0.004	n.s.
	−40	0.0027 ± 0.0010	0.001 ± 0.001	n.s.
Gallopamil	−80	51 ± 4	23 ± 4	0.01
	−40	3.7 ± 0.3	1.1 ± 0.2	0.001
Verapamil	−80	225 ± 60	84 ± 15	0.05
	−40	15 ± 3	1.1 ± 0.2	0.01
Mibefradil	−80	4.9 ± 0.7	4.3 ± 0.3	n.s.
	−40	1.4 ± 0.3	0.9 ± 0.1	n.s.

n.s., not significant.

ner. β_1 subunit partly prevents the drug-induced negative shift in the steady-state inactivation and acceleration of the current inactivation observed for the $Ca_v1.2$-a or $Ca_v1.2$-aβ_3 channel. Furthermore, in a part of all investigated cells, low concentrations of mibefradil caused current activation rather than current inhibition.

The shifts in steady-state inactivation and acceleration of current decay in the presence of the drug are consistent with a state-dependent channel block. Our experiments demonstrated that coexpression of β-subunit significantly influences not only the basic properties of calcium current, but also the state-dependent inhibition of the channel by certain classes of pharmacological agents. β-subunit-dependent modulation of neuronal calcium channel blocks by piperidine was reported by Zamponi and co-authors (1996). The block of expressed $Ca_v1.2$, $Ca_v2.1$ and $Ca_v2.3$ channels by mibefradil was strongly affected by coexpression of the β_{1b} subunit (Jimenez et al. 2000). Sokolov et al. (2001) investigated the mechanism of regulation of the PAA gallopamil block of the expressed $Ca_v1.2$ channel by various β subunits and found a correlation between the β-subunit-dependent amplification of channel inactivation and amplification of drug-induced inhibition. Altogether, we can conclude that auxiliary β subunits significantly affect both the gating-related properties of HVA channels and their interaction with pharmacologically relevant inhibitors.

$\alpha_2\delta$ subunit

Cloning of the $\alpha_2\delta$ subunit family

The $\alpha_2\delta$ subunit with a molecular size of 125.0 kD was cloned by Ellis and co-authors (1988). Structurally, the $\alpha_2\delta$ subunit is a heavily glycosylated 175 kDa

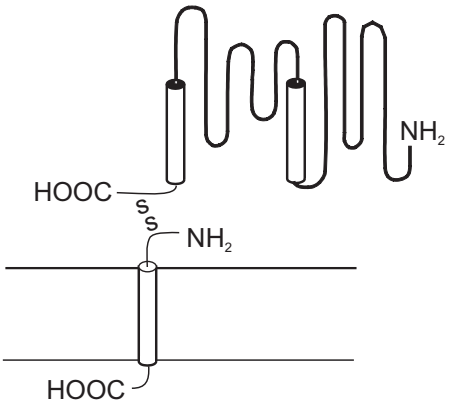

Figure 7. Putative structure of the $\alpha_2\delta$ subunit of the VACC.

protein that is post-translationally cleaved to yield a disulfide-linked α_2 and δ proteins (De Jongh et al. 1990; Jay et al. 1991). The δ part anchors the α_2 protein to membrane *via* a single transmembrane segment (Gurnett et al. 1996). Originally, two transmembrane segments were suggested for the α_2 protein based on hydropathicity analysis (Ellis et al. 1988) and biochemical experiment (Jay et al. 1991). Later experiments with site-directed antibodies (Brickley et al. 1995; Wiser et al. 1996) and *in vitro* translation (Gurnett et al. 1996) revealed a purely extracellular location of the α_2 protein, which is anchored to the calcium channel complex by the membrane-located δ protein (Figure 7). Structural studies have shown that the extracellular α_2 domain provides the structural elements required for channel stimulation (Gurnett et al. 1996). The δ domain, which contains the only transmembrane segment of the $\alpha_2\delta$ complex, harbours the regions important for the shift in the voltage-dependent activation and steady-state inactivation, and for the modulation of the inactivation kinetics (Felix et al. 1997).

Much later, three new members of the $\alpha_2\delta$ subunit family were cloned (Klugbauer et al. 1999b; Gao et al. 2000; Hobom et al. 2000; Hanke et al. 2001; Qin et al. 2002). All four proteins are summarized in Table 6.

Table 6. Sizes of individual cloned $\alpha_2\delta$ subunits of the VACC

Subunit	Molecular weight (kDa)	Number of amino acids	Reference
$\alpha_2\delta$-1	125.0	1106	Ellis et al. 1988
$\alpha_2\delta$-2	129.3	1145	Hobom et al. 2000; Gao et al. 2000
$\alpha_2\delta$-3		1091	Klugbauer et al. 1999b
$\alpha_2\delta$-4	126.0	1120	Qin et al. 2002

Modulatory role of $\alpha_2\delta$ subunits

The role of the $\alpha_2\delta$-1 subunit in regulation of channel function was less extensively investigated than the role of diverse β subunits, and the reported results are

partially inconsistent. Functional coexpression of the $\alpha_2\delta$-1 subunit with various combinations of α_1 and β subunits resulted in an increase in the current amplitude in most (Singer et al. 1991; De Waard et al. 1995; Shistik et al. 1995; Bangalore et al. 1996; Gurnet et al. 1996; Felix et al. 1997; Parent et al. 1997), but not in all cases (Welling et al. 1993a; Qin et al. 1998). Welling and co-authors (1993a) and De Waard and collaborators (1995) also failed to observe any effects of $\alpha_2\delta$-1 coexpression on the time course and voltage dependence of current activation. In contrast, a remarkable acceleration of current activation by $\alpha_2\delta$-1 subunit was reported by Singer et al. (1991), Bangalore et al. (1996) and Qin et al. (1998). A shift of the current-voltage curve in hyperpolarizing direction was observed by Singer et al. (1991) and Felix et al. (1997); however, a shift in the opposite – depolarizing direction was reported by Qin et al. (1998). Acceleration of the time course of current inactivation was consistently observed by all authors who investigated it (Singer et al. 1991; Welling et al. 1993a; De Waard et al. 1995; Felix et al. 1997; Qin et al. 1998; Shirokov et al. 1998). Nevertheless, a hyperpolarizing shift in the steady-state inactivation curve evoked by coexpression of the $\alpha_2\delta$-1 subunit was (Singer et al. 1991; Welling et al. 1993a; Felix et al. 1997), or was not (De Waard et al. 1995; Parent et al. 1997; Qin et al. 1998) observed. The cited authors used different expression systems (*Xenopus* oocytes or mammalian cell lines), different charge carriers (Ba^{2+} or Ca^{2+}), and different combinations of α_1 (L-type $Ca_v1.2$ or $Ca_v2.1$, neuronal $Ca_v2.3$ channels) and β (β_1, β_2, β_3 or β_4) subunits. It is not possible to trace a common pattern in the relation between experimental conditions and observed effects of the $\alpha_2\delta$-1 subunit. However, one should note that though the reported results are inconsistent, they are not contradictory. The authors do not report opposite effects, but rather report presence or absence of individual effects. The only exception is the work of Qin et al. (1998) who observed a depolarizing shift in the current-voltage relation, in contrast to all other authors who observed a hyperpolarizing shift or no shift at all.

The increase in current density could be attributed to improved targeting of expressed α_1 subunit to the cell membrane. Indeed, this effect was directly demonstrated by Shistik et al. (1995). The effects of coexpression of the $\alpha_2\delta$-1 subunit on the time course and/or voltage dependence on current activation and inactivation suggest a more specific modulation of the behaviour of the channel's voltage gate. Shistik et al. (1995) demonstrated that in presence of the $\alpha_2\delta$-1 subunit, the open probability of the channel increases without a change in the mean open time. Both Bangalore et al. (1996) and Qin et al. (1998) showed that coexpression of the $\alpha_2\delta$-1 subunit increases the amount of charge moved during channel activation. This increase was coupled with increased maximal conductance in the L-type $Ca_v1.2$ channel (Bangalore et al. 1996), while no change at maximal conductance was observed in the neuronal $Ca_v2.3$ channel (Qin et al. 1998). Shirokov et al. (1998) reported that $\alpha_2\delta$-1 speeds up the transition of the $Ca_v1.2$ channel into the slow inactivated state and slows down the recovery from this state. These changes in channel gating probably underlie the observed effects on inactivation of whole cell current. The importance of the role of $\alpha_2\delta$-1 in regulation of channel gating is

supported also by the work of Wyatt et al. (1998), who over-expressed the $\alpha_2\delta$-1 subunit in undifferentiated mammalian neuronal NG108-15 cell line and were able to demonstrate the modulation of activation and inactivation of both the L- and T-type channels (however, cf. Lacinová et al. 1999c).

Interactions of various α_1 subunits of the VDCC with $\alpha_2\delta$-2, -3 and -4 subunits have been described only recently. It is possible that the $\alpha_2\delta$-2 subunit interacts with LVA T-type channels by increasing the number of membrane-targeted channels (Gao et al. 2000; Hobom et al. 2000) and accelerating channel inactivation (Hobom et al. 2000). Both the $\alpha_2\delta$-2 and -3 modulate the neuronal HVA channels (Klugbauer et al. 1999b; Hobom et al. 2000). The $\alpha_2\delta$-4 subunit was shown to increase current density of the $Ca_v1.2\beta_3$ channel (Qin et al. 2002).

It was suggested that the mechanism of current enhancement by $\alpha_2\delta$ subunits mimics the mechanism of channel facilitation. When $\alpha_2\delta$-1 or $\alpha_2\delta$-3 were coexpressed together with the $Ca_v1.2$ channel, pre-pulse facilitation of Ca^{2+} current was abolished (Dai et al. 1999; Platano et al. 2000).

Similar to β subunits, $\alpha_2\delta$ subunits may modulate interaction of calcium channels with blockers. The $\alpha_2\delta$-1 subunit was shown to reduce both on-rates and equlibrium inhibition of $Ca_v2.2$ channel by ω-conotoxins GVIA, MVIIA, CVID and analogues (Mould et al. 2004.). Because the expression of the $\alpha_2\delta$ subunit is up-regulated in certain pain states, this finding may have direct clinical implications.

Tissue distribution of $\alpha_2\delta$ subunits

$\alpha_2\delta$ subunits are widely distributed in excitable tissues. The $\alpha_2\delta$-1 subunit is predominantly expressed in skeletal muscles, heart and brain. $\alpha_2\delta$-2 is prominently expressed in the heart, skeletal muscles, lungs, pancreas, testes and brain (Klugbauer et al. 1999b; Gao et al. 2000; Hobom et al. 2000). The $\alpha_2\delta$-3 subunit is mostly expressed in the brain (Klugbauer et al. 1999b). Northern blot analyses revealed expression of the $\alpha_2\delta$-4 gene in the heart and skeletal muscles. Immunohistochemical labelling showed presence of the $\alpha_2\delta$-4 protein in the pituitary gland, adrenal gland, small intestines and foetal liver tissue (Qin et al. 2002).

Regulation of high-voltage-activated calcium channels by the $\alpha_2\delta$-1, -2 and -3 subunits

To elucidate the possible role of the new $\alpha_2\delta$ subunits on the L-type and neuronal HVA channel subfamilies, $Ca_v1.2$ and $Ca_v2.3$ subunits were coexpressed together with β_{2a} or β_3 subunits, respectively, and effects of $\alpha_2\delta$-1 and $\alpha_2\delta$-3 on channel gating were compared. The effect of both $\alpha_2\delta$ subunits on current density was equivalent (Figure 8).

The changes in gating of the $Ca_v1.2$ channel elicited by both subunits were qualitatively similar. The effects of $\alpha_2\delta$-1 and $\alpha_2\delta$-3 on current density, voltage dependence of current activation and inactivation as well as on the time course

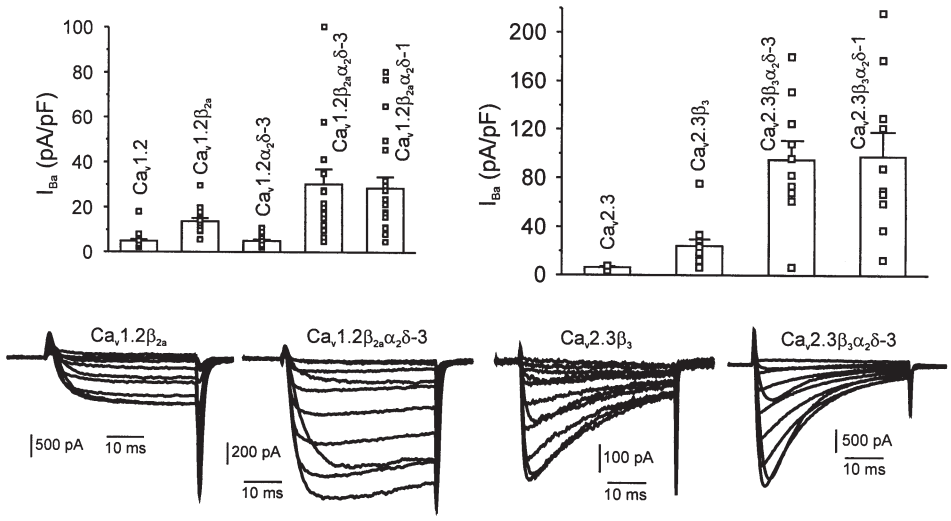

Figure 8. $\alpha_2\delta$-1 and $\alpha_2\delta$-3 subunits affect the amplitude of current through the HVA $Ca_v1.2$ (left panel) and $Ca_v2.3$ (right panel) channels. The differences between current amplitudes in the absence and in presence of each $\alpha_2\delta$ subunit were significant. Original current records are illustrated in lower parts of each panel. Squares represent individual measurements of current amplitude.

of current activation were not quantitatively different. Both the $\alpha_2\delta$-1 and $\alpha_2\delta$-3 subunits accelerated the time course of current inactivation at membrane potential of +20 mV by increasing the proportion of the fast time constant (τ_1). $\alpha_2\delta$-3 changed this time constant from 260 ± 19 ms ($Ca_v1.2\beta_2\alpha_y\delta$-1 channel; n = 11) to 156 ± 10 ms ($Ca_v1.2\beta_2\alpha_2\delta$-3 channel; n = 9). Surprisingly, $\alpha_2\delta$-1 significantly increased the slow time constant (τ_2) from 1.16 ± 0.08 s ($Ca_v1.2\beta_2$ channel; n = 12) to 3.54 ± 0.46 s ($Ca_v1.2\beta_2\alpha_2\delta$-1 channel; n = 11), though this effect is largely screened by the effect of an increased proportion of current inactivating by τ_1 and causing the overall time course of inactivation to be accelerated (Klugbauer et al. 1999b). The effects of both the $\alpha_2\delta$-3 and $\alpha_2\delta$-1 subunits on the whole cell current parameters, which reflect gating of the $Ca_v1.2$ channel, are virtually identical and require the presence of β, in this case, the β_{2a} subunit, to become prominent. In contrast to some previous works (Welling et al. 1993a; Shistik et al. 1995), we found statistically significant effects of $\alpha_2\delta$ coexpression on all measured parameters. However, a direct comparison of our results is not possible because of different experimental conditions – Welling et al. (1993a) used Ca^{2+} as a charge carrier and stably expressed cell lines, and Shistik et al. (1995) used *Xenopus* oocytes as expression system. Moreover, the reported enhancement of charge movement related to both current activation (Bangalore et

al. 1996; Qin et al. 1998) and inactivation (Shirokov et al. 1998) suggests that, in the whole cell current measurements, alteration of all related activation and inactivation parameters could be expected, as we indeed observed in our experiments.

While both the $Ca_v1.2$ and $\alpha_2\delta$-1 subunits are fairly abundant in mammalian tissues, $Ca_v2.3$ and $\alpha_2\delta$-3 are predominantly expressed in neuronal tissue. Therefore, we have selected the $Ca_v2.3$ channel for studies of the effects of $\alpha_2\delta$ subunits. In all experiments, β_3 subunit was coexpressed. This subunit had been suggested to modulate the current through the $Ca_v2.3$ channel (Ludwig et al. 1997). As with the $Ca_v1.2$ channel, both $\alpha_2\delta$-1 and $\alpha_2\delta$-3 affected most of the gating-related parameters except for the time course of current activation during membrane depolarization. Nevertheless, in this case the time constant of activation in absence of $\alpha_2\delta$ already reached the values, which in the case of the $Ca_v1.2\beta_{2a}$ channel required coexpression of $\alpha_2\delta$. Furthermore, the effects of $\alpha_2\delta$-3 and $\alpha_2\delta$-1 on voltage dependence of current activation and inactivation of the $Ca_v2.3\beta_3$ channel were significantly different. The $\alpha_2\delta$-1 subunit shifted both the activation and steady-state inactivation curves in a hyperpolarizing direction, but the change in current activation was not statistically significant. In both curves, the shift invoked by $\alpha_2\delta$-3 was significantly larger. In contrast, the effects of both $\alpha_2\delta$'s on the time course of current inactivation at a membrane potential of +20 mV were identical. Altogether, $\alpha_2\delta$-1 had smaller effect on the $Ca_v2.3$ channel than on the $Ca_v1.2$ channel. $\alpha_2\delta$-3 was found to be equally efficient in modulation of both calcium channel α_1 subunits in the presence of a β subunit. The regulation of the neuronal $Ca_v2.3$ channel by a $\alpha_2\delta$ subunit was not extensively studied before. Parent et al. (1997) reported, consistent with our results, an increase in current density upon coexpression of $\alpha_2\delta$ and, in contrast to our observations, no effect on voltage dependence of the steady-state inactivation curve. However, because of the voltage protocol used in the said study, one may expect a certain level of contamination of inactivated current by tail current. Qin et al. (1998) observed an acceleration of current inactivation, which is apparent in our experiments, too. Nevertheless, in contrast to our results, these authors observed also an acceleration of current activation and no effect on current density or voltage dependence of current inactivation. This discrepancy may again be a result of different expression systems (*Xenopus* oocytes in Qin et al. 1998) and/or different coexpressed β subunit (β_1 in Qin et al. 1998). In our experiments with the $Ca_v2.3$ channel, $\alpha_2\delta$-3 but not $\alpha_2\delta$-1 subunit affected all whole cell parameters related to channel gating except for the time course of channel activation, which was fast already in its absence (see discussion above). Therefore, one could speculate that, as follows also from the works of Bangalore et al. (1996) and Shirokov et al. (1998), $\alpha_2\delta$ subunits in the presence of a β subunit affect both activation and inactivation gating of the α_1 subunit, and that in the neuronal $Ca_v2.3$ channel this is predominantly the role of the new neuronal $\alpha_2\delta$-3 subunit, for which the ubiquitous $\alpha_2\delta$-1 subunit is not an adequate replacement.

Regulation of low-voltage-activated calcium channels by $\alpha_2\delta$-1, -2 and -3 subunits

Functional modulation of a LVA channel by $\alpha_2\delta$ subunits was tested upon coexpression of $\alpha_2\delta$-1, -2 and -3 subunits together with the $Ca_v3.1$ channel in human embryonic kidney (HEK) 293 cells. The current density-voltage relationship for peak and sustained current, kinetics of current activation and inactivation, voltage dependence of current inactivation and time course of recovery from inactivation were analyzed for each type of expressed channel. No significant difference was found for any of the examined parameters.

The lack of modulatory effects of $\alpha_2\delta$-1 and $\alpha_2\delta$-3 subunits contrasts with the finding of Wyatt and co-authors (1998) who overexpressed $\alpha_2\delta$-1 subunit in undifferentiated mammalian neuronal NG108-15 cell line and reported modulation of activation and inactivation of LVA channels. It is possible that the effects observed by Wyatt et al. (1998) upon coexpression of $\alpha_2\delta$ subunit during depolarizing pulses positive to -30 mV reflect the up-regulation of a previously immeasurable L-type channel.

In contrast to $\alpha_2\delta$-1 and $\alpha_2\delta$-3, the $\alpha_2\delta$-2a subunit caused a significant alteration of several $Ca_v3.1$ channel characteristics. Current density was significantly increased (Table 7). A similar finding was reported by Dolphin et al. (1999). Steady-state inactivation was significantly shifted by +4.5 mV in the depolarizing direction (Table 7 and Figure 9). Kinetics of current activation was not significantly altered, but the time course of inactivation was significantly accelerated (Figure 9). The time constant of inactivation saturated at approximately 14.5 ms and 12.5 ms in the absence and in presence of the $\alpha_2\delta$-2 subunit, respectively. Voltage dependence of current activation was slightly shifted in hyperpolarizing direction, but this shift was not significant (Figure 9). From such minute effects, it is hard to judge whether

Table 7. Effect of coexpression of $\alpha_2\delta$-1, $\alpha_2\delta$-2a, and $\alpha_2\delta$-3 subunits on the parameters of current density-voltage relationship of the $Ca_v3.1$ channel. $V_{0.5}$ is the potential of half-maximal current activation or inactivation and k is the corresponding slope factor. Numbers of experiments are given in brackets. Significance of differences between individual parameters for cells expressing the $Ca_v3.1$ subunit only and cells coexpressing an $\alpha_2\delta$ subunit was tested using unpaired Student's *t*-test

Channel	Charge carrier	I (pA/pF)	Activation		Inactivation	
			$V_{0.5}$ (mV)	k (mV)	$V_{0.5}$ (mV)	k (mV)
$Ca_v3.1$	Ba^{2+}	40 ± 10 (9)	−28.4 ± 0.6 (9)	4.0 ± 0.6	−57.3 ± 0.6 (9)	5.6 ± 0.5
$Ca_v3.1\alpha_2\delta$-1	Ba^{2+}	54 ± 12 (10)	−28.1 ± 0.5 (10)	4.4 ± 0.4	−55.9 ± 0.6 (10)	4.2 ± 0.4
$Ca_v3.1\alpha_2\delta$-3	Ba^{2+}	58 ± 12 (11)	−29.8 ± 0.5 (11)	4.1 ± 0.5	−57.2 ± 0.5 (11)	4.6 ± 0.9
$Ca_v3.1$	Ca^{2+}	62 ± 7 (25)	−24.9 ± 1.2 (12)	3.9 ± 0.3	−54.9 ± 1.2 (9)	4.3 ± 0.2
$Ca_v3.1\alpha_2\delta$-2a	Ca^{2+}	93 ± 15* (17)	−22.3 ± 0.8 (12)	4.1 ± 0.2	−50.4 ± 0.7** (11)	4.0 ± 0.2

* $p < 0.5$; ** $p < 0.01$; numbers of cells measured are given in brackets.

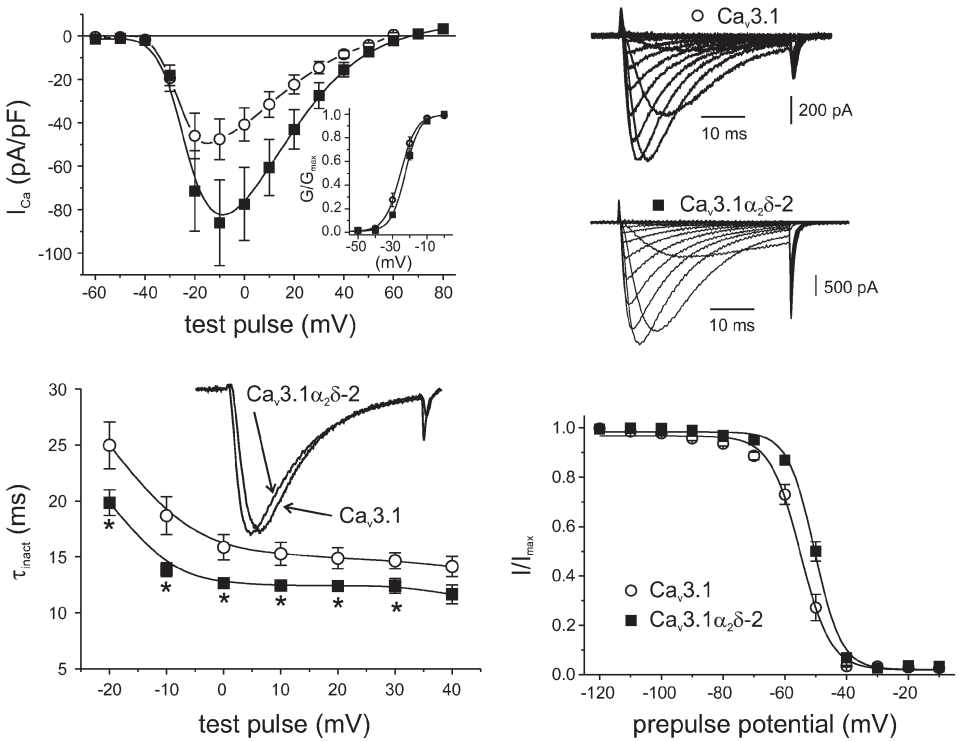

Figure 9. Effect of coexpression of $\alpha_2\delta$-2a subunit on the $Ca_v3.1$ channel. Upper left part demonstrates averaged current-voltage relationships for the $Ca_v3.1$ channel (○) or the $Ca_v3.1\alpha_2\delta$-2a channel (■). The same symbols are used in all parts of the panel. Inset shows normalized conductance-voltage relationships. Conductance was calculated from the current-voltage relationship according to the equation $G = I/(V_{rev} - V_{pulse})$, where G is conductance, I is current amplitude, V_{rev} is reversal potential and V_{pulse} is potential of particular test pulse. Solid lines are fits of averaged experimental points by the Boltzmann equations (see Table 7). Examples of current families recorded during measurement of current-voltage relationships are on the right. Note the different scales for current amplitudes. Time constants of current inactivation in the lower left part of the Figure were obtained by fitting individual current traces from the current-voltage relationships by the Hodgkin–Huxley equation. Inset shows an example of currents recorded during depolarizing pulse to −10 mV. Steady-state inactivation curves are shown in the lower right part of the Figure. Solid lines are fits of averaged experimental points by the Boltzmann equation (see Table 7). * significantly different ($p < 0.05$). Modified from Hobom et al. (2000).

the $\alpha_2\delta$-2 subunit simply facilitates membrane targeting of the $Ca_v3.1$ channel or indeed has a genuine modulatory effect on calcium channel gating.

Modulation of the $Ca_v3.1$ channel as a representative of the LVA channels family, is summarized in Table 8.

Table 8. Effects of coexpression of various $\alpha_2\delta$ subunits on the gating properties of the $Ca_v3.1$ channel. The positive and negative numbers represent shifts of half-maximal voltage for current activation ($V_{0.5act}$) or half-maximal voltage for steady-state inactivation of the current ($V_{0.5inact}$) in the depolarizing and hyperpolarizing direction, respectively. Time constants of current activation (τ_{act}) and inactivation (τ_{inact}) were significantly affected by $\alpha_2\delta$ coexpression either at individual voltages or in the whole range of voltages (marked by "…")

	Enhancement of I_{max}	Shift of $V_{0.5act}$	Shift of $V_{0.5inact}$	τ_{act}	τ_{inact}	τ_{deact}
$\alpha_2\delta$-1	0.95	+1.5	+1.4	n.s.	n.s.	n.s.
$\alpha_2\delta$-2	1.5	+2.6	***+4.5***	−30, +30 mV	−20… +20 mV	n.s.
$\alpha_2\delta$-3	1.2	+1.4	+0.1	n.s.	n.s.	n.s.

n.s., not significantly altered; gray background, $p < 0.01$; bold italics, $p < 0.001$.

Interaction of $\alpha_2\delta$ subunit with gabapentin

Gabapentin (GBP) is an antiepileptic drug that has found application also in pain relief and as an anxiolytic (Welty et al. 1993; Beydoun et al. 1995). GBP was found to bind specifically to $\alpha_2\delta$-1 of VACCs (Gee et al. 1996). This was the first described interaction between a regulatory subunit of a VACC and a pharmaceutical agent. Because VACCs are involved in the control of electrical excitability of neurons, it has been postulated that this drug reduces calcium current by modulating α_1 subunit of HVA channel indirectly through its association with $\alpha_2\delta$-1 (Gee et al. 1996).

The K_d of GBP binding to the porcine brain $\alpha_2\delta$-1 was reported as 9.4 nmol/l (Brown et al. 1998), but as 37.5 nmol/l for porcine $\alpha_2\delta$-1 expressed in COS-7 cells (Brown and Gee 1998) and 16 nmol/l for rabbit $\alpha_2\delta$-1 in COS-7 cells (Gee et al. 1996). Marais and co-authors (2001) found K_d values of 59 nmol/l for $\alpha_2\delta$-1 and 153 nmol/l for $\alpha_2\delta$-2. No specific binding of GBP to $\alpha_2\delta$-3 subunit was found. The reason of variations in K_d values is not clear, but may be attributable to species differences and assay methods.

The effect of GBP on physiological activity of calcium channels is not clearly understood. In patch-clamp studies with hippocampal granule cells, no effect of GBP was reported (Schumacher et al. 1998). However, in other studies, modest to dramatic changes in calcium current were noted. A reduction in the calcium current in isolated neurons (Stefani et al. 1998) and in rat neocortical slices (Fink et al. 2000) upon application of GBP has been described. Calabresi et al. (1999) found GBP to reduce most excitatory properties of striatal spiny neurons, which could account for the anticonvulsant effect of the drug. The calcium channels affected are not known, but candidates are L-type (Stefani et al. 1998) and P/Q-type channel (Fink et al. 2000; Meder and Dooley 2000). We have observed no consistent effect of GBP on $Ca_v1.2$, $Ca_v2.1$, and $Ca_v3.2$ currents in a heterologous HEK 293 expression system (Marais et al. 2001).

Initial studies on GBP binding using rat tissue homogenates showed strong binding in skeletal muscles and the brain, where $\alpha_2\delta$-1 is most highly expressed (Gee et al. 1996). A much lower binding of the drug was seen in the liver and kidney, which express considerable levels of the protein, as judged by Western blotting. A possible explanation for these conflicting results is that the binding of GBP to $\alpha_2\delta$-1 is modulated by other subunits (e.g., the α_1 pore protein). It is possible that the effects of GBP depend on the composition and environment of the channel. The lack of clinical side effects of the drug on skeletal muscles and other $\alpha_2\delta$-1 expressing tissues supports this view (Beydoun et al. 1995). GBP has also been shown to be an agonist of certain $GABA_B$ receptors, and this has also been postulated to be involved in the clinical action of the drug (Ng et al. 2001).

γ subunit

The γ subunit is an integral membrane protein. Originally the γ-1 subunit consisting of 222 amino acids with a predicted molecular mass of 25.1 kDa was purified from rabbit skeletal muscle (Bosse et al. 1990; Jay et al. 1990). Hydrophobicity analysis revealed the existence of four putative transmembrane helices with intracellularly located N- and C-termini (Figure 10A). The presence of two extracellular potential N-glycosylation sites is consistent with the observed strong glycosylation of these subunits (Bosse et al. 1990; Jay et al. 1990).

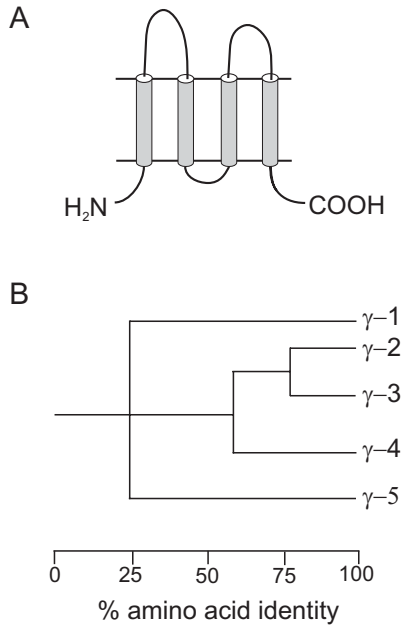

Figure 10. A. Putative structure of the γ subunit. **B.** Phylogenetic comparison of five putative γ subunits of VACCs.

For a long time, the γ subunit was considered unique to skeletal muscles. Later, a second γ-2 subunit was identified in brain. The γ-2 subunit has 25 % identity with the skeletal muscle γ-1 and is expressed mostly in the cerebellum, olfactory bulb, cerebral cortex, thalamus, CA3, and dentate gyrus of the hippocampus (Letts et al. 1998). Additional putative γ subunits γ-3, γ-4, and γ-5 have been identified (Klugbauer et al. 2000). The γ-3 clone is highly homologous to the γ-2 subunit. The γ-4 clone has 25 % identity with the γ-1 subunit. The γ-3 subunit is only distantly related to γ-2, γ-3, and γ-4 (Figure 10B). Burgess and co-authors (2001) identified a cluster of three novel g subunit genes. Structurally, γ-6 subunit is related to γ-1, γ-7 subunit is related to γ-5, and γ-8 subunit is related to γ-4.

Chu and co-workers (2001) analysed γ subunit family in rat, mouse and human. They identified eight γ subunits expressed in rat tissues including three new genes and identified orthologs of these genes in mouse and human. Based on this analysis, authors suggests that protein identified previously as mouse γ-5 subunit (Klugbauer et al. 2000) is not a member of the γ subunit family and introduces the term "protein distantly related to the γ subunit family" (Chu et al. 2001).

Tissue distribution of the novel putative γ subunits was analyzed by Northern blot. γ-3 and γ-4 mRNAs were only detectable in mouse brain and, even after a long time of autoradiography, no signals were seen in other tissues. The γ-5 subunit is highly expressed in the liver, kidney, heart, lung, skeletal muscles, and, with a lower abundance, in testes (Klugbauer et al. 2000).

Coexpression of each γ subunit together with α_1, $\alpha_2\delta$ and β subunits in oocytes induces a left shift in steady-state inactivation curves (Singer et al. 1991; Letts et al. 1998). We have tested for regulatory effects of γ-2, γ-4, and γ-5 upon their coexpression with the $Ca_v1.2$, $Ca_v2.1$, or $Ca_v3.1$ subunits, and also in combination with other auxiliary subunits (Klugbauer et al. 2000). The sequence of the γ-3 subunit is highly homologous with γ-2, so one can expect that they behave similarly.

In the combination of $Ca_v2.1$, β_{1a}, and $\alpha_2\delta$-1, only γ-2 showed a small but significant shift of voltage-dependent activation to more positive potentials. A shift of the steady-state inactivation curve towards more hyperpolarized potentials was observed upon coexpression for the γ-2 and γ-4, but not for the γ-5 subunit. When these experiments were repeated with the neuronal β_{2a} subunit, the same effect on the steady-state inactivation as seen with β_{1a} could be observed with Ca^{2+}, but not with Ba^{2+} as charge carrier (Klugbauer et al. 2000).

Furthermore, we compared the effects of the novel γ subunits with previously published results on the L-type $Ca_v1.2$ channel. Upon coexpression of γ-1 with $Ca_v1.2$-a, cardiac β_{2a} and $\alpha_2\delta$-1, the steady-state inactivation curve was shifted about 30 mV to more negative potentials and current inactivation was accelerated. Using the newly identified subunits, γ-2 and γ-5, we performed coexpression studies with $Ca_v1.2$-a, cardiac β_{2a} and $\alpha_2\delta$-1 with Ba^{2+} as charge carrier. Small but significant shifts of the voltage dependence of activation and inactivation were observed with γ-2, but not with the γ-5 subunit. These results suggest that there is also an interaction between the γ-2 subunit and the L-type $Ca_v1.2$ channel. Coexpression studies with γ-5 have also been performed in the absence of $\alpha_2\delta$-1. The absence of this subunit did not uncover any effects of γ-5 on voltage dependence of activation or on steady-state inactivation of current through the $Ca_v1.2$ channels. Although γ-5 is expressed in at least some of the tissues that also express $Ca_v1.2$ channel, it does not seem to modulate this L-type channel. For these reasons, we suggest that the γ-5 subunit may not be an auxiliary subunit of the HVA channel.

The possibility that the novel γ subunits are auxiliary subunits of the LVA T-type channels was considered and the effects of the γ-2, γ-4 and γ-5 subunits on the $Ca_v3.1$ channel were analyzed. Current density was enhanced upon coexpression of each γ subunit, but this increase was not statistically significant (Table 9). Voltage dependence of current activation was unaffected. Steady-state inactivation

Table 9. Effects of γ subunits on the voltage-dependent activation and inactivation of LVA calcium channels. I_{max} represents averaged current densities for all tested channels. Activation and steady-state inactivation experimental data were fitted by the Boltzmann equation and the resulting $V_{0.5}$ and k values were averaged. The last column shows time constants of recovery from voltage-dependent inactivation. Individual measurements were fitted to an exponential association curve and the resulting τ_s's were averaged. Significance of the differences between parameters measured in the absence and in presence of various auxiliary subunits was tested by unpaired Student's *t*-test. Data are given as mean ± S.E.M. with number of cells in brackets. 20 mmol/l Ca^{2+} was used as a charge carrier in all experiments

Channel	I_{max} (pA/pF)	Activation		Inactivation		Recovery
		$V_{0.5}$ (mV)	k (mV)	$V_{0.5}$ (mV)	k (mV)	τ (ms)
$Ca_v3.1$	61 ± 7 (20)	−24.9 ± 1.2 (12)	3.9 ± 0.3	−54.9 ± 1.2 (9)	4.3 ± 0.2	251 ± 24 (9)
$Ca_v3.1\gamma$-2	87 ± 13 (13)	−24.4 ± 1.6 (10)	3.8 ± 0.2	−51.4 ± 1.4 (10)	4.2 ± 0.2	336 ± 14** (8)
$Ca_v3.1\gamma$-4	79 ± 12 (14)	−23.9 ± 1.3 (10)	4.1 ± 0.2	−50.0 ± 1.4* (11)	3.9 ± 0.2	320 ± 17* (10)
$Ca_v3.1\gamma$-5	73 ± 9 (22)	−24.1 ± 1.0 (12)	3.9 ± 0.2	−51.7 ± 1.2 (11)	4.5 ± 0.2	248 ± 11 (9)
$Ca_v3.1\alpha_2\delta$-2a	93 ± 15* (17)	−22.3 ± 0.8 (12)	4.1 ± 0.2	−50.4 ± 0.7** (11)	4.0 ± 0.2	279 ± 12 (10)
$Ca_v3.1\alpha_2\delta$-2aγ-5	85 ± 12 (18)	−21.4 ± 1.1 (19)	4.2 ± 0.2	−49.3 ± 1.1** (11)	4.1 ± 0.3	296 ± 25 (9)

* $p < 0.05$; ** $p < 0.01$.

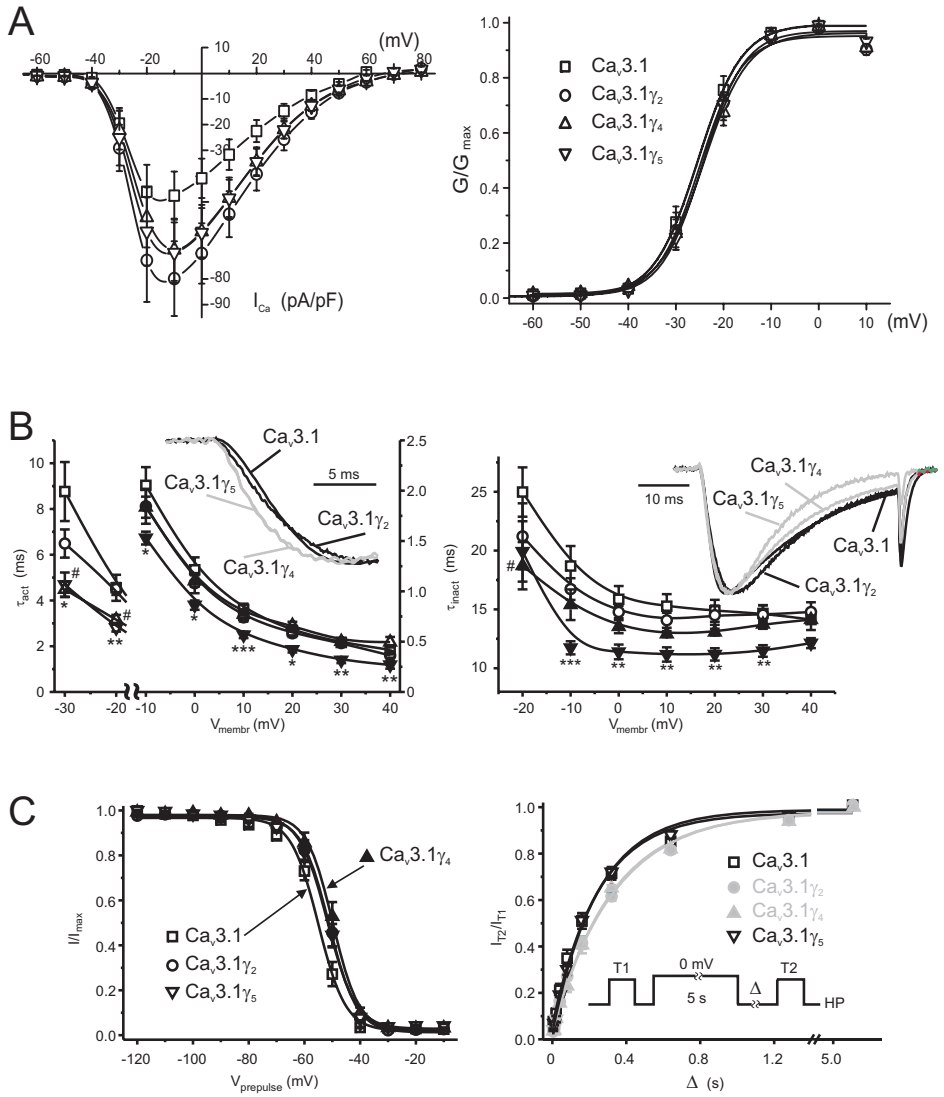

Figure 11. A. Coexpression of the γ-2, γ-4, and γ-5 subunits together with the $Ca_v3.1$ channel enhanced current density (left), but this effect was not significant. Voltage dependence of current activation was not affected (right). **B.** Kinetics of current activation during depolarization was significantly accelerated by the γ-5 subunit, partly also by γ-4, but not by the γ-2 subunit (left). Current inactivation was significantly accelerated by the γ-5 subunit (right). Significance of differences between the parameters observed in the absence and in presence of individual γ subunits was tested by unpaired Student's t-test. * $p < 0.05$, ** $p < 0.01$, *** $p < 0.001$. **C.** Shift of the steady-state inactivation curve caused by coexpression of γ subunits was significant for the γ-4 subunit (left). Recovery from the inactivation was significantly slowed down by the γ-2 and γ-4 subunits (right). Modified from Klugbauer et al. (2000).

curves were slightly shifted to more positive voltages (Table 9 and Figure 11); however, this shift was only significant for the γ-4 subunit. The speed of recovery from voltage-dependent inactivation was significantly slowed down by the γ-2 and γ-4 subunits, but not by the γ-5 subunit (Table 9 and Figure 11). The time course of current activation and inactivation during a depolarizing pulse was fitted by the Hodgkin–Huxley equation. The γ-5 subunit significantly accelerated both processes over the whole range of voltages. This effect indicates that γ-5 could be an auxiliary subunit of LVA channels. In contrast, the γ-4 subunit had similar effects only at voltages above the threshold for current activation and γ-2 was without effect.

To test the possibility that an interaction of the γ-5 subunit with $Ca_v3.1$ requires the presence of an additional auxiliary subunit, the $\alpha_2\delta$-2a subunit was coexpressed together with $Ca_v3.1$ and γ-5. However, the properties of the $Ca_v3.1/\alpha_2\delta$-2a/γ-5 channel were similar to those of the $Ca_v3.1/\alpha_2\delta$-2a channel (Table 9). Another member of LVA channel family, $Ca_v3.3$, is modulated by coexpression of γ-2, but not γ-3 and γ-4 subunits (Green et al. 2001).

In summary, γ-2, γ-3 and γ-4 could be associated with the $Ca_v2.1$, $Ca_v2.2$, and $Ca_v2.3$ channels. γ-5 subunit may modulate LVA T-type channels. Rousset et al. (2001) demonstrated minor modulatory effects of γ-2, γ-3, and γ-4 subunits on electrophysiological characteristics of the $Ca_v2.1$ channel. The role of γ-2 and γ-3 subunits in the neuronal channel complex was underlined by Kang and coauthors (2001), who demonstrated its co-immunoprecipitation with the $Ca_v2.1/2.2$ channels. Furthermore, the γ-2 subunit regulated the $Ca_v2.2$ channel expressed in *Xenopus* oocytes (Kang et al. 2001). The γ-2 subunit downregulated activity of both $Ca_v2.1$ and Ca_v 2.2 channels. Similarly, the γ-1 subunit downregulates calcium current through the $Ca_v1.1$ channel (Freise et al. 2000; Arikkath et al. 2003). This property contrasts with the regulatory role of β and $\alpha_2\delta$ subunits, which generally enhance the activity of VACC.

It is possible that while the modulatory effects of γ-2 through γ-5 on the VACC

Table 10. Effects of coexpression of various γ subunits on gating properties of the $Ca_v3.1$ channel. Positive and negative numbers represent shift of half-maximal voltage for current activation ($V_{0.5act}$) or half-maximal voltage for steady-state inactivation of current ($V_{0.5inact}$) in the depolarizing and hyperpolarizing direction, respectively. Time constants of current activation (τ_{act}) and inactivation (τ_{inact}) were significantly affected by γ coexpression either at individual voltages or in the whole range of voltages (marked by "...")

	Enhancement of I_{max}	Shift of $V_{0.5act}$	Shift of $V_{0.5inact}$	τ_{act}	τ_{inact}	τ_{deact}
γ_2	1.4	+0.5	+3.5	n.s.	n.s.	n.s.
γ_4	1.3	+1.0	***+4.9***	***−20, −10 mV***	***−20 mV***	n.s.
γ_5	1.2	−0.8	+3.2	−30... +30 mV	−10... +30 mV	n.s.

n.s., not significantly altered; bold italics, $p < 0.05$; grey background, $p < 0.01$.

are modest, their principal role is in interaction with other membrane proteins. Chen and co-authors (2000) have shown that γ-2 is responsible for proper targeting of AMPA receptor to the synaptic space.

The possible role of γ subunits in the LVA channel complex is summarized in Table 10.

L-type calcium channel

Subunit composition of the calcium channel

The L-type channel family has currently four known members (see Table 1). The first cloned skeletal muscle $Ca_v1.1$ channel consists of five proteins, the principal α_1 and auxiliary β_1, $\alpha_2\delta$-1 and γ-1 subunits. Subunit composition of another three L-type channels, $Ca_v1.2$, $Ca_v1.3$ and $Ca_v1.4$, is less certain. $Ca_v1.2$ may be coexpressed with various β and $\alpha_2\delta$ subunits in a tissue-dependent manner. Coexpression studies in heterologous systems demonstrated modulation of the $Ca_v1.2$ channel by all four known β subunits. Our results (Klugbauer et al. 2000) suggest that the γ-2 subunit may regulate the $Ca_v1.2$ channel. Subunit composition of the $Ca_v1.3$ channel was not investigated systematically, but coexpression studies confirmed regulation of the channel by the β_2, β_3 and $\alpha_2\delta$-1 subunits. No expression studies have been done so far with the $Ca_v1.4$ channel.

Regulation by calcium channel blockers and activators

Dihydropyridines

Ligands of the L-type channel represent a clinically and experimentally important set of blockers and agonists. The major classes of these drugs are organic channel blockers, such as dihydropyridines (DHP), phenylalkylamines (PAA) and benzothiazepines (BTZ). Different techniques have been used to localize potential binding sites of these drugs on the calcium channel complex. Earlier experimental observations from photoaffinity labelling and peptide mapping studies on the skeletal muscle channel revealed that all three classes bind to the transmembrane region of repeat IV of the α_1 subunit (Regulla et al. 1991; Catterall and Striessnig 1992; Kuniyasu et al. 1998) with additional sites on repeat III (Catterall and Striessnig 1992; Kalasz et al. 1993) and repeat I (Kalasz et al. 1993) for the DHPs. Custom-synthesized DHPs, in which the DHP-moiety was separated from the permanently charged head by a spacer chain with variable length, were most effective in channel inhibition when the length of the spacer chain was ten methylene residues (Baindur et al. 1993; Bangalore et al. 1994). While the permanently charged hydrophilic head stays outside of cell membrane, the active DHP-moiety can reach about 11–14 Å inside the lipid bilayer under these conditions.

The construction of chimeric $Ca_v1.2/Ca_v2.1$ and $Ca_v1.2/Ca_v2.3$ channels and site directed mutagenesis of single amino acids in the $Ca_v1.1$ or $Ca_v1.2$ subunit further refined the location of the DHP-interaction site. Tyr1485, Met1486 and Ile1493 of IVS6 (amino acid numbering is according to the $Ca_v1.2$-b sequence (Biel

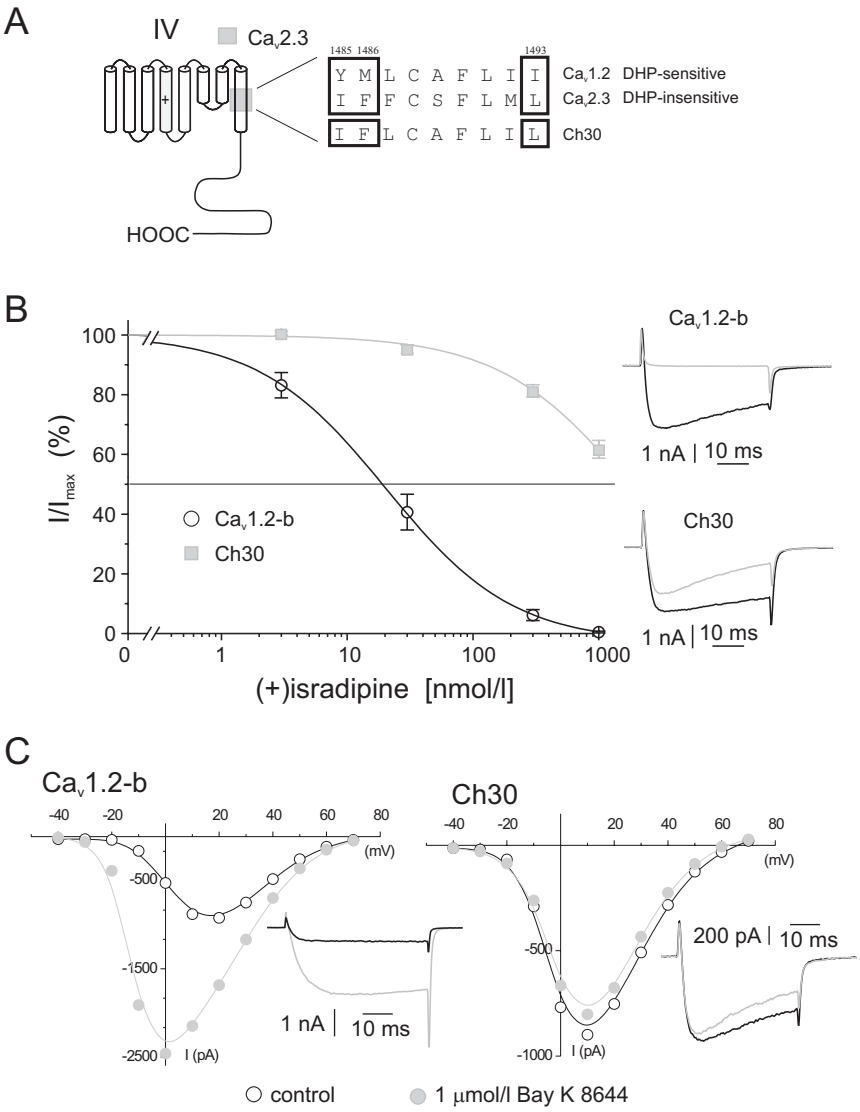

Figure 12. Important determinants of DHP binding to the $Ca_v1.2$ channel are the amino acids of the IVS6 segment. Panel **A.** Amino acid exchange between the $Ca_v1.2$ channel and the DHP insensitive $Ca_v2.3$ channel, yielding the Ch30 channel. Panel **B.** The effect of mutations of the Ch30 channel on IC_{50} for inhibition of the expressed channel by (+)isradipine. The dose-response curve measured at HP of –80 mV is in the left part of the panel. Examples of current traces measured in the absence (black) and in presence (grey) of 1 μmol/l (+)isradipine from either the wild type $Ca_v1.2$ or the Ch30 channel are on the right part of the panel. Panel **C.** The effects of mutations of the Ch30 channel on current enhancement by the Bay K 8644 agonist. Current-voltage relationships and current traces measured under the control conditions and in the presence of 1 μmol/l Bay K 8644 are shown in black and grey, respectively. Reprinted by permission from EMBO J., Schuster et al. (1996), copyright 1996 Macmillan Publishers Ltd.

et al. 1990)) contribute to the DHP-interaction site in a decisive way. Their replacement by the corresponding amino acids from the DHP-insensitive $Ca_v2.3$ channel in chimera 30 (Ch30) channel increased IC_{50} for isradipine inhibition more than 100-fold, from 16 ± 2 nmol/l (wild type channel) to 1.7 ± 0.3 μmol/l (Ch30 channel). These mutations reversed the effect of another DHP Bay K 8644 from agonistic to antagonistic (Figure 12 and Schuster et al. 1996). Both DHPs accelerated current decay of the Ch30 channel.

Further investigations identified additional amino acids participating in the high affinity block of the $Ca_v1.2$ mediated barium current (I_{Ba}) by antagonist DHPs: Thr1061 and Gln1065 in IIIS5 (Ito et al. 1997; He et al. 1997), Ile1175, Ile1178, Met1183 and the conserved Tyr1174 of IIIS6 (Bodi et al. 1997; Peterson

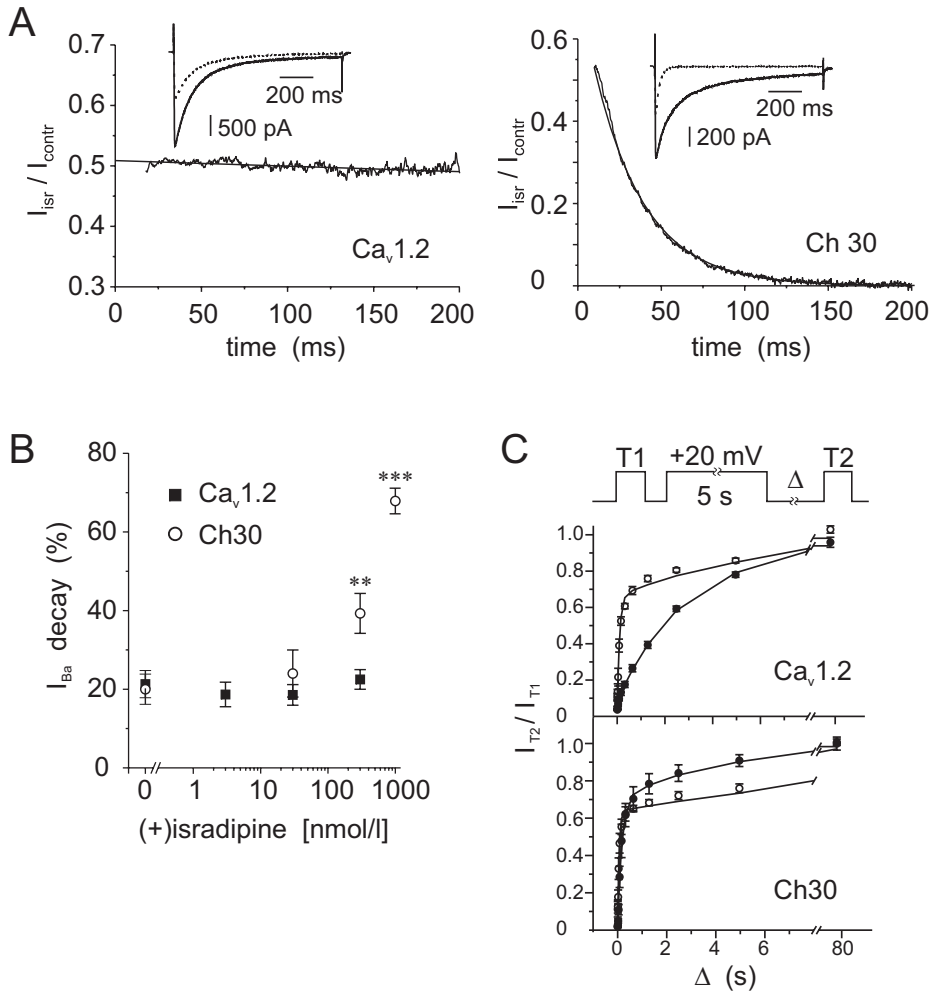

et al. 1997) and the conserved Asp1494 in IVS6 (Peterson et al. 1997). The largest effects were observed with mutation of Thr1061 to Tyr, which lowered the affinity for isradipine more than 1000-fold (He et al. 1997; Ito et al. 1997). The removal of stimulation of I_{Ba} by the DHP agonists Bay K 8644 or (+)S-202-791 required mutation of less amino acids: Thr1061 in IIIS5 (Ito et al. 1997), Tyr1174 in IIIS6 (Bodi et al. 1997) and Tyr1485, Met1486 in IVS6 (Schuster et al. 1996). In contrast to these mutations, the replacement of the L-type channel specific Phe1484 in IVS6 by Ala decreased the IC_{50} for the DHP antagonist isradipine from 6.8 nmol/l to 0.014 nmol/l (Peterson et al. 1997). High affinity binding of DHPs requires Ca^{2+} ions (Schneider et al. 1991), which are coordinated by the pore region glutamates (Mitterdorfer et al. 1995). Mutation of the respective Glu to Gln in the $Ca_v1.1$ pore region III and IV decreased the affinity for isradipine 10- to 40-fold (Peterson and Catterall 1995). Although not completely excluded, it is unlikely that the high affinity binding of DHPs involves direct binding to the pore region glutamates. Most

Figure 13. A. Effect of (+)isradipine on I_{Ba} waveform. The currents recorded from the wild type $Ca_v1.2$ channel (left) or Ch30 channel (right) during a 1 s long depolarizing pulse from the holding potential of −80 mV to +20 mV under control conditions (solid line) and in the presence of 30 nmol/l (wild type) or 1 μmol/l (Ch30) of (+)isradipine (dashed line) are shown in insets. The main graphs were obtained by dividing individual points of the current trace sampled in the presence of (+)isradipine by the corresponding current samples measured under the control conditions. The points preceding the peak of the current trace were omitted. The first 200 ms of each record were analyzed. The solid line for the wild type channel represents a linear fit with a slope of 0.9×10^{-4} ms^{-1}. The solid line for Ch30 channel is a monoexponential fit with a time constant of 30 ms. **B.** Concentration dependence of I_{Ba} decay at the end of a 40 ms long test pulse for $Ca_v1.2$ and Ch30 channels. I_{Ba} decay was calculated as $(1 - I_{end}/I_{peak}) \times 100\,\%$, where I_{end} is the current amplitude measured at the end of a 40 ms test pulse and I_{peak} is the maximal I_{Ba} amplitude during the test pulse. $n = 5$–9 at individual concentrations; ** $p < 0.01$; *** $p < 0.001$ (paired t-test) for the difference between I_{Ba} decay at a given isradipine concentration and in the control solution for the same calcium channel type. **C.** Recovery of the two channels from voltage-dependent inactivation. The voltage protocol used in this set of measurements is shown at the top. A 40 ms long test pulse T1 was followed by a 5 s inactivating pulse to +20 mV. After a variable time recovery interval Δ, a second test pulse T2, identical to the T1 pulse, followed. Between the depolarizing pulses, the membrane was held at the HP of −80 mV. The whole sequence was repeated starting 60 s after the end of T2. The recovery interval Δ varied from 5 ms to 79.36 s. The amplitudes of I_{Ba} measured during the T2 pulse were normalized to the amplitude measured during the T1 pulse. Averaged results from cells expressing the $Ca_v1.2$ channel (upper graph) or Ch30 channel (lower graph) measured under the control conditions (open symbols) or in the presence of isradipine (solid symbols) were fitted to double exponential association curves (solid lines in both panels). The concentration of isradipine was 30 nmol/l ($Ca_v1.2$ channel) or 1 μmol/l (Ch30 channel); $n = 6$ for both calcium channels.

likely, the coordination of Ca^{2+} is required to allow the optimal conformation for high affinity binding.

Removal of high affinity interaction site in the Ch30 channel revealed low affinity interaction with IC_{50} about 1 μmol/l (Schuster et al. 1996). Mechanism of this interaction has typical features of open channel block (Lacinová and Hofmann 1998). Isradipine accelerated current decay in the Ch30 channel, but not in the wild type $Ca_v2.1$ channel, in a concentration-dependent manner (Figure 13A and B). Apparently, prolonged depolarization supported development of channel block in Ch30, but not in the wild type channel. This observation was consistent with an open channel block of the Ch30 channel. Inhibition of current amplitude increased to the same extent with increasing HP in both the wild type and Ch30 channels. Acceleration of current decay by isradipine in the Ch30 channel was independent on HP. Increase in HP increases the proportion of channels in inactivated state and supports the inhibition of current amplitude. We therefore suggested that the inhibition of current amplitude was mainly due to isradipine interaction with an inactivated channel state and that it is this interaction, which is removed by the mutations of the Ch30 channel. The recovery of both channels from voltage-dependent inactivation was biphasic. The presence of isradipine slowed down the recovery of the wild type channel, suggesting that the inactivated channel must unbind the drug before it can recover from inactivation. In contrast, the recovery was faster in the presence of isradipine in the Ch30 channel (Figure 13C), suggesting that the drug-bound channel did not inactivate and could recover fast. Altogether, the mutations in IVS6 yielding the Ch30 channel disturb the high affinity interaction site responsible for DHP interaction with an inactivated channel and reveal an interaction with an open channel state (Lacinová and Hofmann 1998). Possibly, binding to the pore region is involved in this low affinity block.

Identification of DHP interaction site using the loss-of-function chimeric channels was confirmed by construction of gain-of-function chimeras. Transfer of parts of the $Ca_v1.2$ sequence to the DHP insensitive neuronal $Ca_v2.1$ subunit (Grabner et al. 1996; Hockerman et al. 1997b; Sinnegger et al. 1997) or the $Ca_v2.3$ subunit (Ito et al. 1997) showed that the L-type specific and non-conserved amino acids mentioned above had to be present to allow high affinity block and stimulation of these channels by the DHP antagonist isradipine and the Bay K 8644 agonist, respectively. The IC_{50} values for block of the chimeric channels were in the range of 10 to 100 nmol/l. A similar value is obtained with the wild type $Ca_v1.2$ channel at a HP of -80 mV, suggesting that these amino acids transfer the affinity for a "resting block". The high affinity block for DHPs requires inactivation of the L-type Ca^{2+} channel. Inhibition of the inactivated state of the channel measured at more positive HPs of -40 to -30 mV results in IC_{50} values less than 1 nmol/l (Lacinová et al. 2000b). The transfer of the amino acids of the IIIS5, IIIS6 and IVS6 segments described above was not sufficient to reconstruct the voltage dependence of the DHP-induced channel block. The involvement of additional amino acids in the high affinity block of the L-type channel by DHPs is supported by the report about a recently cloned L-type channel α_1 subunit from jellyfish (Jeziorski et al. 1998).

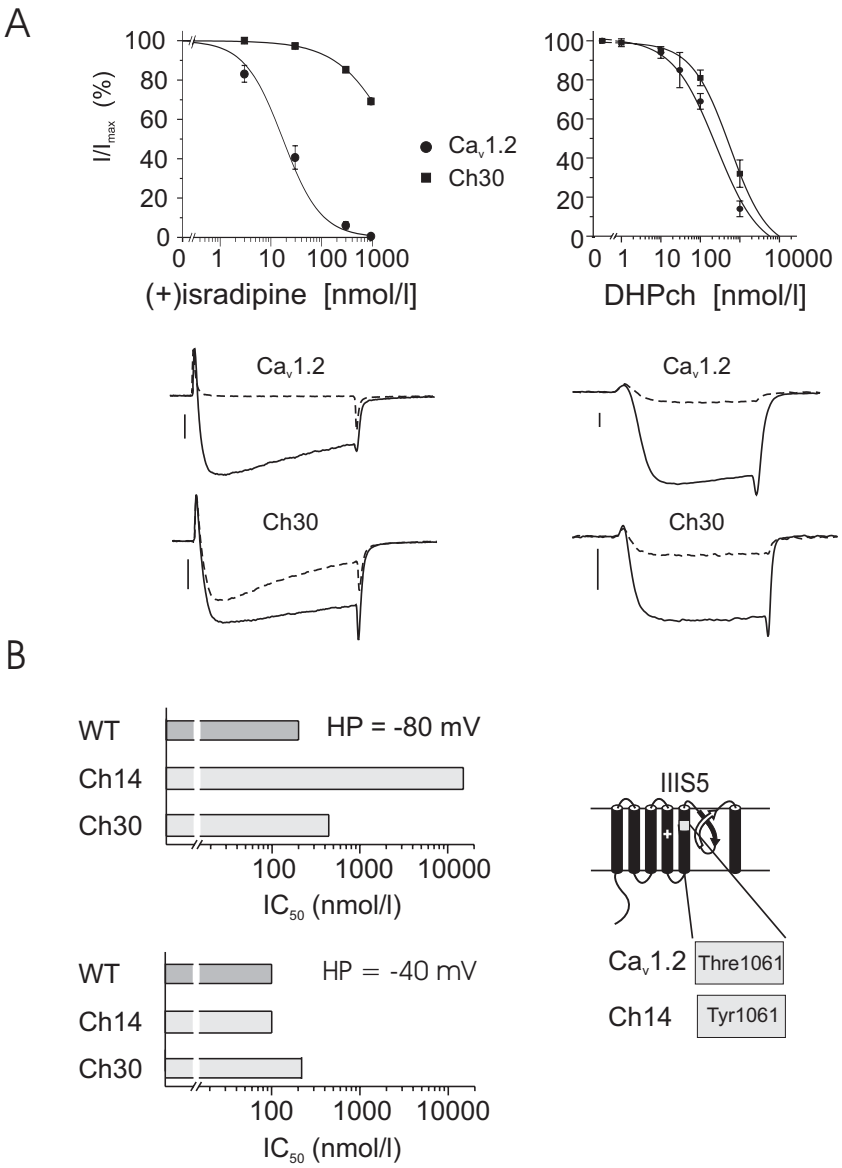

Figure 14. A. Mutations of Ch30 channel (see Figure 12) affect differently the inhibition of the $Ca_v1.2$ channel by the neutral DHP isradipine and charged DHPch. Dose-response curves for wild type (■) and mutated (●) channels are shown in the upper part of the panel. In the lower part, original current records in the absence (solid line) and in presence (dashed line) of 1 μmol/l of each drug are shown. Scale bars, 500 pA. **B.** Left: IC_{50} for DHPch measured for the wild type $Ca_v1.2$ channel and for the Ch14 and Ch30 channels at two HP, 80 mV (top) and −40 mV (bottom). On the right, mutation of the $Ca_v1.2$ channel yielding the Ch14 channel is shown. Modified from Lacinová et al. (1999).

The expressed jellyfish α_1 subunit contained all amino acids identified in IIIS5, IIIS6 and IVS6 that are necessary for high affinity block of the mammalian $Ca_v1.2$ channel. However, this channel is neither blocked by isradipine at submicromolar concentrations, nor stimulated by (−)Bay K 8644.

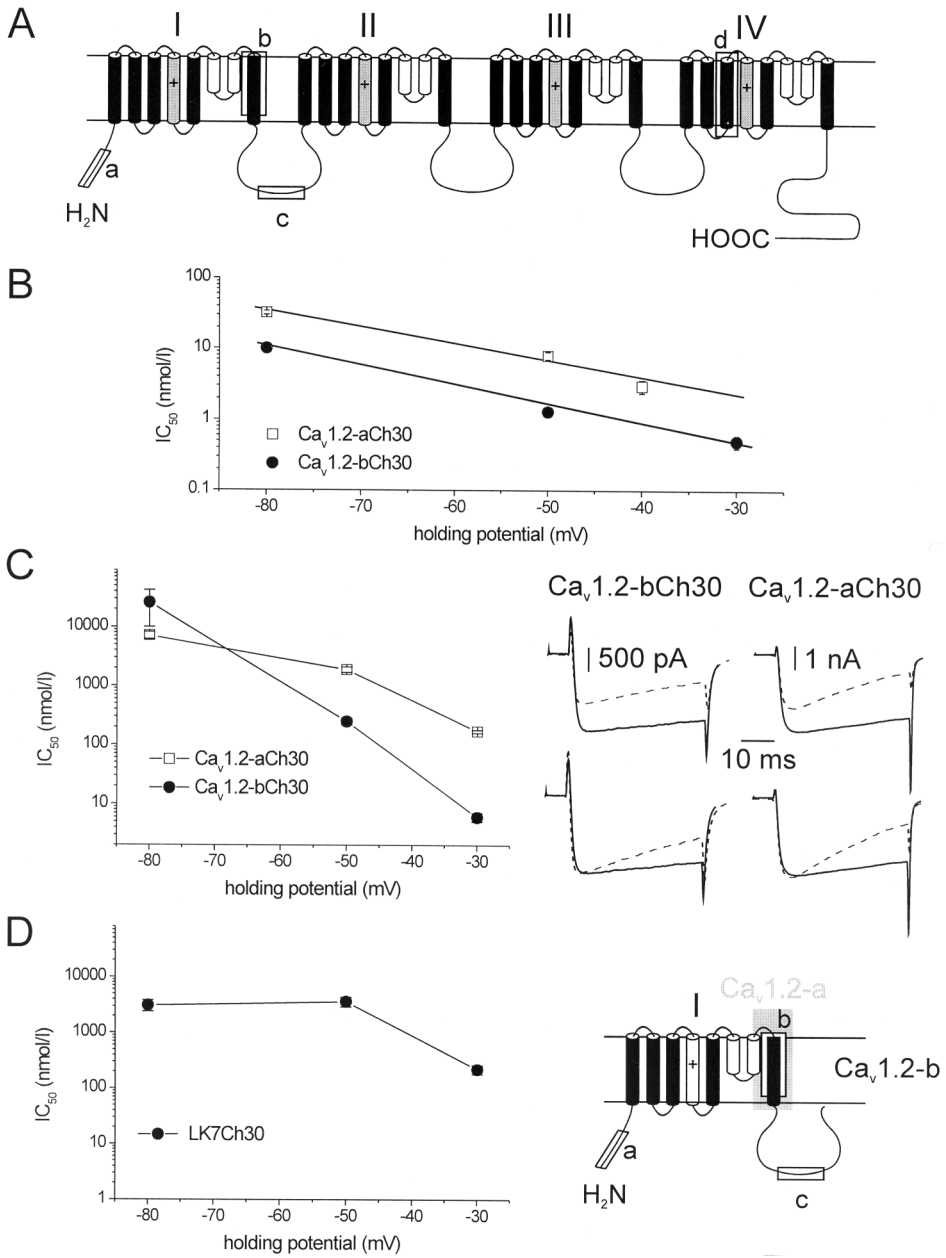

Testing of the different mutations of the $Ca_v1.2$ channel with charged and uncharged DHP analogues (Bangalore et al. 1994; Lacinová et al. 1999b) suggested the presence of an additional site and/or mechanism for interaction of the channel with DHPs. A custom-synthesized dihydropyridine (DHPch), in which the DHP-moiety was separated from the permanently charged head by a spacer chain consisting of ten methylene residues (Baindur et al. 1993; Bangalore et al. 1994) was used in these experiments. Mutations in the IVS6 segment (Ch30) decreased the affinity of the channel for the uncharged DHP isradipine; the charged DHP blocked wild type $Ca_v1.2$ and the mutated Ch30 channel with similar, but relatively low affinity at both the hyperpolarized (−80 mV) and depolarized (−40 mV) HPs (Figure 14). DHPch may bind to a different conformation of the channel and interact with different amino acids than the neutral isradipine used in experiments that mapped the DHP site. This suggestion is further supported by analysis of inhibition of the Ch14 channel with DHPch (Figure 14B). In the Ch14 channel, replacement of Thr1061 in the IIIS5 segment by Tyr completely abolished channel block by isradipine at all HPs (Ito et al. 1997). The mutation had similar effect on the Ch14 channel inhibition by DHPch at HP of −80 mV; however, the mutation was without any effect on channel inhibition at HP of −40 mV (Lacinová et al. 1999b and Figure 14B).

The work of several groups suggested that coexpression of ß, $\alpha_2\delta$ and γ subunits is required for high affinity binding of DHPs (Mitterdorfer et al. 1994; Wei et al. 1995; Suh-Kim et al. 1996a) and/or for high affinity inhibition of the calcium current by DHPs (Wei et al. 1995; Suh-Kim et al. 1996b). So far, it can not be decided whether these subunits help to position the α_1 subunit in the membrane, to ensure correct folding of the α_1 subunit, or influence directly the binding site. In contrast to the above results, other groups reported that high affinity binding of DHPs is observed even when only the $Ca_v1.2$ subunit was expressed alone

Figure 15. A. Amino acid sequences of the cardiac splice variant $Ca_v1.2$-a and the smooth muscle $Ca_v1.2$-b splice variant of the $Ca_v1.2$ channel differ in the four regions (a–d) marked by grey rectangles. **B.** Dependence of IC_{50} for inhibition of cardiac $Ca_v1.2$-aCh30 (□) and smooth muscle $Ca_v1.2$-bCh30 (●) splice variants by (+)isradipine on the holding potential. Solid lines are simple connectors of experimental points. **C.** Left: dependence of IC_{50} for inhibition of the chimeric $Ca_v1.2$-aCh30 (□) and $Ca_v1.2$-bCh30 (●) channels by (+)isradipine on the holding potential. Solid lines are simple connectors of experimental points. Right: examples of current traces recorded from the $Ca_v1.2$-aCh30 and $Ca_v1.2$-bCh30 channels in the absence (solid line) and in presence (dashed line) of 1 μmol/l (+)isradipine. To facilitate comparison of current waveforms, traces were normalized to the same amplitude in the bottom part of the panel. **D.** Left: dependence of IC_{50} for inhibition of the chimeric LK7Ch30 channel (●) by (+)isradipine on the holding potential. Right: in the LK7 channel, the IS6 segment of the smooth muscle $Ca_v1.2$-b channel was replaced by the IS6 segment from the cardiac $Ca_v1.2$-a channel (region b, see panel A). In addition, mutations of Ch30 channel (Figure 12) were introduced in the IVS6 segment. Modified from Lacinová et al. (1999a).

(Welling et al. 1993a). Coexpression of the β_3 subunit did not significantly affect the inhibition of calcium current by isradipine (Lacinová et al. 1995). In the experiments mentioned above, wild type and chimeric channels were always coexpressed with auxiliary subunits. Still, the gain-of-function chimeras failed to reconstruct the voltage dependence of the high affinity channel inhibition by DHPs. Additional channel structures may be involved in this interaction. Analysis of cardiac and smooth muscle splice variants of the $Ca_v1.2$ subunit offered an additional insight into this problem (Welling et al. 1993b). It is known that the smooth muscle splice variant is more susceptible to channel inhibition by DHP. Originally, different sensitivities were attributed to the different resting membrane potentials of the two tissues. Molecular cloning of calcium channels, Northern blot and *in situ* analysis revealed that different splice variants of the L-type channel are expressed in both tissues (Welling et al. 1997). Amino acid sequences of the $Ca_v1.2$-a (cardiac) and $Ca_v1.2$-b (smooth muscle) splice variants differ only at four sites (Figure 15A). In spite of these structural differences, basic electrophysiological properties of both channels are identical (Lacinová et al. 2000b). The mechanism of the block of channels expressed by isradipine is also identical, but the $Ca_v1.2$-b channel is blocked at lower concentrations of the drug at each investigated potential (Figure 15B). IC_{50} values for isradipine are 32 nmol/l and 8 nmol/l at HP of -80 mV, and 10 nmol/l and 1.3 nmol/l at HP of -50 mV, for $Ca_v1.2$-a and $Ca_v1.2$-b, respectively (Lacinová et al. 2000b and Figure 15). The mutations of Ch30 (see Figure 12) affected the channels differently. The voltage dependence of current inhibition, which is related to high affinity interaction with an inactivated channel, was disturbed in the $Ca_v1.2$-a, but not in the $Ca_v1.2$-b channel (Figure 15C). In contrast, the acceleration of current decay during a depolarizing pulse that reflects low affinity open channel block was not affected (Figure 15C). An in-depth analysis showed that the alternative exon 8a or 8b, which codes for the IS6 segment, is responsible for the difference (Welling et al. 1997; Lacinová et al. 2000b and Figure 15D). The double chimera LK7Ch30, consisting of the $Ca_v1.2$-b channel with IS6 segment from the $Ca_v1.2$-a channel and mutations of Ch30 in IVS6 segment (see Figure 12) mimicked the properties of the $Ca_v1.2$-aCh30 channel (Welling et al. 1997; Lacinová et al. 2000b. and Figure 15D). Similar results were reported by Zühlke and co-workers (1998) and Morel and co-workers (1998), proving that the IS6 segment significantly affects the DHP block. Additional splice variations at the IIIS2 segment and in the intracellular carboxyterminal sequences can also contribute to alterations in DHP affinity (Zühlke et al. 1998).

Contribution of the IS6 segment to the voltage dependence of channel inhibition by DHPs was further investigated in gain-of-function chimeras. The DHP interaction site was reconstructed in the $Ca_v2.3$ channel by mutating eight amino acids of the IIIS5, IIIS6 and IVS6 segments. These mutations yielded the chimeric channel rEC10 (Figure 16A). Study of the voltage dependence of the block of inactivated channels must take into account the voltage dependence of steady-state inactivation of the investigated channels. The $Ca_v2.3$ channel as well as the chimeric rEC10 channel inactivate at 50 mV more negative membrane potentials than the

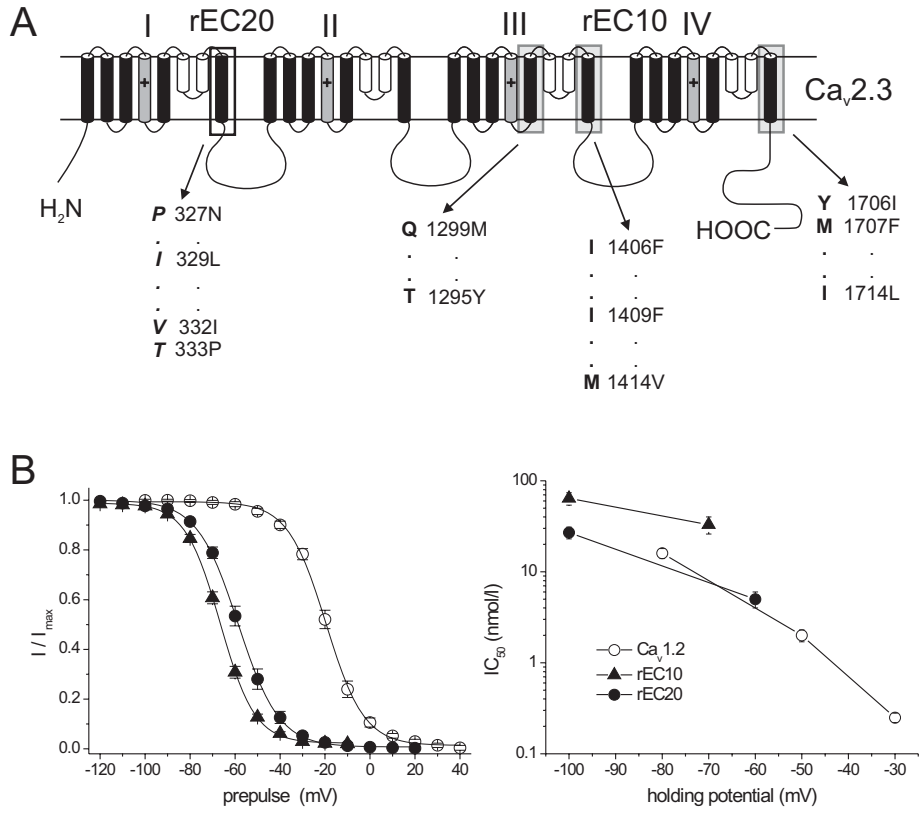

Figure 16. A. Construction of the chimeric rEC10 and rEC20 channels. In the rEC10 chimera, amino acids of the $Ca_v2.3$ sequence were replaced by the corresponding amino acids of the $Ca_v1.2$ sequence (bold letters) in the IIIS5, IIIS6, and IVS6 segments, as indicated. In the rEC20 chimera, besides that, amino acids of the IS6 segment from the $Ca_v1.2$ sequence (bold italics) were introduced into the $Ca_v2.3$ sequence. Numbering of amino acids is according to the $Ca_v2.3$ sequence (Schneider et al. 1994). **B.** Left: voltage dependence of steady-state inactivation for the $Ca_v1.2$ channel (○, $n = 14$), chimeric rEC10 channel (▲, $n = 8$) and chimeric rEC20 channel (●, $n = 7$). Fitting of experimental data by the Boltzmann function resulted in voltages for half-maximal inactivation: -19.6 ± 0.3 mV, -66.6 ± 0.1 mV and -58.6 ± 0.2 mV for the $Ca_v1.2$, rEC10 and rEC20 channel, respectively. Right: dependence of IC_{50} for inhibition of the channels by (+)isradipine on holding potential. Symbols have the same meaning as in the left panel. IC_{50} were calculated by fitting the dose-response curves measured for 7 to 9 cells for each investigated channel by the Hill equation (see Lacinová et al. 1999a).

$Ca_v1.2$ channel (Lacinová et al. 1999a and Figure 16B). Therefore, IC_{50} for inhibition of the chimeric channel should be evaluated at a more negative HP than IC_{50} for inhibition of the wild type $Ca_v1.2$ channel. No channels are inactivated at HPs of -80 mV and -100 mV for the $Ca_v1.2$ channel and chimeric rEC10 channel,

respectively. IC_{50} for inhibition by (+)isradipine at these HPs were 16 ± 2 nmol/l and 64 ± 10 nmol/l for the $Ca_v1.2$ and chimeric rEC10 channels, respectively. Both values decreased in a voltage dependent manner; nevertheless, the slope of the voltage dependence for the rEC10 channel was less steep compared to the slope for the $Ca_v1.2$ channel (Figure 16B). Introduction of amino acids of the IS6 segment, which are responsible for increased sensitivity of the smooth muscle $Ca_v1.2$-b channel, into the rEC10 channel yielded the gain-of-function chimera rEC20 (Figures 15 and 16). This chimera was: more sensitive to inhibition by (+)isradipine than rEC10 (IC_{50} = 27 ± 4 nmol/l) and voltage dependence of its inhibition by (+)isradipine had a more steep slope close to that of the $Ca_v1.2$ channel (Figure 16B). Together with the earlier photoaffinity results (Kalasz et al. 1993) these observations further support the suggestion that amino acids of the IS6 segment contribute directly to the DHP-binding pocket.

Phenylalkylamines and benzothiazepines

Phenylalkylamines (PAA), such as verapamil, gallopamil or devapamil, block L-type current in a use-dependent manner from the intracellular side of the membrane (Hescheler et al. 1982) and affect binding of DHPs by allosteric interaction (Glossmann and Striessnig 1990). In addition, benzothiazepines (BTZ), such as diltiazem, interact allosterically with binding of DHPs (Glossmann and Striessnig 1990). In contrast to PAAs, BTZs label extracellular sites in the linker sequence between IVS5 and IVS6 in the $Ca_v1.1$ subunit (Watanabe et al. 1993), in agreement with a recent report that the quaternary 1,5-BTZ DTZ417 blocks the cardiac L-type channel only when applied from the extracellular site (Kurokawa et al. 1997). More recently, it was shown that similar to the PAA devapamil (Catterall and Striessnig 1992), the 1,4-BTZ semotiadil labels a short sequence of the IVS6 segment (Kuniyasu et al. 1998). The PAA verapamil blocks the L-type $Ca_v1.2$ Ca^{2+} channel and the non-L-type $Ca_v2.1$ and $Ca_v2.3$ Ca^{2+} channels at similar concentrations in a state-dependent manner (Cai et al. 1997), whereas diltiazem blocked all three channels at similar concentrations, but only the $Ca_v1.2$ Ca^{2+} channel in a state-dependent manner.

Extent of the inhibition of L-type channel by PAAs increased, when the extent of VDCC inactivation increased (Sokolov et al. 2001; Hering 2002). Use of Ca^{2+} instead of Ba^{2+} as a charge carrier potentiated inhibition of the L-type $Ca_v1.2$ Ca^{2+} channel by both PAAs and BTZs, however, this effect was independent of potentiation of Ca-dependent channel inactivation. Potentiation of BTZs and PAAs block of $Ca_v1.2$ channel depends on the interaction of Ca^{2+} ions with pore glutamates, as demonstrated Dilmac and co-authors (Dilmac et al. 2003, 2004).

Molecular analysis of the $Ca_v1.2$ subunit (Schuster et al. 1996; Hockerman et al. 1995, 1997a) showed that the L-type channel specific Ile1175 and the conserved Tyr1174, Phe1186 and Val1187 in IIIS6 and the L-type channel specific Tyr1485, Ala1489 and Ile1492 in IVS6 are necessary to form a high affinity PAA site. In addition, the two glutamates (Glu1140 and Glu1441) in pore regions of repeats III and IV are necessary (amino acid numbering is according to the $Ca_v1.2$-b sequence

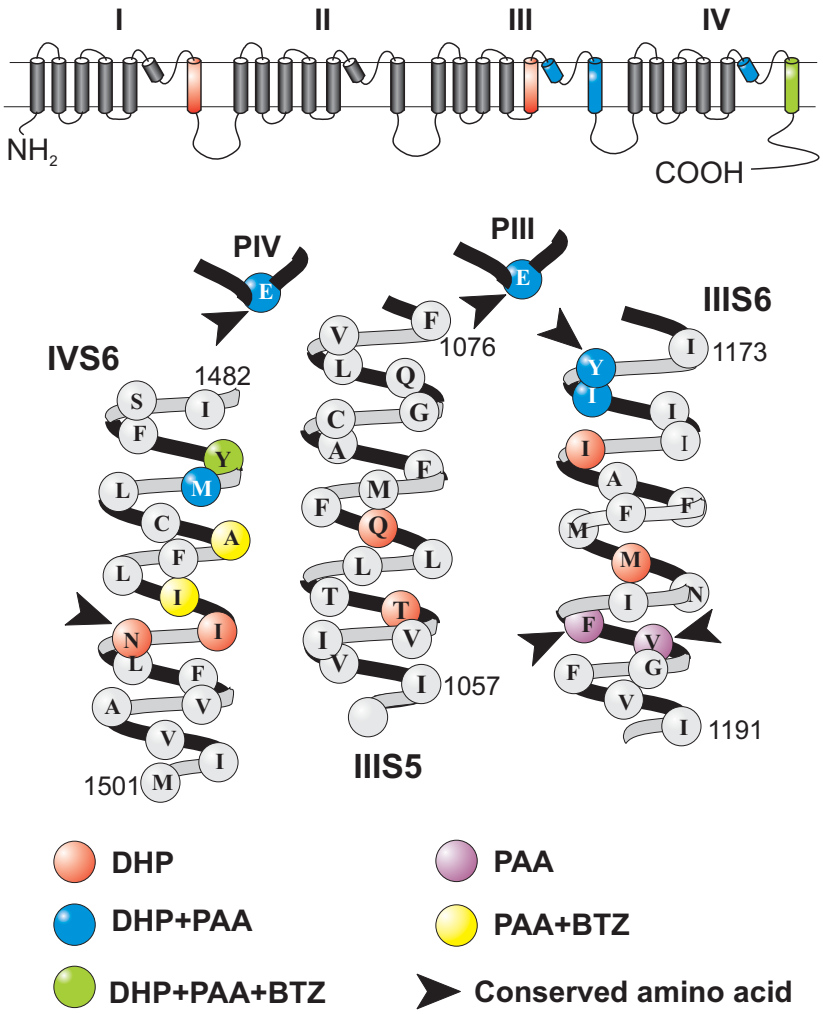

Figure 17. Amino acids interacting with DHPs (red), PAA (purple), PAAs+BTZs (yellow), DHPs+PAAs (blue) and all three blocker types DHPs+PAAs+BTZs (green) are shown. Amino acids conserved between the DHP-sensitive L-type channels and DHP-insensitive, non-L-type channels are marked by an arrow head. The IS6 segment contributes significantly to high affinity binding of DHP to the smooth muscle L-type channel. Numbering of amino acids is according to the $Ca_v1.2$-b sequence (Biel et al. 1990).

(Biel et al. 1990; Hockerman et al. 1997a). The effect of mutation of the conserved Tyr1174 depends on the substituent amino acid. Substitution by phenylalanine decreased the affinity for devapamil 18-fold, whereas substitution by alanine increased the affinity 7-fold (Hockerman et al. 1997a). The increased affinity of the Y1174A

mutant is most likely caused by a shift of −11 mV of the steady-state inactivation curve. Transfer of the three IVS6 amino acids Tyr1485, Ala1489 and Ile1492 from the $Ca_v1.2$ to the $Ca_v2.1$ subunit introduced PAA and BTZ sensitivity, when measured in a use-dependent protocol (Hering et al. 1996). Furthermore, it was shown that the triple mutation Y1485A, A1489S and I1492A in IVS6 of the $Ca_v1.2$ channel reduced the use-dependent block of the three PAAs, devapamil, verapamil and gallopamil, reduced the resting and depolarized blocks of devapamil, but affected poorly the resting and depolarized blocks of verapamil and gallopamil (Johnson et al. 1996).

Together, these results show that the IVS6 segment interacts with various PAAs and BTZs. The state-dependent block of the L-type channel is mediated by the same three amino acid residues in IVS6 for diltiazem and devapamil. However, different amino acids are required to allow high affinity interaction at resting state for diltiazem, verapamil and gallopamil. A further problem arises from the finding that DHPs, PAAs, and BTZs interact with the same (Tyr1485) or with adjacent (Ile1492 and Ile1493) amino acid side chain. It is difficult to reconcile this close location of interacting site chains with the previously described allosteric modulation of DHP binding by diltiazem or PAAs (Glossmann and Striessnig 1990). Amino acids known to contribute to interaction sites for antagonists DHPs, PAAs, and BTZs are summarized in the Figure 17.

In addition, for the interaction of agonists DHP, e.g., (–)Bay K 8644 and FLP-64176 with L-type channel are essential amino acids located in IIIS5-S6 (Yamaguchi et al. 2003). The replacement of Phe1112 by Ala almost abolished current potentiation by DHP agonist and the replacement of Phe1112 and Ser1115 by alanines turned the potentiation into weak inhibition.

Inactivation of L-type calcium channels

HVA channels inactivate by a dual mechanism: voltage-dependent, observable during prolonged depolarization, and calcium-dependent, caused by Ca^{2+} ions entering the cell during channel opening (Brehm and Eckert 1978).

The inactivation mechanism of L-type channels has been studied most extensively. Among the HVA channels, the L-type channels have the most prominent calcium-dependent inactivation. Most authors reported presence of two time constants in the time course of inactivation of L-type channels: a fast one, corresponding to Ca^{2+}-dependent inactivation, and a slow one, corresponding to voltage-dependent inactivation. This was found for freshly isolated native cells from smooth muscle (Ganitkevich et al. 1986), ventricular myocytes (Richard et al. 1993; Masaki et al. 1997) and neuronal cells (Cox and Dunlap 1994; Johnson and Byerly 1994) as well as for the $Ca_v1.2$ channel expressed in mammalian cell lines (Zong and Hofmann 1996; Shirokov 1999) or in *Xenopus* oocytes (Bernatchez et al. 1998; Cens et al. 1999). Time constants measured by different authors in native cells vary between 7 ms (Richard et al. 1993) and 50 ms (Ganitkevich et al. 1986) for the fast time constant, and between 65 ms (Masaki et al. 1997) and 400 ms (Johnson and Byerly 1994) for the slow time constant. In expression systems, slightly higher

values between 20 ms (Zong and Hofmann 1996) and 100 ms (Cens et al. 1999) for the fast time constant, and between 160 ms (Zong and Hofmann 1996) and 2000 ms (Cens et al. 1999) for the slow time constant were reported.

Calcium-dependent inactivation

While the signal for VACC activation is solely the change of the transmembrane voltage, both the voltage and entering calcium ions serve as a negative feedback signal and cause transition of the channels into a non-conducting inactivated state. The calcium-dependent inactivation of a voltage-operated channel was first described by Brehm and Eckert (1978). Initially it was recognized as a property of L-type channels. Later this inactivation mechanism was described also for N-type (Cox and Dunlap 1994; Shirokov 1999) and P/Q-type channels (Lee A. et al. 1999, 2000). The hallmark of calcium-dependent inactivation of all mentioned HVA channels is a slower inactivation of Ba^{2+} current compared to inactivation of Ca^{2+} current. Nevertheless, inactivation of Ba^{2+} current through L-type channels still has a minor divalent cation-dependent component (Ferreira et al. 1997). Another feature is the dependence of inactivation kinetics on extracellular and intracellular calcium concentrations. R-type channels inactivate with the same kinetics when Ca^{2+} or Ba^{2+} is used as a charge carrier, but their inactivation is slowed down when the current is carried by monovalent Na^{+} ions (Jouvenceau et al. 2000). Therefore, these authors have hypothesized that also the R-type channel is inactivated by a divalent-cations-dependent mechanism.

Another, faster component of calcium-dependent inactivation was defined in cardiac myocytes. This component represents a so-called release-dependent inactivation and is caused by calcium ions released from sarcoplasmic reticulum stores. The time constant of this process is between 6 and 15 ms (Sham et al. 1995; Sham 1997) and corresponds to the fastest time constants observed in native cells (Richard et al. 1993).

Initially, the Ca^{2+}-dependent inactivation was attributed to calcium binding to the so-called EF-hand motif on the carboxy terminus of the α_1 subunit of the L-type channel (de Leon et al. 1995; Bernatchez et al. 1998). Other authors (Adams and Tanabe 1997; Zhou et al. 1997; Zühlke and Reuter 1998) located a putative calcium binding site into other regions of the carboxy terminus and/or the whole $Ca_v1.2$ sequence. Finally, a series of papers from three different laboratories (Peterson et al. 1999; Qin et al. 1999; Zühlke et al. 1999) identified calmodulin (CaM) and its binding to the $Ca_v2.1$ channel as a mediator of calcium-dependent inactivation. A similar Ca^{2+}/CaM-mediated inactivation mechanism was described for the $Ca_v2.1$ channel (Lee A. et al. 1999). Ca^{2+} must be bound to CaM in order to start the process of calcium-dependent inactivation (Zühlke et al. 1999). The EF-hand motif may be involved in the process of transduction of Ca^{2+}-CaM binding into channel inactivation (Peterson et al. 2000). As there is only one inactivation mechanism, the various fast time constants reported under various experimental conditions most probably reflect variability in the time-dependent concentration of Ca^{2+} ions in the vicinity of the inner channel mouth.

Voltage-dependent inactivation

While the calcium-dependent inactivation need not be a universal property of all VACCs and has not been proved yet for the $Ca_v2.3$ and $Ca_v3.x$ channels, all VACCs undergo a voltage-dependent inactivation. In order to analyze the kinetics of purely voltage-dependent inactivation, the calcium-dependent inactivation must be eliminated. Using Ba^{2+} instead of Ca^{2+} as a permeant ion is not sufficient, as Ferreira et al. (1997) reported charge carrier-dependent channel inactivation caused by Ba^{2+} ions. Replacement of all divalent cations in external solution by monovalent cations eliminates also this inactivation mechanism. However, with Na^+ as a charge carrier the current inactivation during the depolarizing pulse still has two time constants in both isolated mammalian cardiomyocytes (Boyett et al. 1994; Mitarai et al. 2000) and in expressed $Ca_v1.2$ channel (Lacinová et al. 2000d; Lacinová and Hoffmann 2005). The second, ultra-slow component of voltage-dependent inactivation, has a time constant of several seconds (Boyet et al. 1994; Lacinová et al. 2000d; Lacinová and Hoffmann 2005, but see Mitarai et al. 2000), so that even a 5 s long conditioning pre-pulse to positive membrane potentials was not sufficient to fully inactivate the Na^+ current through the $Ca_v1.2$ channel (Lacinová et al. 2000d; Lacinová and Hoffmann 2005). From these experiments, we could conclude that the inactivation mechanism of L-type channels may consist of three processes: a fast, Ca^{2+}-dependent process, and two purely voltage-dependent processes.

Neuronal calcium channels

The $Ca_v2.1$ channel

Transcripts of the $Ca_v2.1$ channel are present at high levels in the mammalian brain and in peripheral nervous system (Mori et al. 1991; Starr et al. 1991). Because the $Ca_v2.1$ channel transcripts are expressed in many neurons shown to possess P- and Q-type channels and because the properties of $Ca_v2.1$ channel exhibit similarities with both of these channels (Stea et al. 1994), the $Ca_v2.1$ cDNA is referred to as P/Q-type channel.

The $Ca_v2.2$ channel

The $Ca_v2.2$ channel gene has been cloned exclusively from brain (Dubel et al. 1992; Williams et al. 1992a; Fujita et al. 1993). Expression studies using dysgenic myotubes or *Xenopus* oocytes revealed that $Ca_v2.2$ channel induced a barium current which is inhibited by low concentrations of ω-conotoxin GVIA (Williams et al. 1992a; Fujita et al. 1993). These results identify the $Ca_v2.2$ channel as the neuronal N-type channel. The $Ca_v2.2$ subunit also binds the ω-conotoxin GVIA with high affinity (Dubel et al. 1992) in extracellular space (Ellinor et al. 1994). Chimeras between the $Ca_v2.2$ and $Ca_v2.1$ subunits indicate that each repeat contributes to the binding pocket with the pore region of repeat III, which is the most important determinant (Ellinor et al. 1994).

The $Ca_v2.3$ channel

The sixth gene has been cloned from rat, rabbit and human brain libraries (Niidome et al. 1992; Soong et al. 1993; Schneider et al. 1994; Williams et al. 1994). Initially, this channel was characterized as an LVA T-type channel (Soong et al. 1993). However, later studies showed (Schneider et al. 1994; Williams et al. 1994), that the expressed $Ca_v2.3$ channel has the activation and inactivation kinetics of a HVA neuronal channel. The human and rat $Ca_v2.3$ currents have some properties in common with the R-type currents observed in the cerebellar granule cells (Ellinor et al. 1993; Randall and Tsien 1997).

Low-voltage-activated calcium channels

Low-voltage-activated (LVA) channels are characterized by threshold membrane potential for activation of macroscopic inward current of about –60 mV, which is below the threshold potential for action potential generation, and is far more negative than for the HVA channels. LVA channels open and inactivate very fast, but deactivate about 10 to 100 times slower than HVA channels. Single channel conductance of LVA channels is very low and is between 5 and 9 pS. For these reasons, they are also called T-type, T for transient (fast inactivation) and tiny (small conductance). LVA channels can be detected in various tissues such as heart, brain, dorsal root ganglia and adrenal gland. In the heart, T-type channels may contribute to generation of action potential in the sino-atrial node, to depolarization of cell membranes and to propagation of the atrio-ventricular calcium action potential. Calcium entry *via* T-type channel plays a significant role in initiating Ca^{2+}-induced Ca^{2+} release in the developing heart (Kitchens et al. 2003). The functional role of T-type channels in generating low-threshold spikes and rebound burst-firing has been demonstrated in neurons from the inferior olive, thalamus, hippocampus and neocortex (Huguenard 1996). In the adrenal gland, T-type channels are postulated to be involved in hormone secretion (Cohen et al. 1988). There is also evidence that genetic abnormalities in T-type channel genes give rise to absence epilepsy and cardiomyopathy (Sen and Smith 1994; Tsakiridou et al. 1995; Talley et al. 2000).

Cloning of low-voltage-activated calcium channels

The cloning strategy used to identify the T-type channels is an example of refined search of sequence databases using the motifs common to the family of voltage-gated calcium and sodium channels. Since the degree of homology between the LVA and HVA channels is rather low, standard techniques such as library screening or polymerase chain reaction amplification with degenerate primers are not applicable. The use of different search algorithms on mammalian expressed sequence-tagged cDNAs or on similar sequences of the nematode *Caenorhabditis elegans* led to identification of several genes, three of which encode LVA channels (Cribbs et al. 1998; Perez-Reyes et al. 1998; Klugbauer et al. 1999a; Lee et al. 1999a; Williams

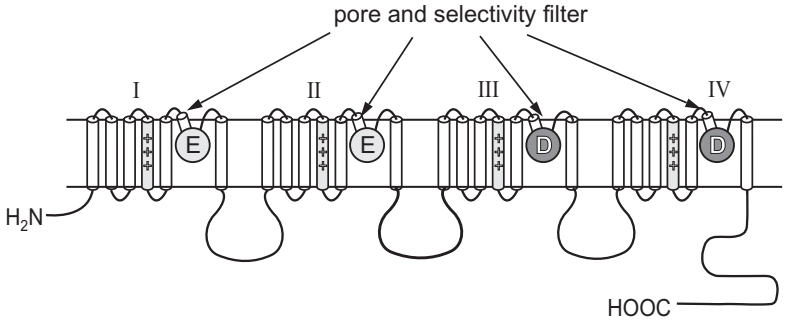

Figure 18. α_1 subunit of a T-type channel. The predicted structure is analogous to the α_1 subunit of HVA type channels, but instead of four pore glutamates it contains glutamates in repeats I and II, and aspartates in repeats III and IV.

et al. 1999). They were named $Ca_v3.1$, $Ca_v3.2$, and $Ca_v3.3$ channels. The genes for murine $Ca_v3.1$ and $Ca_v3.2$ channels were mapped to chromosomes 11 (Perez-Reyes et al. 1998) and 17 (Cribbs et al. 1998), respectively. The genes for human $Ca_v3.1$, $Ca_v3.2$, and $Ca_v3.3$ channels were mapped to chromosomes 17 (Perez-Reyes et al. 1998), 16 (Cribbs et al. 1998), and 22 (Mittman et al. 1999), respectively.

Hydrophobicity analysis revealed that T-type channels – like HVA channels – contain four homologous repeats, each consisting of six transmembrane segments (Figure 18). A comparison of the negatively charged residues in the pore loops shows that all T-type channels have a glutamate in repeats I and II and an aspartate in repeats III and IV (EEDD), whereas HVA channels have glutamates in all four repeats (EEEE). The positively charged residues of the HVA S4 voltage sensor are also conserved in the LVA channels (Figure 4). Overall amino acid sequences of the $Ca_v3.1$ and $Ca_v3.2$ channels exhibit 57% homology and their putative transmembrane segments are 90% identical (Cribbs et al. 2000). The whole amino acid sequence of the $Ca_v3.3$ channel is 59.3% identical with the $Ca_v3.1$ sequence, and 56.9% identical with the $Ca_v3.2$ sequence (Lee et al. 1999a). Its transmembrane segments are only 80% identical with the transmembrane segments of the $Ca_v3.1$ and $Ca_v3.2$ channels (Lee et al. 1999a). Different splice variants of the $Ca_v3.1$ channel have been reported for the rat, mouse and human brain (for review, see Lacinová et al. 2000a). Differentially spliced sequences are found in the intracellular loops connecting repeats II-III and III-IV and at the carboxy terminus.

Tissue distribution of T-type mRNA was analysed by Northern blot and *in situ* hybridizations. Transcripts of $Ca_v3.1$ were identified in rat, human and mouse in the brain and, at lower levels, in the heart (Perez-Reyes et al. 1998; Klugbauer et al. 1999a). Transcripts of $Ca_v3.2$ are expressed more ubiquitously. High concentrations of the transcripts were identified in human kidney, liver and heart, and lower levels were present in the brain, placenta, lung, skeletal muscle and pancreas (Cribbs et al. 1998; Williams et al. 1999). $Ca_v3.3$ mRNA of 10.5 kb was only found in the

brain on a rat multiple tissue blot. However, smaller fragments were also detectable in the kidney, thymus and liver (Lee et al. 1999a).

In situ hybridization analysis of rat and mouse brain revealed that all three mRNAs are differentially expressed (for review see Lacinova 2004). Transcripts of $Ca_v3.1$ were found to be widely, but not uniformly, spread in mouse brain (Klugbauer et al. 1999a), with high expression level in the cerebellum, hippocampus, thalamus and olfactory bulb. Talley et al. (1999) found that expression of the three genes was largely complementary in the rat central and peripheral nervous system. $Ca_v3.2$ riboprobes hybridized strongest to sensory ganglia, pituitary, dentate gyrus granule neurons and thalamic reticular neurons. The latter contained also $Ca_v3.3$ mRNA. Expression was found to be high in the olfactory tubercules for $Ca_v3.3$ and $Ca_v3.2$, and the subthalamic nucleus for $Ca_v3.3$ and $Ca_v3.1$.

Subunit composition of T-type calcium channels

The activation, inactivation and deactivation kinetics of expressed $Ca_v3.1$ and $Ca_v3.2$ channels mimics the kinetics observed in native T-type channels (for review, see Lacinová et al. 2000a). Furthermore, the amino acid sequence of all three cloned α_1 subunits lacks the AID identified in α_1 subunits of HVA channels. The AID domain was shown to be necessary for interaction between HVA channel α_1 subunit with a β subunit (for review, see Hofmann et al. 1999). Elimination of the four known β subunits by transfection of nodus ganglion neurons (Lambert et al. 1997) or mammalian neuronal NG108-15 cells (Leuranguer et al. 1998) with antisense oligonucleotides, or overexpression of the neuronal β_{2a} subunit (Wyatt et al. 1998) did not affect the size or voltage-dependence of native T-type current. It was therefore considered as improbable that a β subunit could function as an auxiliary subunit in the LVA channel complex. However, recently an increased current amplitude and improved membrane traficking of all three cloned α_1 subunits by β_{1b} subunit was described (Dubel et al. 2004), leaving this question open.

In earlier studies, coexpression of the $Ca_v3.1$ subunit with the $\alpha_2\delta$-1 or $\alpha_2\delta$-3 subunit did not modulate the T-type current (Lacinová et al. 1999c), or did so only minimally (Dolphin et al. 1999). In contrast, Dubel and co-authors (2004) reported that coexpression of the $\alpha_2\delta$-1 subunit enhanced current through all three Ca_v3 channels at least 2-fold. Some expression studies support the notion that the $\alpha_2\delta$-2 (Hobom et al. 2000) and the γ-5 subunit (Klugbauer et al. 2000) may moderately modulate the current through the $Ca_v3.1$ channel (see also chapters above). When expressed in *Xenopus* oocytes, $\alpha_2\delta$-2 increased the peak current amplitude of the $Ca_v3.1$ channel 1.8-fold (Gao et al. 2000). Recently, minor modulation of gating currents of the $Ca_v3.1$ channel by the $\alpha_2\delta$-2 and the γ-5 subunits was demonstrated (Lacinová and Klugbauer 2004b).

Activation and inactivation kinetics of the expressed $Ca_v3.3$ channel is slower than the kinetics of native T-type current (Klöckner et al. 1999; Kozlov et al. 1999; Lee et al. 1999a). This observation together with the reported dependence of channel kinetics on expression system (Lee et al. 1999a) suggests that this LVA channel is regulated by an auxiliary subunit and/or other factors endogenously present

either in HEK 293 cells or in *Xenopus* oocytes. Alternatively, the predominant $Ca_v3.3$ subunit may have another carboxy terminus because of the extraordinary short C-terminus and insertion of a repetitive sequence that is not present in the human sequence (Dunham et al. 1999).

Permeability properties of T-type calcium channels

Instead of the highly conserved glutamates in all four pore regions, all three cloned T-type channels have glutamates in pore regions I and II, but aspartates in pore regions III and IV. Indirect evidence suggests that the aspartates of pore regions III and IV control the relatively low unit conductance. The expressed $Ca_v3.1$ channel has a single-channel conductance of 7.5 pS (Perez-Reyes et al. 1998). For the $Ca_v3.2$ channel, a slightly lower conductance of 5.3 pS (Cribbs et al. 1998) and a slightly higher value of 9.1 pS (Williams et al. 1999) have been reported. The expressed $Ca_v3.3$ channel has the highest single-channel conductance of 11.0 pS (Lee et al. 1999a; Monteil et al. 2000b). The unit conductances reported for all three channels are 3-fold lower compared to those of the L-type channels. T-type channels, in contrast to HVA channels, are not selective for Ba^{2+} over Ca^{2+}. The permeability ratios of expressed $Ca_v3.1$ channels are Ba^{2+}/Ca^{2+} $\sim$0.96 and Sr^{2+}/Ca^{2+} $\sim$1.35 (Monteil et al. 2000a). Unlike any of the HVA channels, T-type channels inactivate faster with Ba^{2+} than Ca^{2+} as charge carrier (Klöckner et al. 1999; Klugbauer et al. 1999a; Monteil et al. 2000a, and Figure 19).

Voltage-dependent activation and inactivation of T-type calcium channels

Gating of T-type channels contrasts in many aspects the gating of L-type channels. When compared with L-type channels, the voltage dependence of T-type channel activation is shifted by 20–30 mV in the hyperpolarized direction, inactivation is rapid and not inherently voltage-dependent, and deactivation is slow.

Parameters of voltage-dependent activation depend on the concentration of charge carrier used, but are not influenced by the choice of Ba^{2+} or Ca^{2+} ions (Klöckner et al. 1999; Klugbauer et al. 1999a; for review, see Lacinová et al. 2000a). The membrane potential for half-maximal current peak is approximately -45 mV at physiologically low charge carrier concentrations of 1–2 mmol/l (Perez-Reyes et al. 1998; Klöckner et al. 1999; Kozlov et al. 1999). These values are common for all three $Ca_v3.x$ channels. Detailed analysis of tail current-voltage relations revealed two components of current activation in the $Ca_v3.1$ and $Ca_v3.2$ channels. For the $Ca_v3.1$ channel, potentials for half-maximal activation voltages ($V_{0.5act}$) were -41.8 mV and -14.7 mV in 2 mmol/l Ca^{2+} with corresponding slope factors of 5.1 and 11.9 (Monteil et al. 2000a). Similar values of -37.1 mV and 0.0 mV for $V_{0.5act}$, and 4.5 mV and 13.7 mV for activation slopes were reported by Lacinová and co-authors (2002). For the $Ca_v3.2$ channel, potentials for $V_{0.5act}$ were -25.1 mV and $+25.5$ mV and the corresponding slope factors were 7.5 and 14.7 in 15 mmol/l Ba^{2+} (Williams et al. 1999).

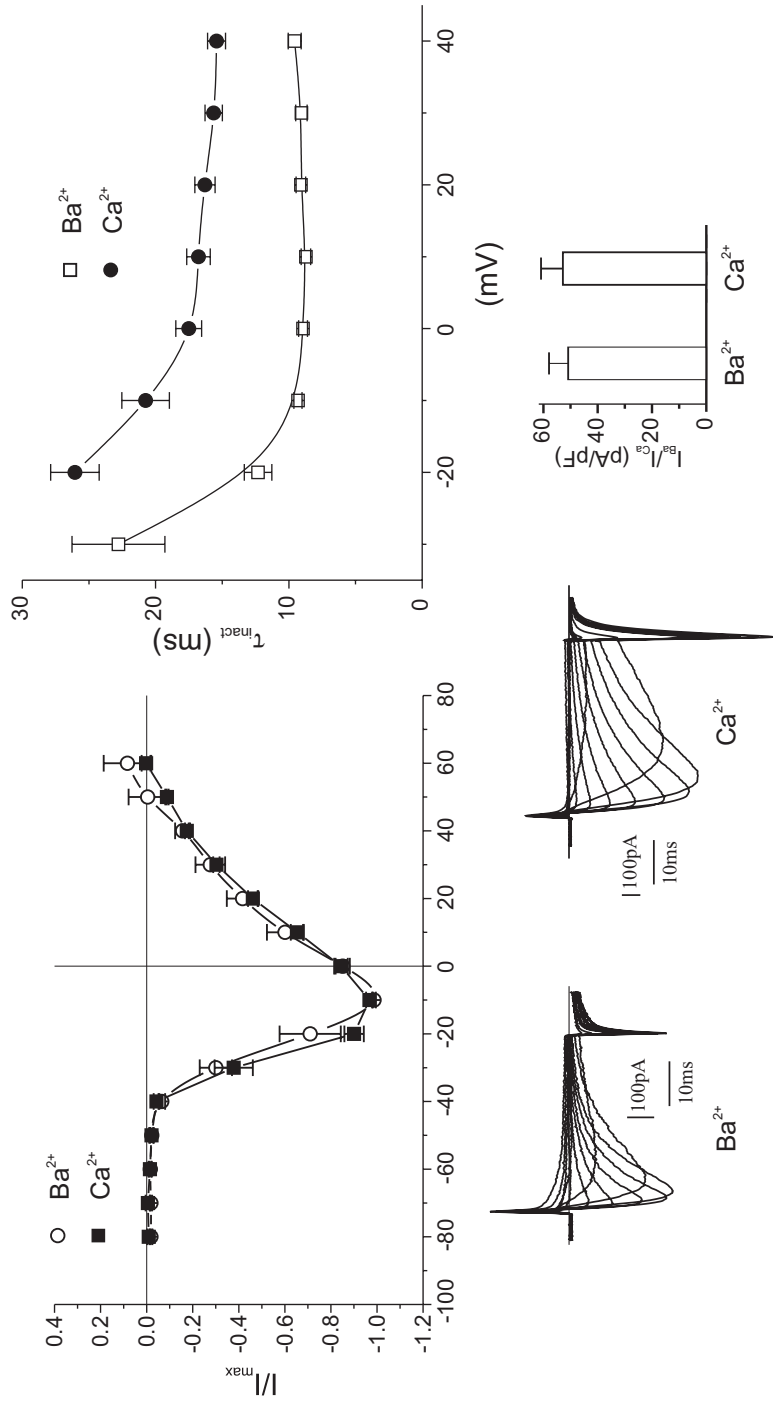

Figure 19. Ba^{2+} (open symbols) and Ca^{2+} (filled symbols) currents through an expressed $Ca_v3.1$ channel. Current-voltage relation had identical shapes for both ions (upper left). The time constant of current inactivation was significantly accelerated by Ba^{2+} ions (upper right). Original current traces are shown bellow together with averaged current densities. Modified from Klugbauer et al. (1999a). With kind permission of Springer Science and Business Media.

The time course of current activation could be described by a single time constant, which decreases sharply with increasing amplitude of the depolarizing pulse. In case of the $Ca_v3.1$ and $Ca_v3.2$ channels, this time constant varies from 8–10 ms just above the activation threshold to hundreds of microseconds for pulse amplitudes positive relative to the peak of the current-voltage relationship (Perez-Reyes et al. 1998; Klöckner et al. 1999; Klugbauer et al. 1999a; Williams et al. 1999). In case of the $Ca_v3.3$ channel, the activation time constant decreases from approximately 50 to 5 ms with increasing pulse amplitude when calcium channels are expressed in mammalian HEK 293 cells (Klöckner et al. 1999; Kozlov et al. 1999; Lee et al. 1999a). The time constant is two times slower when the channel is expressed in *Xenopus* oocytes (Lee et al. 1999a). The activation time constants of the $Ca_v3.1$ and $Ca_v3.2$ channels are independent of the expression system (Perez-Reyes et al. 1998; Klugbauer et al. 1999a; Williams et al. 1999).

The rates of inactivation (Figure 19) and recovery from inactivation of T-type channels are much faster than in any HVA channel. The time course of current decay during a single depolarizing pulse can be fitted by a single exponential. Just above the activation threshold, the time constant is about 50 ms for the expressed $Ca_v3.1$ and $Ca_v3.2$ channels. With increasing amplitude of the depolarizing pulse, the current decay becomes faster and its time constant saturates at a virtually voltage independent value of 10–15 ms (Cribbs et al. 1998; Perez-Reyes et al. 1998; Klöckner et al. 1999; Klugbauer et al. 1999a; Kozlov et al. 1999; Williams et al. 1999). This time constant is independent of the charge carrier concentration and of the expression system. Curiously, both the $Ca_v3.1$ and $Ca_v3.2$ channels inactivate faster with Ba^{2+} than Ca^{2+} as a charge carrier (Klöckner et al. 1999; Klugbauer et al. 1999a; Monteil et al. 2000a). In spite of the fast inactivation, there is a sustained current component corresponding to about 1–2 % of non-inactivated channels (Serrano et al. 1999). Recovery from inactivation caused by a 5 s long pulse to 0 mV is fast and monoexponential, with a time constant of 200 ms at a membrane potential of −100 mV (Klugbauer et al. 1999a). When a 1 s long inactivating pulse was used, in addition to the fast time constant in the range of ≈100 ms, a slow time constant in the range of ≈1 s was identified in $Ca_v3.1$ and $Ca_v3.2$ channels (Satin and Cribbs 2000). The relative amplitude of the slow time constant was about 20 % for the $Ca_v3.1$ channel and about 80 % for the $Ca_v3.1$ channel. The slower apparent recovery from inactivation of the $Ca_v3.1$ channel seems to be the only significant difference in electrophysiological profiles of the $Ca_v3.1$ and $Ca_v3.2$ channel isoforms. Serrano et al. (1999) suggested a model in which the $Ca_v3.2$ channel inactivates from any of four closed states and an open state. The rate constants of channel inactivation and recovery in this model are state- but not voltage-dependent. Talavera and collaborators (2003) suggested a similar model with three closed and one open state. In their model, the transitions between the C1-C2-C3-O states and the I1-I2-I3-IO states are voltage-dependent, while inactivation and/or recovery from each closed/open state is a voltage-independent process.

Inactivation properties of the $Ca_v3.3$ channel differ from those of the $Ca_v3.1$ and $Ca_v3.2$ channels. When expressed in HEK 293 cells, the channel inactivates

much more slowly, with time constants ranging from about 200 ms at depolarizing pulses just above activation threshold to 50–100 ms at more positive depolarizing pulses (Klöckner et al. 1999; Kozlov et al. 1999; Lee et al. 1999a; Monteil et al. 2000b). The inactivation rate is even slower when the channel is expressed in *Xenopus* oocytes (Lee et al. 1999a). Recovery from the inactivation of the α_{1I} channel is monoexponential, with time constant of 297 ms (Monteil et al. 2000b).

Deactivation of T-type channels is very slow in comparison with the HVA channels. Time courses of tail current decay can be fitted by a single exponential. At extremely hyperpolarized membrane potentials below −100 mV, the time constant of tail current decay reaches a voltage-independent value of 1–2 ms for the $Ca_v3.1$ and $Ca_v3.2$ channels. At membrane potentials positive to −100 mV, this time constant increases non-linearly (Serrano et al. 1999) and reaches a value of 10–12 ms at −40 mV (Cribbs et al. 1998; Perez-Reyes et al. 1998; Klugbauer et al. 1999a). In other words, current decay and current inactivation of the $Ca_v3.1$ and $Ca_v3.2$ channels converge to the same voltage-independent rate. The deactivation kinetics of the $Ca_v3.1$ channel is independent of the charge carrier (Ba^{2+}/Ca^{2+}; Klugbauer et al. 1999a). Expressed $Ca_v3.3$ channels deactivate faster, with a time constant ranging from 0.3–0.5 ms at extremely hyperpolarized membrane potentials to 2 ms at membrane potential of −40 mV (Klöckner et al. 1999; Kozlov et al. 1999; Monteil et al. 2000b).

While the kinetics of expressed $Ca_v3.1$ and $Ca_v3.2$ channels resemble closely the properties of T-type channels observed in native cells, the activation and inactivation kinetics of expressed $Ca_v3.3$ channels was very slow. Chemin and co-authors (2001b) have shown that kinetics of the $Ca_v3.3$ channels could be accelerated by expression of the channel in the neuroblastoma/glioma NG 108-15 cell line. To a smaller extent, this effect was observed also when HEK 293 cell line was used as an expression system rather than *Xenopus* oocyte (Chemin et al. 2001b). Because expression of the $Ca_v3.3$ channel is predominantly restricted to neuronal tissue, it is possible that this tissue endogenously contains a modulatory factor missing in the *Xenopus* oocyte expression system.

Pharmacology of recombinant T-type calcium channels

Cloning of the family of α_1 subunits of LVA channels enabled studies of the pharmacology of T-type channels. In native tissues, T-type currents are masked to a considerable extent by HVA currents and have to be dissected using pharmacological and/or biophysical techniques. Published results show a considerable variability (Huguenard 1996), which has been attributed to the putative existence of multiple channel types. This hypothesis was confirmed by isolation of three genes, $Ca_v3.1$, $Ca_v3.2$ and $Ca_v3.3$. Initial studies (Williams et al. 1999; Lacinová et al. 2000c; Perchenet et al. 2000) revealed considerable differences between the $Ca_v3.1$ and $Ca_v3.2$ channels. The $Ca_v3.2$ channel appears to be more sensitive than the $Ca_v3.1$ channel to several T-type channel blockers characterized on the native channels. Pharmacology of the $Ca_v3.3$ channel has been studied less extensively.

Table 11. Inhibition of expressed LVA calcium channels by inorganic ions

Ion	Channel	Charge carrier	Effect	Reference
Ni^{2+}	$Ca_v3.1$	10 mmol/l Ba^{2+}	IC_{50} = 250 μmol/l	Lee et al. 1999b
		20 mmol/l Ba^{2+}	IC_{50} = 470 μmol/l	Lacinová et al. 2000c
		20 mmol/l Ca^{2+}	IC_{50} = 1130 μmol/l	Lacinová et al. 2000c
		2 mmol/l Ca^{2+}	IC_{50} = 133 μmol/l	Monteil et al. 2000a
	$Ca_v3.2$	15 mmol/l Ba^{2+}	IC_{50} = 6.6 μmol/l	Williams et al. 1999
		10 mmol/l Ba^{2+}	IC_{50} = 12 μmol/l	Lee et al. 1999b
		5 mmol/l Ca^{2+}	IC_{50} (1) = 1.9 μmol/l	Perchenet et al. 2000
			IC_{50} (2) = 1350 μmol/l	
	$Ca_v3.3$	10 mmol/l Ba^{2+}	IC_{50} = 216 μmol/l	Lee et al. 1999b
		2 mmol/l Ca^{2+}	IC_{50} = 184 μmol/l	Monteil et al. 2000b
Cd^{2+}	$Ca_v3.1$	20 mmol/l Ba^{2+}	IC_{50} = 162 μmol/l	Lacinová et al. 2000c
		20 mmol/l Ca^{2+}	IC_{50} = 658 μmol/l	Lacinová et al. 2000c
	$Ca_v3.2$	15 mmol/l Ba^{2+}	IC_{50} = 104 μmol/l	Williams et al. 1999
		5 mmol/l Ca^{2+}	IC_{50} = 218 μmol/l	Perchenet et al. 2000

Block by inorganic cations

The high sensitivity of native T-type current to block by Ni^{2+} was considered to be one of the signatures of this channel. However, IC_{50} values observed in numerous native tissues varied between 30 μmol/l and 780 μmol/l (reviewed in Huguenard 1996). Experiments with recombinant channels revealed that expressed $Ca_v3.1$ and $Ca_v3.3$ channels have low affinity to Ni^{2+} (see Table 11). A high affinity block by Ni^{2+} was found only with the expressed $Ca_v3.2$ channel. More detailed analyses have shown that this apparent high affinity block may actually consist of high and low affinity sites (see Table 11). This observation is supported by the findings of Lee et al. (1999b) that the Hill coefficient for inhibition of the α_{1H} channel by Ni^{2+} is significantly lower than one. Interaction of Ni^{2+} with all three cloned T-type channels is complex. The ion shifts the voltage dependence of current activation towards more positive membrane voltages, increases the slope of voltage dependence of current activation and accelerates channel deactivation of the $Ca_v3.1$ channel (Lacinová et al. 2000c). Ni^{2+} slows the inactivation time course of the $Ca_v3.2$ channel (Lee et al. 1999b). Block by Ni^{2+} is voltage-dependent in all three expressed channels and may be relieved at very positive membrane voltages around +100 mV (Lee et al. 1999b).

Another divalent cation channel blocker, Cd^{2+}, blocks $Ca_v3.2$ slightly more effectively than $Ca_v3.1$ (Table 11). In addition to the block of current amplitude, Cd^{2+} accelerates the time constant of deactivation of the expressed $Ca_v3.1$ channel (Lacinová et al. 2000c).

More efficient inorganic blockers, trivalent cations, inhibit the expressed $Ca_v3.1$ channel in nanomolar concentrations. The reported IC_{50} for current carried by 20 mmol/l Ba^{2+} were (in nmol/l): Y^{3+} 28, Er^{3+} 69, Gd^{3+} 87, Ce^{3+} 87, Ho^{3+} 100,

Yb^{3+} 113, Nd^{3+} 148, La^{3+} 184, Sc^{3+} 3946 (Beedle et al. 2002). A somewhat higher IC_{50} value of 700 nmol/l was found for inhibition by La^{3+} when calcium current was carried by 2 mmol/l Ca^{2+} (Lacinová et al. 2002).

Organic blockers

Selective inhibition of T-type channels may have clinical importance in cardiovascular diseases (Katz 1999) and some forms of epilepsy (Macdonald and Kelly 1995). An overview of the effects of organic channel blockers on expressed LVA channels, together with the corresponding references, is given in Table 12. The only organic blocker effective at submicromolar concentrations, identified previously for native T-type channels, was mibefradil (for review, see Clozel et al. 1997). Mibefradil also inhibits expressed $Ca_v3.1$, $Ca_v3.2$ and $Ca_v3.3$ channels in nanomolar concentrations. The $Ca_v3.3$ channel has the lowest affinity with IC_{50} of 2.3 μmol/l. Mibefradil was designed as a selective T-type channel antagonist, however, it's active metabolite inhibits also HVA channels. Huang and co-authors (2004) synthetized nonhydrolyzable analog of mibefradil, NNC 55-0396. This substance appears to be selective T-type channel blocker. In contrast to several reports on native T-type channels (for references see Lacinová et al. 2000a), both channels are resistant to both agonistic and antagonistic DHPs. The charged DHP amlodipine inhibited the $Ca_v3.2$ channel with IC_{50} of 31 μmol/l. Verapamil inhibited the predominantly cardiac $Ca_v3.2$ channel in micromolar concentrations.

The availability of a cloned $Ca_v3.1$ channel enabled identification of the scorpion toxin kurtoxin, which has a high affinity for both the $Ca_v3.1$ and $Ca_v3.2$ channels. Its analog, kurtoxin-like I, is only a weak inhibitor of the $Ca_v3.3$ channel, suggesting selectivity of the kurtoxins family towards $Ca_v3.1$ and $Ca_v3.2$ channels. The $Ca_v3.2$ channel was resistant to ω-Aga IVA, ω-CTx MVIIC, and ω-CgTx GVIA toxins, which are known as inhibitors of neuronal HVA channels. Other $Ca_v3.x$ channels were not tested with these toxins. A tetrodotoxin (TTX)-sensitive LVA Ca^{2+} current has been identified in cardiac and neuronal preparations (Aggarwal et al. 1997; Balke et al. 1999). This current was insensitive to low concentrations of Ni^{2+} and its kinetics resembled that of a T-type channel. Both the $Ca_v3.1$ and $Ca_v3.2$ channels are insensitive to TTX and therefore cannot contribute to this type of calcium conductance in native tissues.

It is possible, that at least a part of clinical action of antiepileptics, antipsychotics and anaesthetics is mediated *via* inhibition of T-type channels. The expressed $Ca_v3.1$ channel has a low sensitivity to the antiepileptic drugs valproate and ethosuximide and is moderately sensitive to phenytoin. Gomora and co-authors (2001) reported similarly a low sensitivity of the human variant of $Ca_v3.1$ channel to ethosuximide. All three LVA channels were moderately sensitive to an active metabolite of methosuximide, α-methyl-α-phenylsuccinimide (MPS). The $Ca_v3.2$ channel is sensitive to ethosuximide. Therefore inhibition of T-type current by phenytoin and ethosuximide may contribute to their clinical action. Several neuroleptics inhibit all three LVA channels in clinically relevant concentrations (Santi et al. 2002). In contrast, Osipenko and co-authors (2003) reported significantly

higher concentrations necessary for T-type current inhibition and full block of inward current could not be reached. Discrepancy may be caused by different expression systems (HEK tsa201 cells in Santi et al. 2002, *Xenopus* oocytes in Osipenko et al. 2003). Nitrous oxide inhibits selectively the $Ca_v3.2$, but not the $Ca_v3.1$ channel (Todorovic et al. 2001). Whole range anaesthetics inhibits the $Ca_v3.1$ channel with IC_{50} close to their therapeutic plasma concentration (Todorovic et al. 2000). This inhibition may be important part of their clinical action.

The $Ca_v3.2$, but not the $Ca_v3.1$ channel is potentiated by stimulation of Ca^{2+}/CaM-dependent protein kinase (Wolfe et al. 2002; Welsby et al. 2003). Furthermore, $Ca_v3.2$ channel expressed in *Xenopus* oocytes is potentiated *via* activation of protein kinase C by phorbol-12-myristate-13-acetate (Park et al. 2003). Imatinib-mesylate, an inhibitor of protein tyrosine kinase (PTK), inhibits expressed $Ca_v3.3$ channel with an IC_{50} of 56.9 μmol/l (Cataldi et al. 2004). Nevertheless, this effect was not related to the inhibition of PTK.

Amiloride is a highly selective T-type channel blocker with an IC_{50} of 167 μmol/l for the $Ca_v3.2$ channel, but with an $IC_{50} > 5$ mmol/l for the $Ca_v3.1$ channel. T-type current is inhibited by two endogenous substances, arachidonic acid and endocannabinoid anandamide. This modulation may have pathophysiological significance. Anandamide inhibits all three channels in submicromolar concentration (Chemin et al. 2001a). Micromolar concentrations of arachidonic acid inhibit $Ca_v3.1$ and $Ca_v3.2$ channels (Zhang et al. 2000; Talavera et al. 2004). External acidification from pH 8.2 to 5.5 modulates the activity of the $Ca_v3.2$ channel in a complex way (Delisle and Satin 2000). At pH 5.5, current amplitude is inhibited and voltage dependence of both activation and inactivation of the channel is shifted in depolarizing direction. Activation gating is slowed, while deactivation is accelerated. Paradoxically, acidification increases macroscopic slope conductance. Altogether, acidification attenuates the activity of the $Ca_v3.2$ channel and could contribute to the protection against abnormal rhythm generation during ischemia.

An overview of effects of organic blockers is given in Table 12.

Gating of T-type calcium channels

Opening and closing of a voltage-dependent ion channel is accompanied by movement of the S4 transmembrane segments. The traditional model presupposed movements in outward and inward directions, respectively. Recently, a novel model was suggested for the voltage-dependent K^+ channel, in which the S4 segment along with the second part of the S3 segment form a paddle extended from the channel core into the membrane's fluid interior (Jiang et al. 2003a). When the channel is closed, these paddles are located inside the membrane, near the intracellular surface, and move across the membrane from the inside outward, when the channel opens (Jiang et al. 2003b). In any case, as the S4 segments are rich in positively

Steady-state activation of calcium current cannot be evaluated reliably from a current-voltage relationship. Analysis of voltage dependences of tail current amplitudes revealed two components of voltage dependence of activation of the T-type channel (Williams et al. 1999; Monteil et al. 2000a; Lacinová et al. 2002). Peak tail

Table 12. Effects of organic blockers on the $Ca_v3.1$, $Ca_v3.2$, and $Ca_v3.3$ channels

Drug	$Ca_v3.1$	$Ca_v3.2$	$Ca_v3.3$	Therapeutic plasma concentration (Flanagan 1998)	Reference
Cardiovascular agents					
Mibefradil	$IC_{50} = 0.39$ μmol/l			0.5–1 μmol/l	Klugbauer et al. 1999a
Mibefradil		$IC_{50} \approx 1.2$ μmol/l		0.5–1 μmol/l	Cribs et al. 1998 Williams et al. 1999 Perchenet et al. 2000
NNC 55-0396	$IC_{50} \sim 7$ μmol/l				Huang et al. 2004
Amlodipine		$IC_{50} = 30.9$ μmol/l		15 nmol/l	Perchenet et al. 2000
Nimodipine		$IC_{50} \geq 10$ μmol/l			Williams et al. 1999
Isradipine	$IC_{50} \gg 1$ μmol/l				Lacinová et al. 2000c
Nifedipine	$IC_{50} \gg 10$ μmol/l				Lacinová et al. 2000c
PPK-12 (nifedipine-analogue)	$IC_{50} = 1.65$ μmol/l				Kumar et al. 2002
PPK-5 (nifedipine-analogue)	$IC_{50} = 1.14$ μmol/l				Kumar et al. 2002
Bay K 8644		10 μmol/l min. effect			Williams et al. 1999
Bay K 8644	1 μmol/l min. effect				Lacinová et al. 2000c
Verapamil		$IC_{50} > 1$ μmol/l		250–800 nmol/l	Williams et al. 1999
Verapamil	IC_{50} at -130 mV ~ 21 μmol/l, IC_{50} at -90 mV $\sim 9\mu$mol/l	IC_{50} at -130 mV ~ 27 μmol/l, IC_{50} at -130 mV ~ 20 μmol/l		250–800 nmol/l	Freeze et al. 2004

(continued)

Table 12. (continued)

Drug	$Ca_v3.1$	$Ca_v3.2$	$Ca_v3.3$	Plasma concentration	Reference
Peptide toxins					
Kurtoxin	IC_{50} = 15 nmol/l	IC_{50} = 61 nmol/l			Chuang et al. 1998
Kurtoxin-like I			IC_{50} > 700 nmol/l		Olamendi-Portugal et al. 2002
ω-Aga IVA		60 nmol/l no effect			Perchenet et al. 2000
ω-CTx MVIIC		1 μmol/l no effect			Perchenet et al. 2000 Williams et al. 1999
ω-CgTx GVIA		1 μmol/l no effect			Perchenet et al. 2000 Williams et al. 1999
TTX	10 μmol/l no effect				Lacinová et al. 2000c
TTX		30 μmol/l no effect			Perchenet et al. 2000
Antiepileptics					
Valproate	max. block 10 % at 1 mmol/l			300–600 μmol/l	Lacinová et al. 2000c
Phenytoin	IC_{50} = 74 μmol/l			80 μmol/l	Lacinová et al. 2000c
Ethosuximide		IC_{50} < 300 μmol/l		700 μmol/l	Williams et al. 1999
Ethosuximide	IC_{50} > 3 mmol/l			700 μmol/l	Lacinová et al. 2000c
MPS	1.95 mmol/l	3.03 mmol/l	1.82 mmol/l	700 μmol/l	Gomora et al. 2001
Lamotrigine	inhib. 10 % at 100 μmol/l		no effect	40 μmol/l	Hainsworth et al. 2003
Sipatrigine	$IC_{50} \approx$ 15 μmol/l	$IC_{50} \approx$ 15 μmol/l	IC_{50} = 14 μmol/l		McNaughton et al. 2000a

(continued)

Table 12. (continued)

Drug	$Ca_v3.1$	$Ca_v3.2$	$Ca_v3.3$	Plasma concentration	Reference
Antipsychotics					
Pimozide	IC_{50} = 35 nmol/l	IC_{50} = 54 nmol/l	IC_{50} = 30 nmol/l	40 nmol/l	Santi et al. 2002
Pimozide	IC_{50} = 2 μmol/l max. block 40 %	IC_{50} = 15 μmol/l max. block 30 %	IC_{50} = 1.6 μmol/l max. block 25 %	40 nmol/l	Osipenko et al. 2003
Penfluoridol	IC_{50} = 93 nmol/l	IC_{50} = 64 nmol/l	IC_{50} = 72 nmol/l	40 nmol/l	Santi et al. 2002
Haloperidol	$IC_{50} \approx 1$ μmol/l	$IC_{50} \approx 1$ μmol/l	$IC_{50} \approx 1$ μmol/l	0.5 μmol/l	Santi et al. 2002
Haloperidol	IC_{50} = 1.5 μmol/l max. block 60 %	IC_{50} = 3 μmol/l max. block 55 %	IC_{50} = 35 μmol/l max. block 86 %	0.5 μmol/l	Osipenko et al. 2003
Flunarizine	$IC_{50} \leq 1$ μmol/l	$IC_{50} > 1$ μmol/l	$IC_{50} \leq 1$ μmol/l	0.25 μmol/l	Santi et al. 2002
Fluspirilene	IC_{50} = 12 μmol/l max. block 80 %	IC_{50} = 7 μmol/l max. block 80 %	IC_{50} = 12 μmol/l max. block 62 %		Osipenko et al. 2003
Anaesthetics					
NO_2	not sensitive	IC_{50} = 58 % max. block 66 %		50 %	Todorovic et al. 2001
Propofol	IC_{50} = 21 μmol/l			50 μmol/l	Todorovic et al. 2000
Etomidate	IC_{50} = 161 μmol/l			2 μmol/l	Todorovic et al. 2000
Octanol	IC_{50} = 160 μmol/l				Todorovic et al. 2000
Isoflurane	IC_{50} = 277 μmol/l			100 μmol/l	Todorovic et al. 2000
Ketamine	IC_{50} = 1.2 mmol/l			20 μmol/l	Todorovic et al. 2000
Thiopental	IC_{50} = 280 μmol/l			20 μmol/l	Todorovic et al. 2000
Pentobarbital	IC_{50} = 310 μmol/l			22 μmol/l	Todorovic et al. 2000
Phenobarbital	IC_{50} = 1.5 mmol/l			170 μmol/l	Todorovic et al. 2000

(continued)

Table 12. (continued)

Drug	$Ca_v3.1$	$Ca_v3.2$	$Ca_v3.3$	Plasma concentration	Reference
Other compounds					
Anandamide	$IC_{50} = 4.15$ μmol/l	$IC_{50} = 330$ nmol/l	$IC_{50} = 1.10$ μmol/l		Chemin et al. 2001a
Arachidonic acid		$IC_{50} \leq 10$ μmol/l			Zhang et al. 2000
Arachidonic acid	$IC_{50} = 3.9$ μmol/l				Talavera et al. 2004
Amiloride		$IC_{50} = 167$ μmol/l		220 nmol/l	Williams et al. 1999
Amiloride	$IC_{50} \geq 5$ mmol/l			220 nmol/l	Lacinová et al. 2000c
SB-209712			$IC_{50} < 500$ nmol/l		McNaughton et al. 2000b

charged amino acids, the movement of these segments causes a measurable current known as the gating current or non-linear charge movement.

Due to the low level of expression of T-type channels in native tissues, the charge movements are too small to be detected. Cloning of the $Ca_v3.x$ channel family (reviewed in Lacinová et al. 2000a) enabled to reach a high expression of these channels in heterologous expression systems and, consequently, also analyze the gating currents reflecting their activation.

When calcium current through an expressed $Ca_v3.1$ channel was blocked by La^{3+}, an asymmetric charge movement could be observed (Lacinová et al. 2002 and Figure 20). The voltage threshold for detection of the gating current was between -70 and -60 mV and the current saturated at about $+80$ mV. ON-charge movements (Q_{on}) observed after the start of depolarizing pulses have a smaller amplitude and slower kinetics than OFF-charge movements (Q_{off}) observed after the depolarizing pulses have finished. The voltage dependence of both Q_{on} and Q_{off} followed a single Boltzmann distribution. $V_{0.5act}$ and slopes were $+12.9 \pm 1.4$ mV and 22.4 ± 0.4 mV for Q_{on}, and $+12.3 \pm 0.7$ mV and 18.1 ± 0.4 mV for Q_{off} ($n = 25$). Asymmetric currents were detected exclusively in cells expressing the $Ca_v3.1$ channel (Lacinová et al. 2002). The amplitudes of Q_{off} did not differ significantly from the amplitudes of Q_{on} from the same cell (Figure 20C). The charge amplitude increased with the current amplitude. The average amount of charge moved was 0.20 ± 0.02 fC/pA and 0.20 ± 0.01 fC/pA ($n = 25$) for Q_{on} and Q_{off}, respectively (Figure 20D).

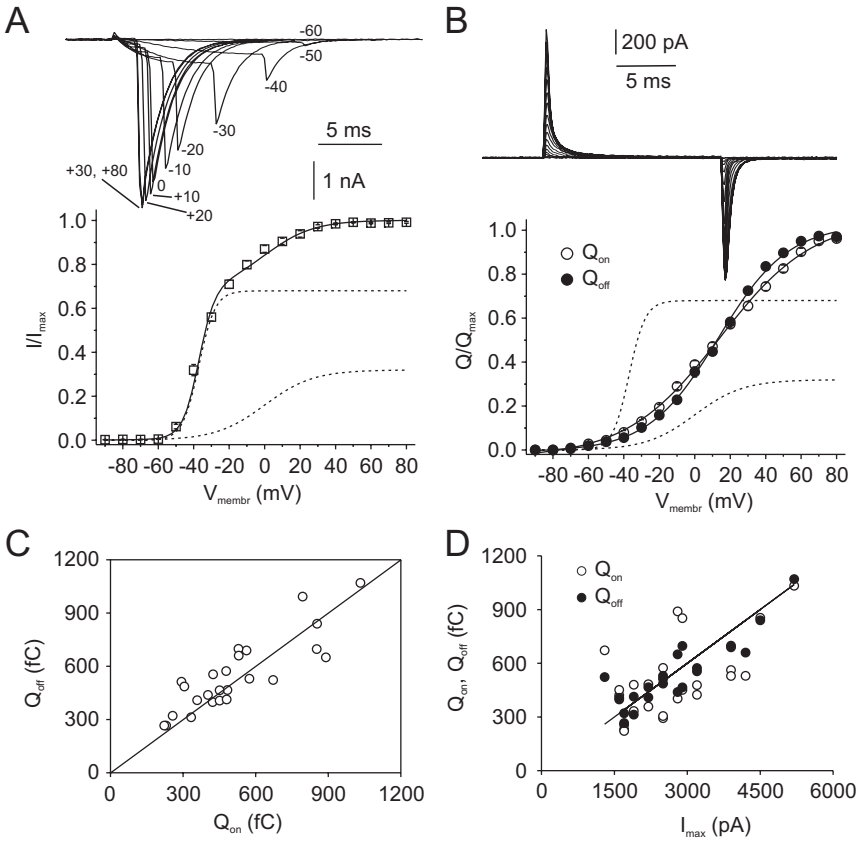

Figure 20. Voltage dependence of activation of ionic and gating currents of the $Ca_v3.1$ channel. **A.** Activation of ionic current was evaluated from the amplitudes of tail currents measured at a constant repolarizing potential of −100 mV after depolarization to potentials between −90 and +80 mV. The length of the depolarizing pulse was adjusted according to time-to-peak of the inward current observed at each potential. An example of tail currents measured according to the described protocol is shown. Depolarization potentials are marked next to each trace. Normalized amplitudes of tail currents (□) could be fitted by a double Boltzmann distribution whose individual components are shown by dashed lines. **B.** Families of gating currents measured from a cell expressing the $Ca_v3.1$ channel in the presence of 1 mmol/l La^{3+}. The total charge moved during each pulse was calculated by integrating the area under the gating currenht records. Individual measurements were normalized and averaged. Both Q_{on}- and Q_{off}-voltage relations were fitted by a single Boltzmann functions (shown as solid lines). Dashed lines demonstrate the two components of current activation as evaluated from the data presented in panel A. **C.** The maximal value of Q_{off} measured for each individual cell plotted against the maximal Q_{on} value from the same cell (○). Straight line represents unity line. Points above the unity line represent the cells in which Q_{off} was bigger than Q_{on}. Points under the unity line represent the cells in which Q_{off} was smaller than Q_{on}. Cells with equal Q_{off} and Q_{on} lie on the unity line. **D.** The maximal Q_{on} or Q_{off} values plotted against current amplitude measured at the peak of the current-voltage relationship (I_{max}) in the same cell. The slope of the straight line is 0.20. Modified from Lacinová et al. (2002).

current amplitude was measured at a constant post-pulse repolarization potential of −100 mV following depolarization pulses to voltages between −90 and +80 mV. Conductance was calculated by dividing the peak tail amplitude by the effective driving force −100 mV − E_{Ca}, and normalized to the maximal conductance (G_{max}) measured after the largest prepulse potential +80 mV. When averaged data points were fitted by a double Boltzmann distribution (Figure 20A), 68 % of the total activation had a steep slope of 4.5 ± 0.4 mV and $V_{0.5act}$ of −37.1±0.7 mV, while activation of 32 % of the channels followed a shallow slope of 13.7±0.8 mV and had $V_{0.5act}$ 0.0 ± 3.8 mV ($n = 11$). The start of both Q_{on} and Q_{off} preceded the start of the fast component of current activation by about 10 mV, and the start of the slow component of current activation by more than 30 mV. The fast component of current activation saturated at a membrane potential above −10 mV, when about 30 % of gating charge was transferred.

Gating of expressed $Ca_v1.2$ or $Ca_v2.2$ channels preceded channel activation by 30 to 40 mV (Jones et al. 1997; Josephson 1997). The value found for the $Ca_v3.1$ channel was smaller, but similar to the values found for an expressed $Ca_v2.3$ channel (Jones et al. 1998; Qin et al. 1998). These channels are sometimes considered as intermediates between HVA and LVA channels because of their fast kinetics and relatively negative threshold for current activation (reviewed in Hofmann et al. 1999). Voltage dependencies of gating currents measured from native L-type channels (Shirokov et al. 1992) or expressed $Ca_v1.2$ (Josephson 1997), $Ca_v2.2$ (Jones et al. 1997) and $Ca_v2.3$ channels (Olcese et al. 1996; Jones et al. 1998) have a slightly steeper slope (between 15 and 18 mV) than that found for the $Ca_v3.1$ channel (18 to 22 mV, Lacinová et al. 2002). Furthermore, in contrast to $Ca_v3.1$ channels, no difference in slope was found between the Q_{on}-V and Q_{off}-V relationships in HVA channels. While a single Boltzmann component was found for the $Ca_v3.1$ channel, a second component with a steep slope of about 5–8 mV was reported for the $Ca_v2.2$ (Jones et al. 1999) or $Ca_v2.3$ (Olcese et al. 1996) channel. These differences suggest that the mechanism of transitions between closed, open and inactivated states may differ in the $Ca_v3.1$ channel.

While the current through the $Ca_v3.1$ channel decayed rapidly during the depolarizing pulse due to inactivation and/or deactivation, the amplitude of Q_{off} remained constant when the length of the depolarizing pulse was prolonged from 10 ms to 55 ms (Lacinová et al. 2002 and Figure 21). The transition that caused a decay of inward calcium current did not immobilize gating charge. The amplitude and time course of the OFF-charge transient remained unaffected even when the depolarizing pulse was prolonged to 5 s (Figure 21). Immobilization of charge movement coupled to voltage-dependent channel inactivation was reported for native L-type channel (Hadley and Lederer 1991) and for expressed non-L-type $Ca_v2.2$ channel (Jones et al. 1999). The mechanism of T-type channel gating seems to be different. The structural determinants and molecular processes underlying inactivation of LVA channels are largely unknown. Serrano et al. (1999) proposed that the decay of current during a depolarizing pulse represents a mixture of voltage-dependent deactivation and nearly-voltage-independent inactivation. A “ball-and-

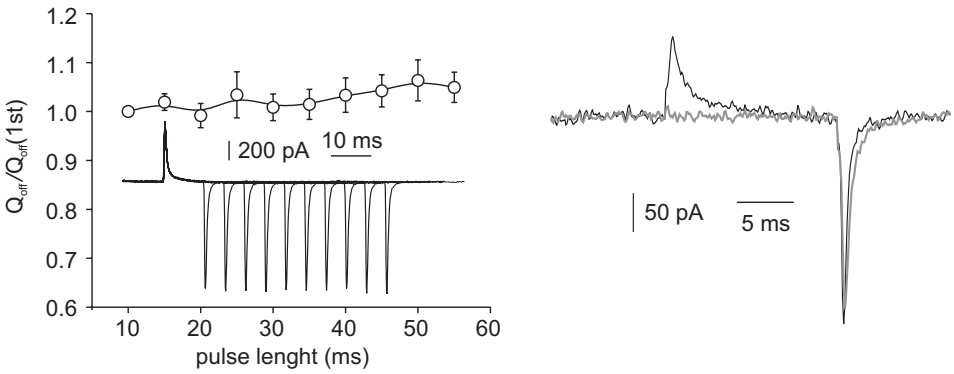

Figure 21. Gating current of the $Ca_v3.1$ channel is not immobilized by prolonged depolarization. Currents were activated by depolarizing pulses from the HP of −100 mV to −20 mV (peak of the current-voltage relationship) with lengths increasing from 10 to 55 ms at 0.2 Hz. Charge movement was recorded in the presence of 1 mmol/l La^{3+}. Amplitudes of Q_{off} evaluated at the end of each individual pulse were normalized to the Q_{off} measured at the end of a 10 ms long pulse, averaged, and plotted against the pulse length (left). An example of charge movements recorded during the described voltage protocol is given in the inset. Charge movement recorded during a 15 ms long depolarizing pulse to −20 mV with (grey) or without (black) a 5 s long conditioning prepulse to 0 mV is shown on the right. Modified from Lacinová et al. (2002).

chain" mechanism including a highly negatively charged region of 23 amino acids at the amino side of the intracellular carboxy terminus of the $Ca_v3.1$ channel as a putative "ball" was suggested (Staes et al. 2001). Involvement of the IIIS6 segment in channel inactivation was demonstrated by Marksteiner and collaborators (2001). Here we have shown that the process by which a depolarizing pulse transfers $Ca_v3.1$ channels into non-conducting state does not result in a restriction of movement of charged parts of the channel. Our observations support a model in which the process that causes the decay of the $Ca_v3.1$ channel current during the depolarizing step does not involve a voltage-dependent movement of charged parts.

Acknowledgements. While working on this manuscript, L. L. was supported by grants from Volkswagen Stiftung, VEGA 2/4009/04, and APVT-51-013802.

References

Adams B., Tanabe T. (1997): Structural regions of the cardiac Ca channel α subunit involved in Ca-dependent inactivation. J. Gen. Physiol. **110,** 379—389

Aggarwal R., Shorofsky S. R., Goldman L., Balke C. W. (1997): Tetrodotoxin-blockable calcium currents in rat ventricular myocytes; a third type of cardiac cell sodium current. J. Physiol. **505,** 353—369

Arikkath J., Chen C. C., Ahern C., Allamand V., Flanagan J. D., Coronado R., Gregg R. G., Campbell K. P. (2003): γ_1 subunit interactions within the skeletal muscle L-type voltage-gated calcium channels. J. Biol. Chem. **278,** 1212—1219

Baindur N., Rutledge A., Triggle D. J. (1993): A homologous series of permanently charged 1,4-dihydropyridines: novel probes designed to localize drug binding sites on ion channels. J. Med. Chem. **36,** 3743—3745

Balke C. W., Goldman L., Aggarwal R., Shorofsky S. (1999): Whether "slip-mode conductance" occurs? Science **284,** 711a

Bangalore R., Baindur N., Rutledge A., Triggle D. J., Kass R. S. (1994): L-type calcium channels: asymmetrical intramembrane binding domain revealed by variable length, permanently charged 1,4-dihydropyridines. Mol. Pharmacol. **46,** 660—666

Bangalore R., Mehrke G., Gingrich K., Hofmann F., Kass R. S. (1996): Influence of L-type Ca channel α_2/δ-subunit on ionic and gating current in transiently transfected HEK 293 cells. Am. J. Physiol. **270,** H1521—1528

Beedle A. M., Hamid J., Zamponi G. W. (2002): Inhibition of transiently expressed low- and high-voltage-activated calcium channels by trivalent metal cations. J. Membr. Biol. **187,** 225—238

Bech-Hansen N. T., Naylor M. J., Maybaum T. A., Pearce W. G., Koop B., Fishman G. A., Mets M., Musarella M. A., Boycott K. M. (1998): Loss-of-function mutations in a calcium-channel α_1-subunit gene in Xp11.23 cause incomplete X-linked congenital stationary night blindness. Nat. Genet. **19,** 264—267

Bernatchez G., Talwar D., Parent L. (1998): Mutations in the EF-hand motif impair the inactivation of barium currents of the cardiac α_{1C} channel. Biophys. J. **75,** 1727—1739

Berrow N. S., Campbell V., Fitzgerald E. M., Brickley K., Dolphin A. C. (1995): Antisense depletion of β-subunits modulates the biophysical and pharmacological properties of neuronal calcium channels. J. Physiol. **482,** 481—491

Beydoun A., Uthman B. M., Sackellares J. C. (1995): Gabapentin: pharmacokinetics, efficacy, and safety. Clin. Neuropharmacol. **18,** 469—481

Biel M., Ruth P., Bosse E., Hullin R., Stuhmer W., Flockerzi V., Hofmann F. (1990): Primary structure and functional expression of a high voltage activated calcium channel from rabbit lung. FEBS Lett. **269,** 409—412

Biel M., Hullin R., Freundner S., Singer D., Dascal N., Flockerzi V., Hofmann F. (1991): Tissue-specific expression of high-voltage-activated dihydropyridine-sensitive L-type calcium channels. Eur. J. Biochem. **200,** 81—88

Birnbaumer L., Campbell K. P., Catterall W. A., Harpold M. M., Hofmann F., Horne W. A., Mori Y., Schwartz A., Snutch T. P., Tanabe T., et al. (1994): The naming of voltage-gated calcium channels. Neuron **13,** 505—506

Birnbaumer L., Qin N., Olcese R., Tareilus E., Platano D., Costantin J., Stefani E. (1998): Structures and functions of calcium channel β subunits. J. Bioenerg. Biomembr. **30,** 357—375

Bodi I., Yamaguchi H., Hara M., He M., Schwartz A., Varadi G. (1997): Molecular studies on the voltage dependence of dihydropyridine action on L-type Ca^{2+} channels. Critical involvement of tyrosine residues in motif IIIS6 and IVS6. J. Biol. Chem. **272,** 24952—24960

Borsotto M., Barhanin J., Fosset M., Lazdunski M. (1985): The 1,4-dihydropyridine receptor associated with the skeletal muscle voltage-dependent Ca^{2+} channel. Purification and subunit composition. J. Biol. Chem. **260,** 14255—14263

Bosse E., Regulla S., Biel M., Ruth P., Meyer H. E., Flockerzi V., Hofmann F. (1990): The cDNA and deduced amino acid sequence of the γ subunit of the L-type calcium channel from rabbit skeletal muscle. FEBS Lett. **267,** 153—156

Boyett M. R., Honjo H., Harrison S. M., Zang W. J., Kirby M. S. (1994): Ultra-slow voltage-dependent inactivation of the calcium current in guinea-pig and ferret ventricular myocytes. Pflügers. Arch. **428,** 39—50

Brehm P., Eckert R. (1978): Calcium entry leads to inactivation of calcium channel in Paramecium. Science **202,** 1203—1206

Brickley K., Campbell V., Berrow N., Leach R., Norman R. I., Wray D., Dolphin A. C., Baldwin S. A. (1995): Use of site-directed antibodies to probe the topography of the α2 subunit of voltage-gated Ca^{2+} channels. FEBS Lett. **364,** 129—133

Brown J. P., Gee N. S. (1998): Cloning and deletion mutagenesis of the $\alpha_2\delta$ calcium channel subunit from porcine cerebral cortex. Expression of a soluble form of the protein that retains [3H]gabapentin binding activity. J. Biol. Chem. **273,** 25458—25465

Brown J. P., Dissanayake V. U., Briggs A. R., Milic M. R., Gee N. S. (1998): Isolation of the [3H]gabapentin-binding protein/$\alpha_2\delta$ Ca^{2+} channel subunit from porcine brain: development of a radioligand binding assay for $\alpha_2\delta$ subunits using [3H]leucine. Anal. Biochem. **255,** 236—243

Burgess D. L., Gefrides L. A., Foreman P. J., Noebels J. L. (2001): A cluster of three novel Ca^{2+} channel γ subunit genes on chromosome 19q13.4: evolution and expression profile of the γ subunit gene family. Genomics **71,** 339—350

Cai D., Mulle J. G., Yue D. T. (1997): Inhibition of recombinant Ca^{2+} channels by benzothiazepines and phenylalkylamines: class-specific pharmacology and underlying molecular determinants. Mol. Pharmacol. **51,** 872—881

Calabresi P., Centonze D., Marfia G. A., Pisani A., Bernardi G. (1999): An in vitro electrophysiological study on the effects of phenytoin, lamotrigine and gabapentin on striatal neurons. Br. J. Pharmacol. **126,** 689—696

Canti C., Bogdanov Y., Dolphin A. C. (2000): Interaction between G proteins and accessory subunits in the regulation of α_{1B} calcium channels in Xenopus oocytes. J. Physiol. **527,** 419—432

Castellano A., Wei X., Birnbaumer L., Perez-Reyes E. (1993a): Cloning and expression of a third calcium channel β subunit. J. Biol. Chem. **268,** 3450—3455

Castellano A., Wei X., Birnbaumer L., Perez-Reyes E. (1993b): Cloning and expression of a neuronal calcium channel β subunit. J. Biol. Chem. **268,** 12359—12366

Cataldi M., Gaudino A., Lariccia V., Russo M., Amoroso S., di Renzo G., Annunziato L. (2004): Imatinib-mesylate blocks recombinant T-type calcium channels expressed in human embryonic kidney-293 cells by a protein tyrosine kinase-independent mechanism. J. Pharmacol. Exp. Ther. **309,** 208—215

Catterall W. A., Striessnig J. (1992): Receptor sites for Ca^{2+} channel antagonists. Trends Pharmacol. Sci. **13,** 256—262

Cens T., Restituito S., Galas S., Charnet P. (1999): Voltage and calcium use the same molecular determinants to inactivate calcium channels. J. Biol. Chem. **274,** 5483—5490

Chemin J., Monteil A., Perez-Reyes E., Nargeot J., Lory P. (2001a): Direct inhibition of T-type calcium channels by the endogenous cannabinoid anandamide. EMBO J. **20,** 7033—7040

Chemin J., Monteil A., Dubel S., Nargeot J., Lory P. (2001b): The α_{1I} T-type calcium channel exhibits faster gating properties when overexpressed in neuroblastoma/glioma NG 108-15 cells. Eur. J. Neurosci. **14,** 1678—1686

Chen L., Chetkovich D. M., Petralia R. S., Sweeney N. T., Kawasaki Y., Wenthold R. J., Bredt D. S., Nicoll R. A. (2000): Stargazin regulates synaptic targeting of AMPA receptors by two distinct mechanisms. Nature **408,** 936—943

Chen Y. H., Li M. H., Zhang Y., He L. L., Yamada Y., Fitzmaurice A., Shen Y., Zhang H., Tong L., Yang J. (2004): Structural basis of the α_1-β subunit interaction of voltage-gated Ca^{2+} channels. Nature **429,** 675—680

Chu P. J., Robertson H. M., Best P. M. (2001): Calcium channel γ subunits provide insights into the evolution of this gene family. Gene **280,** 37—48

Chuang R. S., Jaffe H., Cribbs L., Perez-Reyes E., Swartz K. J. (1998): Inhibition of T-type voltage-gated calcium channels by a new scorpion toxin. Nat. Neurosci. **1,** 668—674

Clozel J. P., Ertel E. A., Ertel S. I. (1997): Discovery and main pharmacological properties of mibefradil (Ro 40-5967), the first selective T-type calcium channel blocker. J. Hypertens. (Suppl.) **15,** S17—25

Cohen C. J., McCarthy R. T., Barrett P. Q., Rasmussen H. (1988): Ca channels in adrenal glomerulosa cells: K^+ and angiotensin II increase T-type Ca channel current. Proc. Natl. Acad. Sci. U.S.A. **85,** 2412—2416

Cox D. H., Dunlap K. (1994): Inactivation of N-type calcium current in chick sensory neurons: calcium and voltage dependence. J. Gen. Physiol. **104,** 311—336

Cribbs L. L., Lee J. H., Yang J., Satin J., Zhang Y., Daud A., Barclay J., Williamson M. P., Fox M., Rees M., Perez-Reyes E. (1998): Cloning and characterization of α_{1H} from human heart, a member of the T-type Ca^{2+} channel gene family. Circ. Res. **83,** 103—109

Cribbs L. L., Gomora J. C., Daud A. N., Lee J. H., Perez-Reyes E. (2000): Molecular cloning and functional expression of $Ca_v3.1c$, a T-type calcium channel from human brain. FEBS Lett. **466,** 54—58

Curtis B. M., Catterall W. A. (1984): Purification of the calcium antagonist receptor of the voltage-sensitive calcium channel from skeletal muscle transverse tubules. Biochemistry **23,** 2113—2118

Dai S., Klugbauer N., Zong X., Seisenberger C., Hofmann F. (1999): The role of subunit composition on prepulse facilitation of the cardiac L-type calcium channel. FEBS Lett. **442,** 70—74

De Jongh K. S., Warner C., Catterall W. A. (1990): Subunits of purified calcium channels α_2 and δ are encoded by the same gene. J. Biol. Chem. **265,** 14738—14741

de Leon M., Wang Y., Jones L., Perez-Reyes E., Wei X., Soong T. W., Snutch T. P., Yue D. T. (1995): Essential Ca^{2+}-binding motif for Ca^{2+}-sensitive inactivation of L-type Ca^{2+} channels. Science **270,** 1502—1506

De Waard M., Campbell K. P. (1995): Subunit regulation of the neuronal α_{1A} Ca^{2+} channel expressed in Xenopus oocytes. J. Physiol. **485,** 619—634

De Waard M., Pragnell M., Campbell K. P. (1994): Ca^{2+} channel regulation by a conserved β subunit domain. Neuron **13,** 495—503

De Waard M., Scott V. E., Pragnell M., Campbell K. P. (1996): Identification of critical amino acids involved in α_1-β interaction in voltage-dependent Ca^{2+} channels. FEBS Lett. **380,** 272—276

Delisle B. P., Satin J. (2000): pH modification of human T-type calcium channel gating. Biophys. J. **78,** 1895—1905

Dilmac N., Hilliard N., Hockerman G. H. (2003): Molecular determinants of Ca^{2+} potentiation of diltiazem block and Ca^{2+}-dependent inactivation in the pore region of $Ca_v1.2$. Mol. Pharmacol. **64,** 491—501

Dilmac N., Hilliard N., Hockerman G. H. (2004): Molecular determinants of frequency

dependence and Ca^{2+} potentiation of verapamil block in the pore region of $Ca_v1.2$. Mol. Pharmacol. **66,** 1236—1247

Dolphin A. C., Wyatt C. N., Richards J., Beattie R. E., Craig P., Lee J. H., Cribbs L. L., Volsen S. G., Perez-Reyes E. (1999): The effect of α_2-δ and other accessory subunits on expression and properties of the calcium channel α_{1G}. J. Physiol. **519,** 35—45

Dubel S. J., Starr T. V., Hell J., Ahlijanian M. K., Enyeart J. J., Catterall W. A., Snutch T. P. (1992): Molecular cloning of the α-1 subunit of an ω-conotoxin-sensitive calcium channel. Proc. Natl. Acad. Sci. U.S.A. **89,** 5058—5062

Dubel S. J., Altier C., Chaumont S., Lory P., Bourinet E., Nargeot J. (2004): Plasma membrane expression of T-type calcium channel α_1 subunits is modulated by high voltage-activated auxiliary subunits. J. Biol. Chem. **279,** 29263—29269

Dunham I., Shimizu N., Roe B. A., Chissoe S., Hunt A. R., Collins J. E., Bruskiewich R., Beare D. M., Clamp M., Smink L. J., Ainscough R., Almeida J. P., Babbage A., Bagguley C., Bailey J., Barlow K., Bates K. N., Beasley O., Bird C. P., Blakey S., Bridgeman A. M., Buck D., Burgess J., Burrill W. D., O'Brien K. P., et al. (1999): The DNA sequence of human chromosome 22. Nature **402,** 489—495

Ellinor P. T., Zhang J. F., Randall A. D., Zhou M., Schwarz T. L., Tsien R. W., Horne W. A. (1993): Functional expression of a rapidly inactivating neuronal calcium channel. Nature **363,** 455—458

Ellinor P. T., Zhang J. F., Horne W. A., Tsien R. W. (1994): Structural determinants of the blockade of N-type calcium channels by a peptide neurotoxin. Nature **372,** 272—275

Ellis S. B., Williams M. E., Ways N. R., Brenner R., Sharp A. H., Leung A. T., Campbell K. P., McKenna E., Koch W. J., Hui A., et al. (1988): Sequence and expression of mRNAs encoding the α_1 and α_2 subunits of a DHP-sensitive calcium channel. Science **241,** 1661—1664

Ertel E. A., Campbell K. P., Harpold M. M., Hofmann F., Mori Y., Perez-Reyes E., Schwartz A., Snutch T. P., Tanabe T., Birnbaumer L., Tsien R. W., Catterall W. A. (2000): Nomenclature of voltage-gated calcium channels. Neuron **25,** 533—535

Fatt P., Katz B. (1953): The electrical properties of crustacean muscle fibres. J. Physiol. **120,** 171—204

Felix R., Gurnett C. A., De Waard M., Campbell K. P. (1997): Dissection of functional domains of the voltage-dependent Ca^{2+} channel $\alpha_2\delta$ subunit. J. Neurosci. **17,** 6884—6891

Ferreira G., Yi J., Rios E., Shirokov R. (1997): Ion-dependent inactivation of barium current through L-type calcium channels. J. Gen. Physiol. **109,** 449—461

Fink K., Meder W., Dooley D. J., Gothert M. (2000): Inhibition of neuronal Ca^{2+} influx by gabapentin and subsequent reduction of neurotransmitter release from rat neocortical slices. Br. J. Pharmacol. **130,** 900—906

Flanagan R. J. (1998): Guidelines for the interpretation of analytical toxicology results and unit of measurement conversion factors. Ann. Clin. Biochem. **35,** 261—267

Flockerzi V., Oeken H. J., Hofmann F. (1986): Purification of a functional receptor for calcium-channel blockers from rabbit skeletal-muscle microsomes. Eur. J. Biochem. **161,** 217—224

Fox A. P., Nowycky M. C., Tsien R. W. (1987): Kinetic and pharmacological properties distinguishing three types of calcium currents in chick sensory neurones. J. Physiol. **394,** 149—172

Freeze B. S., McNulty M. M., Hanck D. A. (2004): Verapamil block of human T-type Ca^{2+} channels. Biophys. J. **86,** B307

Freise D., Held B., Wissenbach U., Pfeifer A., Trost C., Himmerkus N., Schweig U., Freichel M., Biel M., Hofmann F., Hoth M., Flockerzi V. (2000): Absence of the γ subunit of the skeletal muscle dihydropyridine receptor increases L-type Ca^{2+} currents and alters channel inactivation properties. J. Biol. Chem. **275,** 14476—14481

Fujita Y., Mynlieff M., Dirksen R. T., Kim M. S., Niidome T., Nakai J., Friedrich T., Iwabe N., Miyata T., Furuichi T., et al. (1993): Primary structure and functional expression of the ω-conotoxin-sensitive N-type calcium channel from rabbit brain. Neuron **10,** 585—598

Ganitkevich V., Shuba M. F., Smirnov S. V. (1986): Potential-dependent calcium inward current in a single isolated smooth muscle cell of the guinea-pig taenia caeci. J. Physiol. **380,** 1—16

Gao B., Sekido Y., Maximov A., Saad M., Forgacs E., Latif F., Wei M. H., Lerman M., Lee J. H., Perez-Reyes E., Bezprozvanny I., Minna J. D. (2000): Functional properties of a new voltage-dependent calcium channel $\alpha_2\delta$ auxiliary subunit gene (CACNA2D2). J. Biol. Chem. **275,** 12237—12242

Garcia R., Carrillo E., Rebolledo S., Garcia M. C., Sanchez J. A. (2002): The β_{1a} subunit regulates the functional properties of adult frog and mouse L-type Ca^{2+} channels of skeletal muscle. J. Physiol. **545,** 407—419

Gee N. S., Brown J. P., Dissanayake V. U., Offord J., Thurlow R., Woodruff G. N. (1996): The novel anticonvulsant drug, gabapentin (Neurontin), binds to the $\alpha_2\delta$ subunit of a calcium channel. J. Biol. Chem. **271,** 5768—5776

Glauner K. S., Mannuzzu L. M., Gandhi C. S., Isacoff E. Y. (1999): Spectroscopic mapping of voltage sensor movement in the Shaker potassium channel. Nature **402,** 813—817

Glossmann H., Striessnig J. (1990): Molecular properties of calcium channels. Rev. Physiol. Biochem. Pharmacol. **114,** 1—105

Gomora J. C., Daud A. N., Weiergraber M., Perez-Reyes E. (2001): Block of cloned human T-type calcium channels by succinimide antiepileptic drugs. Mol. Pharmacol. **60,** 1121—1132

Grabner M., Wang Z., Hering S., Striessnig J., Glossmann H. (1996): Transfer of 1,4-dihydropyridine sensitivity from L-type to class A (BI) calcium channels. Neuron **16,** 207—218

Green P. J., Warre R., Hayes P. D., McNaughton N. C., Medhurst A. D., Pangalos M., Duckworth D. M., Randall A. D. (2001): Kinetic modification of the α_{1I} subunit-mediated T-type Ca^{2+} channel by a human neuronal Ca^{2+} channel γ subunit. J. Physiol. **533,** 467—478

Gurnett C. A., De Waard M., Campbell K. P. (1996): Dual function of the voltage-dependent Ca^{2+} channel $\alpha_2\delta$ subunit in current stimulation and subunit interaction. Neuron **16,** 431—440

Hadley R. W., Lederer W. J. (1991): Properties of L-type calcium channel gating current in isolated guinea pig ventricular myocytes. J. Gen. Physiol. **98,** 265—285

Hagiwara S., Ozawa S., Sand O. (1975): Voltage clamp analysis of two inward current mechanisms in the egg cell membrane of a starfish. J. Gen. Physiol. **65,** 617—644

Hainsworth A. H., McNaughton N. C., Pereverzev A., Schneider T., Randall A. D. (2003): Actions of sipatrigine, 202W92 and lamotrigine on R-type and T-type Ca^{2+} channel currents. Eur. J. Pharmacol. **467,** 77—80

Hanke S., Bugert P., Chudek J., Kovacs G. (2001): Cloning a calcium channel $\alpha_2\delta$-3 subunit gene from a putative tumor suppressor gene region at chromosome 3p21.1 in conventional renal cell carcinoma. Gene **264,** 69—75

He M., Bodi I., Mikala G., Schwartz A. (1997): Motif III S5 of L-type calcium channels is involved in the dihydropyridine binding site. A combined radioligand binding and electrophysiological study. J. Biol. Chem. **272,** 2629—2633

Hering S. (2002): β-subunits: fine tuning of Ca^{2+} channel block. Trends Pharmacol. Sci. **23,** 509—513

Hering S., Aczel S., Grabner M., Doring F., Berjukow S., Mitterdorfer J., Sinnegger M. J., Striessnig J., Degtiar V. E., Wang Z., Glossmann H. (1996): Transfer of high sensitivity for benzothiazepines from L-type to class A (BI) calcium channels. J. Biol. Chem. **271,** 24471—24475

Hescheler J., Pelzer D., Trube G., Trautwein W. (1982): Does the organic calcium channel blocker D600 act from inside or outside on the cardiac cell membrane? Pflügers Arch. **393,** 287—291

Hibino H., Pironkova R., Onwumere O., Rousset M., Charnet P., Hudspeth A. J., Lesage F. (2003): Direct interaction with a nuclear protein and regulation of gene silencing by a variant of the Ca^{2+}-channel β_4 subunit. Proc. Natl. Acad. Sci. U.S.A. **100,** 307—312

Hobom M., Dai S., Marais E., Lacinova L., Hofmann F., Klugbauer N. (2000): Neuronal distribution and functional characterization of the calcium channel $\alpha_2\delta$-2 subunit. Eur. J. Neurosci. **12,** 1217—1226

Hockerman G. H., Johnson B. D., Scheuer T., Catterall W. A. (1995): Molecular determinants of high affinity phenylalkylamine block of L-type calcium channels. J. Biol. Chem. **270,** 22119—22122

Hockerman G. H., Johnson B. D., Abbott M. R., Scheuer T., Catterall W. A. (1997a): Molecular determinants of high affinity phenylalkylamine block of L-type calcium channels in transmembrane segment IIIS6 and the pore region of the α_1 subunit. J. Biol. Chem. **272,** 18759—18765

Hockerman G. H., Peterson B. Z., Sharp E., Tanada T. N., Scheuer T., Catterall W. A. (1997b): Construction of a high-affinity receptor site for dihydropyridine agonists and antagonists by single amino acid substitutions in a non-L-type Ca^{2+} channel. Proc. Natl. Acad. Sci. U.S.A. **94,** 14906—14911

Hodgkin A. L., Huxley A. F. (1952a): Currents carried by sodium and potassium ions through the membrane of the giant axon of *Loligo*. J. Physiol. **116,** 473—496

Hodgkin A. L., Huxley A. F. (1952b): The components of membrane conductance in the giant axon of *Loligo*. J. Physiol. **116,** 473—496

Hodgkin A. L., Huxley A. F. (1952c): The dual effect of membrane potential on sodium conductance in the giant axon of *Loligo*. J. Physiol. **116,** 497—506

Hodgkin A. L., Huxley A. F. (1952d): A quantitative description of membrane current and its application to conduction and excitation in nerve. J. Physiol. **117,** 500—544

Hofmann F., Lacinová L., Klugbauer N. (1999): Voltage-dependent calcium channels: from structure to function. Rev. Physiol. Biochem. Pharmacol. **139,** 33—87

Horne W. A., Ellinor P. T., Inman I., Zhou M., Tsien R. W., Schwarz T. L. (1993): Molecular diversity of Ca^{2+} channel α_1 subunits from the marine ray Discopyge ommata. Proc. Natl. Acad. Sci. U.S.A. **90,** 3787—3791

Huang L., Keyser B. M., Tagmose T. M., Hansen J. B., Taylor J. T., Zhuang H., Zhang M., Ragsdale D. S., Li M. (2004): NNC 55-0396 [(1S,2S)-2-(2-(N-[(3-benzimidazol-2-yl)propyl]-N-methylamino)ethyl)-6-fluo ro-1,2,3,4-tetrahydro-1-isopropyl-2-naphtyl cyclopropanecarboxylate dihydrochloride]: a new selective inhibitor of T-type calcium channels. J. Pharmacol. Exp. Ther. **309,** 193—199

Huguenard J. R. (1996): Low-threshold calcium currents in central nervous system neurons. Annu. Rev. Physiol. **58,** 329—348

Hullin R., Singer-Lahat D., Freichel M., Biel M., Dascal N., Hofmann F., Flockerzi V. (1992): Calcium channel β subunit heterogeneity: functional expression of cloned cDNA from heart, aorta and brain. EMBO J. **11,** 885—890

Hümmer A., Delzeith O., Gomez S. R., Moreno R. L., Mark M. D., Herlitze S. (2003): Competitive and synergistic interactions of G protein β_2 and Ca^{2+} channel β_{1b} subunits with $Ca_v2.1$ channels, revealed by mammalian two-hybrid and fluorescence resonance energy transfer measurements. J. Biol. Chem. **278,** 49386—49400

Ihara Y., Yamada Y., Fujii Y., Gonoi T., Yano H., Yasuda K., Inagaki N., Seino Y., Seino S. (1995): Molecular diversity and functional characterization of voltage-dependent calcium channels (CACN4) expressed in pancreatic β-cells. Mol. Endocrinol. **9,** 121—130

Ito H., Klugbauer N., Hofmann F. (1997): Transfer of the high affinity dihydropyridine sensitivity from L-type to non-L-type calcium channel. Mol. Pharmacol. **52,** 735—740

Jay S. D., Ellis S. B., McCue A. F., Williams M. E., Vedvick T. S., Harpold M. M., Campbell K. P. (1990): Primary structure of the γ subunit of the DHP-sensitive calcium channel from skeletal muscle. Science **248,** 490—492

Jay S. D., Sharp A. H., Kahl S. D., Vedvick T. S., Harpold M. M., Campbell K. P. (1991): Structural characterization of the dihydropyridine-sensitive calcium channel α_2-subunit and the associated δ peptides. J. Biol. Chem. **266,** 3287—3293

Jeziorski M. C., Greenberg R. M., Clark K. S., Anderson P. A. (1998): Cloning and functional expression of a voltage-gated calcium channel α_1 subunit from jellyfish. J. Biol. Chem. **273,** 22792—22799

Jiang Y., Lee A., Chen J., Ruta V., Cadene M., Chait B. T., MacKinnon R. (2003a): X-ray structure of a voltage-dependent K^+ channel. Nature **423,** 33—41

Jiang Y., Ruta V., Chen J., Lee A., MacKinnon R. (2003b): The principle of gating charge movement in a voltage-dependent K^+ channel. Nature **423,** 42—48

Jimenez C., Bourinet E., Leuranguer V., Richard S., Snutch T. P., Nargeot J. (2000): Determinants of voltage-dependent inactivation affect Mibefradil block of calcium channels. Neuropharmacology **39,** 1—10

Johnson B. D., Byerly L. (1994): Ca^{2+} channel Ca^{2+}-dependent inactivation in a mammalian central neuron involves the cytoskeleton. Pflügers Arch. **429,** 14—21

Johnson B. D., Hockerman G. H., Scheuer T., Catterall W. A. (1996): Distinct effects of mutations in transmembrane segment IVS6 on block of L-type calcium channels by structurally similar phenylalkylamines. Mol. Pharmacol. **50,** 1388—1400

Jones L. P., Patil P. G., Snutch T. P., Yue D. T. (1997): G-protein modulation of N-type calcium channel gating current in human embryonic kidney cells (HEK 293). J. Physiol. **498,** 601—610

Jones L. P., Wei S. K., Yue D. T. (1998): Mechanism of auxiliary subunit modulation of neuronal α_{1E} calcium channels. J. Gen. Physiol. **112,** 125—143

Jones L. P., DeMaria C. D., Yue D. T. (1999): N-type calcium channel inactivation probed by gating-current analysis. Biophys. J. **76,** 2530—2552

Josephson I. R. (1997): Kinetic components of the gating currents of human cardiac L-type Ca^{2+} channels. Pflügers Arch. **433,** 321—329

Josephson I. R., Varadi G. (1996): The β subunit increases Ca^{2+} currents and gating charge movements of human cardiac L-type Ca^{2+} channels. Biophys. J. **70,** 1285—1293

Jouvenceau A., Giovannini F., Bath C. P., Trotman E., Sher E. (2000): Inactivation properties of human recombinant class E calcium channels. J. Neurophysiol. **83,** 671—684

Kalasz H., Watanabe T., Yabana H., Itagaki K., Naito K., Nakayama H., Schwartz A., Vaghy P. L. (1993): Identification of 1,4-dihydropyridine binding domains within the primary structure of the α_1 subunit of the skeletal muscle L-type calcium channel. FEBS Lett. **331,** 177—181

Kamp T. J., Perez-Garcia M. T., Marban E. (1996): Enhancement of ionic current and charge movement by coexpression of calcium channel β_{1A} subunit with α_{1C} subunit in a human embryonic kidney cell line. J. Physiol. **492,** 89—96

Kang M. G., Chen C. C., Felix R., Letts V. A., Frankel W. N., Mori Y., Campbell K. P. (2001): Biochemical and biophysical evidence for γ_2 subunit association with neuronal voltage-activated Ca^{2+} channels. J. Biol. Chem. **276,** 32917—32924

Katz A. M. (1999): T-type calcium channels may provide a unique target for cardiovascular therapy. Eur. Heart J. **1,** H18—23

Kitchens S. A., Burch J., Creazzo T. L. (2003): T-type Ca^{2+} current contribution to Ca^{2+}-induced Ca^{2+} release in developing myocardium. J. Mol. Cell. Cardiol. **35,** 515—523

Klöckner U., Lee J. H., Cribbs L. L., Daud A., Hescheler J., Pereverzev A., Perez-Reyes E., Schneider T. (1999): Comparison of the Ca^{2+} currents induced by expression of three cloned α_1 subunits, α_{1G}, α_{1H} and α_{1I}, of low-voltage-activated T-type Ca^{2+} channels. Eur. J. Neurosci. **11,** 4171—4178

Klugbauer N., Marais E., Lacinová L., Hofmann F. (1999a): A T-type calcium channel from mouse brain. Pflügers Arch. **437,** 710—715

Klugbauer N., Lacinová L., Marais E., Hobom M., Hofmann F. (1999b): Molecular diversity of the calcium channel $\alpha_2\delta$ subunit. J. Neurosci. **19,** 684—691

Klugbauer N., Dai S., Specht V., Lacinová L., Marais E., Bohn G., Hofmann F. (2000): A family of γ-like calcium channel subunits. FEBS Lett. **470,** 189—197

Koch W. J., Ellinor P. T., Schwartz A. (1990): cDNA cloning of a dihydropyridine-sensitive calcium channel from rat aorta. Evidence for the existence of alternatively spliced forms. J. Biol. Chem. **265,** 17786—17791

Koschak A., Reimer D., Huber I., Grabner M., Glossmann H., Engel J., Striessnig J. (2001): α_{1D} ($Ca_v1.3$) subunits can form L-type Ca^{2+} channels activating at negative voltages. J. Biol. Chem. **276,** 22100—22106

Kozlov A. S., McKenna F., Lee J. H., Cribbs L. L., Perez-Reyes E., Feltz A., Lambert R. C. (1999): Distinct kinetics of cloned T-type Ca^{2+} channels lead to differential Ca^{2+} entry and frequency-dependence during mock action potentials. Eur. J. Neurosci. **11,** 4149—4158

Kumar P. P., Stotz S. C., Paramashivappa R., Beedle A. M., Zamponi G. W., Rao A. S. (2002): Synthesis and evaluation of a new class of nifedipine analogs with T-type calcium channel blocking activity. Mol. Pharmacol. **61,** 649—658

Kuniyasu A., Itagaki K., Shibano T., Iino M., Kraft G., Schwartz A., Nakayama H. (1998): Photochemical identification of transmembrane segment IVS6 as the binding region of semotiadil a new modulator for the L-type voltage-dependent Ca^{2+} channel. J. Biol. Chem. **273,** 4635—4641

Kurokawa J., Adachi-Akahane S., Nagao T. (1997): 1,5-benzothiazepine binding domain is located on the extracellular side of the cardiac L-type Ca^{2+} channel. Mol. Pharmacol. **51,** 262—268

Lacerda A. E., Kim H. S., Ruth P., Perez-Reyes E., Flockerzi V., Hofmann F., Birnbaumer L., Brown A. M. (1991): Normalization of current kinetics by interaction between the α_1 and β subunits of the skeletal muscle dihydropyridine-sensitive Ca^{2+} channel. Nature **352,** 527—530

Lacinová L. (2004): Pharmacology of recombinant low-voltage activated calcium channels. Curr. Drug Targets CNS Neurol. Disord. **3,** 105—111

Lacinová L., Hofmann F. (1998): Isradipine interacts with the open state of the L-type calcium channel at high concentrations. Recept. Channels **6,** 153—164

Lacinová L., Klugbauer N. (2004): Modulation of gating currents of the $Ca_v3.1$ calcium channel by $\alpha_2\delta$-2 and γ_5 subunits. Arch. Biochem. Biophys. **425,** 207—213

Lacinová L., Hofmann F. (2005): Ca^{2+}- and voltage-dependent inactivation of the expressed L-type $Ca_v1.2$ calcium channel. Arch. Biochem. Biophys. **437,** 42–50

Lacinová L., Ludwig A., Bosse E., Flockerzi V., Hofmann F. (1995): The block of the expressed L-type calcium channel is modulated by the β_3 subunit. FEBS Lett. **373,** 103—107

Lacinová L., Klugbauer N., Hu M., Hofmann F. (1999a): Reconstruction of the dihydropyridine site in a non-L-type calcium channel: the role of the IS6 segment. FEBS Lett. **451,** 152—156

Lacinová L., An R. H., Xia J., Ito H., Klugbauer N., Triggle D., Hofmann F., Kass R. S. (1999b): Distinctions in the molecular determinants of charged and neutral dihydropyridine block of L-type calcium channels. J. Pharmacol. Exp. Ther. **289,** 1472—1479

Lacinová L., Klugbauer N., Hofmann F. (1999c): Absence of modulation of the expressed calcium channel α_{1G} subunit by $\alpha_2\delta$ subunits. J. Physiol. **516,** 639—645

Lacinová Ľ., Klugbauer N., Hofmann F. (2000a): Low voltage activated calcium channels: from genes to function. Gen. Physiol. Biophys. **19,** 121—136

Lacinová L., Klugbauer N., Hofmann F. (2000b): State- and isoform-dependent interaction of isradipine with the α_{1C} L-type calcium channel. Pflügers Arch. **440,** 50—60

Lacinová L., Klugbauer N., Hofmann F. (2000c): Regulation of the calcium channel α_{1G} subunit by divalent cations and organic blockers. Neuropharmacology **39,** 1254—1266

Lacinová L., Klugbauer N., Hofmann F. (2000d): Effect of Ca^{2+} ions on the inactivation of L-type and T-type calcium channels. Proceedings of 4th Czech-French-Slovak Symposium New Frontiers in Basic Cardiovascular Research, pp. 22—23

Lacinová L., Klugbauer N., Hofmann F. (2002): Gating of the expressed $Ca_v3.1$ calcium channel. FEBS Lett. **531,** 235—240

Lambert R. C., Maulet Y., Mouton J., Beattie R., Volsen S., De Waard M., Feltz A. (1997): T-type Ca^{2+} current properties are not modified by Ca^{2+} channel β subunit depletion in nodosus ganglion neurons. J. Neurosci. **17,** 6621—6628

Lee A., Wong S. T., Gallagher D., Li B., Storm D. R., Scheuer T., Catterall W. A. (1999): Ca^{2+}/calmodulin binds to and modulates P/Q-type calcium channels. Nature **399,** 155—159

Lee A., Scheuer T., Catterall W. A. (2000): Ca^{2+}/calmodulin-dependent facilitation and inactivation of P/Q-type Ca^{2+} channels. J. Neurosci. **20,** 6830—6838

Lee J. H., Daud A. N., Cribbs L. L., Lacerda A. E., Pereverzev A., Klöckner U., Schneider T., Perez-Reyes E. (1999a): Cloning and expression of a novel member of the low voltage-activated T-type calcium channel family. J. Neurosci. **19,** 1912—1921

Lee J. H., Gomora J. C., Cribbs L. L., Perez-Reyes E. (1999b): Nickel block of three cloned T-type calcium channels: low concentrations selectively block α_{1H}. Biophys. J. **77,** 3034—3042

Letts V. A., Felix R., Biddlecome G. H., Arikkath J., Mahaffey C. L., Valenzuela A., Bartlett F. S., Mori Y., Campbell K. P., Frankel W. N. (1998): The mouse stargazer gene encodes a neuronal Ca^{2+}-channel γ subunit. Nat. Genet. **19,** 340—347

Leung A. T., Imagawa T., Block B., Franzini-Armstrong C., Campbell K. P. (1988): Biochemical and ultrastructural characterization of the 1,4-dihydropyridine receptor from rabbit skeletal muscle. Evidence for a 52,000 Da subunit. J. Biol. Chem. **263,** 994—1001

Leuranguer V., Bourinet E., Lory P., Nargeot J. (1998): Antisense depletion of β-subunits fails to affect T-type calcium channels properties in a neuroblastoma cell line. Neuropharmacology **37,** 701—708

Llinas R., Yarom Y. (1981): Electrophysiology of mammalian inferior olivary neurones in vitro. Different types of voltage-dependent ionic conductances. J. Physiol. **315,** 549—567

Llinas R., Sugimori M., Lin J. W., Cherksey B. (1989): Blocking and isolation of a calcium channel from neurons in mammals and cephalopods utilizing a toxin fraction (FTX) from funnel-web spider poison. Proc. Natl. Acad. Sci. U.S.A. **86,** 1689—1693

Logothetis D. E., Movahedi S., Satler C., Lindpaintner K., Nadal-Ginard B. (1992): Incremental reductions of positive charge within the S4 region of a voltage-gated K^+ channel result in corresponding decreases in gating charge. Neuron **8,** 531—540

Ludwig A., Flockerzi V., Hofmann F. (1997): Regional expression and cellular localization of the α_1 and β subunit of high voltage-activated calcium channels in rat brain. J. Neurosci. **17,** 1339—1349

Macdonald R. L., Kelly K. M. (1995): Antiepileptic drug mechanisms of action. Epilepsia **36 (**Suppl. 2**)** S2—12

Marais E., Klugbauer N., Hofmann F. (2001): Calcium channel $\alpha_2\delta$ subunits-structure and Gabapentin binding. Mol. Pharmacol. **59,** 1243—1248

Marksteiner R., Schurr P., Berjukow S., Margreiter E., Perez-Reyes E., Hering S. (2001): Inactivation determinants in segment IIIS6 of $Ca_v3.1$. J. Physiol. **537,** 27—34

Masaki H., Sato Y., Luo W., Kranias E. G., Yatani A. (1997): Phospholamban deficiency alters inactivation kinetics of L-type Ca^{2+} channels in mouse ventricular myocytes. Am. J. Physiol. **272,** H606—612

McNaughton N. C., Hainsworth A. H., Green P. J., Randall A. D. (2000a): Inhibition of recombinant low-voltage-activated Ca^{2+} channels by the neuroprotective agent BW619C89 (Sipatrigine). Neuropharmacology **39,** 1247—1253

McNaughton N. C., Warre R., Cooper D. G., Nasir S., Ranson J. L., Randall A. (2000b): Potent inhibition of a recombinant low voltage-activated Ca^{2+} channel by SB-209712. Eur. J. Pharmacol. **407,** 53—60

Meder W. P., Dooley D. J. (2000): Modulation of K^+-induced synaptosomal calcium influx by gabapentin. Brain Res. **875,** 157—159

Mikami A., Imoto K., Tanabe T., Niidome T., Mori Y., Takeshima H., Narumiya S., Numa S. (1989): Primary structure and functional expression of the cardiac dihydropyridine-sensitive calcium channel. Nature **340,** 230—233

Mitarai S., Kaibara M., Yano K., Taniyama K. (2000): Two distinct inactivation processes related to phosphorylation in cardiac L-type Ca^{2+} channel currents. Am. J. Physiol. **279,** C603—610

Mitterdorfer J., Froschmayr M., Grabner M., Striessnig J., Glossmann H. (1994): Calcium channels: the β-subunit increases the affinity of dihydropyridine and Ca^{2+} binding sites of the α_1-subunit. FEBS Lett. **352,** 141—145

Mitterdorfer J., Sinnegger M. J., Grabner M., Striessnig J., Glossmann H. (1995): Coordination of Ca^{2+} by the pore region glutamates is essential for high-affinity dihydropyridine binding to the cardiac Ca^{2+} channel α_1 subunit. Biochemistry **34,** 9350—9355

Mittman S., Guo J., Agnew W. S. (1999): Structure and alternative splicing of the gene encoding α_{1G} a human brain T calcium channel α_1 subunit. Neurosci. Lett. **274,** 143—146

Monteil A., Chemin J., Bourinet E., Mennessier G., Lory P., Nargeot J. (2000a): Molecular and functional properties of the human α_{1G} subunit that forms T-type calcium channels. J. Biol. Chem. **275,** 6090—6100

Monteil A., Chemin J., Leuranguer V., Altier C., Mennessier G., Bourinet E., Lory P., Nargeot J. (2000b): Specific properties of T-type calcium channels generated by the human α_{1I} subunit. J. Biol. Chem. **275,** 16530—16535

Morel N., Buryi V., Feron O., Gomez J. P., Christen M. O., Godfraind T. (1998): The action of calcium channel blockers on recombinant L-type calcium channel α_1-subunits. Br. J. Pharmacol. **125,** 1005—1012

Mori Y., Friedrich T., Kim M. S., Mikami A., Nakai J., Ruth P., Bosse E., Hofmann F., Flockerzi V., Furuichi T., et al. (1991): Primary structure and functional expression from complementary DNA of a brain calcium channel. Nature **350,** 398—402

Mould J., Yasuda T., Schroeder C. I., Beedle A. M., Doering C. J., Zamponi G. W., Adams D. J., Lewis R. J. (2004): The $\alpha_2\delta$ auxiliary subunit reduces affinity of ω-conotoxins for recombinant N-type ($Ca_v2.2$) calcium channels. J. Biol. Chem. **279,** 34705—34714

Nakashima Y. M., Todorovic S. M., Pereverzev A., Hescheler J., Schneider T., Lingle C. J. (1998): Properties of Ba^{2+} currents arising from human α_{1E} and $\alpha_{1E}\beta_3$ constructs expressed in HEK 293 cells: physiology, pharmacology, and comparison to native T-type Ba^{2+} currents. Neuropharmacology **37,** 957—972

Neely A., Wei X., Olcese R., Birnbaumer L., Stefani E. (1993): Potentiation by the β subunit of the ratio of the ionic current to the charge movement in the cardiac calcium channel. Science **262,** 575—578

Ng G. Y., Bertrand S., Sullivan R., Ethier N., Wang J., Yergey J., Belley M., Trimble L., Bateman K., Alder L., Smith A., McKernan R., Metters K., O'Neill G. P., Lacaille J. C., Hebert T. E. (2001): γ-aminobutyric acid type B receptors with specific heterodimer composition and postsynaptic actions in hippocampal neurons are targets of anticonvulsant gabapentin action. Mol. Pharmacol. **59,** 144—152

Niidome T., Kim M. S., Friedrich T., Mori Y. (1992): Molecular cloning and characterization of a novel calcium channel from rabbit brain. FEBS Lett. **308,** 7—13

Nowycky M. C., Fox A. P., Tsien R. W. (1985): Three types of neuronal calcium channel with different calcium agonist sensitivity. Nature **316,** 440—443

Olamendi-Portugal T., Garcia B. I., Lopez-Gonzalez I., Van Der Walt J., Dyason K., Ulens C., Tytgat J., Felix R., Darszon A., Possani L. D. (2002): Two new scorpion toxins that target voltage-gated Ca^{2+} and Na^+ channels. Biochem. Biophys. Res. Commun. **299,** 562—568

Olcese R., Qin N., Schneider T., Neely A., Wei X., Stefani E., Birnbaumer L. (1994): The amino terminus of a calcium channel β subunit sets rates of channel inactivation independently of the subunit's effect on activation. Neuron **13,** 1433—1438

Olcese R., Neely A., Qin N., Wei X., Birnbaumer L., Stefani E. (1996): Coupling between charge movement and pore opening in vertebrate neuronal α_{1E} calcium channels. J. Physiol. **497,** 675—686

Osipenko V. N., Naidenov V. G., Kostyuk P. G., Shuba Y. M. (2003): Blocking of cloned low-threshold Ca^{2+} channels by neuroleptic drugs. Neurophysiology **35,** 7—16

Parent L., Schneider T., Moore C. P., Talwar D. (1997): Subunit regulation of the human brain α_{1E} calcium channel. J. Membr. Biol. **160,** 127—140

Park J. Y., Jeong S. W., Perez-Reyes E., Lee J. H. (2003): Modulation of $Ca_v3.2$ T-type Ca^{2+} channels by protein kinase C. FEBS Lett. **547,** 37—42

Perez-Reyes E., Castellano A., Kim H. S., Bertrand P., Baggstrom E., Lacerda A. E., Wei X. Y., Birnbaumer L. (1992): Cloning and expression of a cardiac/brain β subunit of the L-type calcium channel. J. Biol. Chem. **267,** 1792—1797

Perez-Reyes E., Cribbs L. L., Daud A., Lacerda A. E., Barclay J., Williamson M. P., Fox M., Rees M., Lee J. H. (1998): Molecular characterization of a neuronal low-voltage-activated T-type calcium channel. Nature **391,** 896—900

Perchenet L., Benardeau A., Ertel E. A. (2000): Pharmacological properties of $Ca_v3.2$, a low voltage-activated Ca^{2+} channel cloned from human heart. Naunyn Schmiedebergs Arch. Pharmacol. **361,** 590—599

Peterson B. Z., Catterall W. A. (1995): Calcium binding in the pore of L-type calcium channels modulates high affinity dihydropyridine binding. J. Biol. Chem. **270,** 18201—18204

Peterson B. Z., Johnson B. D., Hockerman G. H., Acheson M., Scheuer T., Catterall W. A. (1997): Analysis of the dihydropyridine receptor site of L-type calcium channels by alanine-scanning mutagenesis. J. Biol. Chem. **272,** 18752—18758

Peterson B. Z., DeMaria C. D., Adelman J. P., Yue D. T. (1999): Calmodulin is the Ca^{2+} sensor for Ca^{2+}-dependent inactivation of L-type calcium channels. Neuron **22,** 549—558

Peterson B. Z., Lee J. S., Mulle J. G., Wang Y., de Leon M., Yue D. T. (2000): Critical determinants of Ca^{2+}-dependent inactivation within an EF-hand motif of L-type Ca^{2+} channels. Biophys. J. **78,** 1906—1920

Platano D., Qin N., Noceti F., Birnbaumer L., Stefani E., Olcese R. (2000): Expression of the $\alpha_2\delta$ subunit interferes with prepulse facilitation in cardiac L-type calcium channels. Biophys. J. **78,** 2959—2972

Pragnell M., De Waard M., Mori Y., Tanabe T., Snutch T. P., Campbell K. P. (1994): Calcium channel β-subunit binds to a conserved motif in the I-II cytoplasmic linker of the α_1-subunit. Nature **368,** 67—70

Qin N., Olcese R., Zhou J., Cabello O. A., Birnbaumer L., Stefani E. (1996): Identification of a second region of the β-subunit involved in regulation of calcium channel inactivation. Am. J. Physiol. **271,** C1539—1545

Qin N., Olcese R., Stefani E., Birnbaumer L. (1998): Modulation of human neuronal α_{1E}-type calcium channel by $\alpha_2\delta$-subunit. Am. J. Physiol. **274,** C1324—1331

Qin N., Olcese R., Bransby M., Lin T., Birnbaumer L. (1999): Ca^{2+}-induced inhibition of the cardiac Ca^{2+} channel depends on calmodulin. Proc. Natl. Acad. Sci. U.S.A. **96,** 2435—2438

Qin N., Yagel S., Momplaisir M. L., Codd E. E., D'Andrea M. R. (2002): Molecular cloning and characterization of the human voltage-gated calcium channel $\alpha_2\delta$-4 subunit. Mol. Pharmacol. **62,** 485—496

Randall A. D., Tsien R. W. (1997): Contrasting biophysical and pharmacological properties of T-type and R-type calcium channels. Neuropharmacology **36,** 879—893

Regulla S., Schneider T., Nastainczyk W., Meyer H. E., Hofmann F. (1991): Identification of the site of interaction of the dihydropyridine channel blockers nitrendipine and azidopine with the calcium-channel α 1 subunit. EMBO J. **10,** 45—49

Richard S., Charnet P., Nerbonne J. M. (1993): Interconversion between distinct gating pathways of the high threshold calcium channel in rat ventricular myocytes. J. Physiol. **462,** 197—228

Rousset M., Cens T., Restituito S., Barrere C., Black J. L. 3rd, McEnery M. W., Charnet P. (2001): Functional roles of γ_2, γ_3 and γ_4, three new Ca^{2+} channel subunits, in P/Q-type Ca^{2+} channel expressed in Xenopus oocytes. J. Physiol. **532,** 583—593

Ruth P., Rohrkasten A., Biel M., Bosse E., Regulla S., Meyer H. E., Flockerzi V., Hofmann F. (1989): Primary structure of the β subunit of the DHP-sensitive calcium channel from skeletal muscle. Science **245,** 1115—1118

Santi C. M., Cayabyab F. S., Sutton K. G., McRory J. E., Mezeyova J., Hamming K. S., Parker D., Stea A., Snutch T. P. (2002): Differential inhibition of T-type calcium channels by neuroleptics. J. Neurosci. **22,** 396—403

Satin J., Cribbs L. L. (2000): Identification of a T-type Ca^{2+} channel isoform in murine atrial myocytes (AT-1 cells). Circ. Res. **86,** 636—642

Schneider T., Regulla S., Hofmann F. (1991): The devapamil-binding site of the purified skeletal muscle receptor for organic-calcium channel blockers is modulated by micromolar and millimolar concentrations of Ca^{2+}. Eur. J. Biochem. **200,** 245—253

Schneider T., Wei X., Olcese R., Costantin J. L., Neely A., Palade P., Perez-Reyes E., Qin N., Zhou J., Crawford G. D., et al. (1994): Molecular analysis and functional expression of the human type E neuronal Ca^{2+} channel α_1 subunit. Recept. Channels **2,** 255—270

Scholze A., Plant T. D., Dolphin A. C., Nurnberg B. (2001): Functional expression and characterization of a voltage-gated $Ca_v1.3$ (α_{1D}) calcium channel subunit from an insulin-secreting cell line. Mol. Endocrinol. **15,** 1211—1221

Schumacher T. B., Beck H., Steinhauser C., Schramm J., Elger C. E. (1998): Effects of phenytoin, carbamazepine, and gabapentin on calcium channels in hippocampal granule cells from patients with temporal lobe epilepsy. Epilepsia **39,** 355—363

Schuster A., Lacinova L., Klugbauer N., Ito H., Birnbaumer L., Hofmann F. (1996): The IVS6 segment of the L-type calcium channel is critical for the action of dihydropyridines and phenylalkylamines. EMBO J. **15,** 2365—2370

Seino S., Chen L., Seino M., Blondel O., Takeda J., Johnson J. H., Bell G. I. (1992): Cloning of the α_1 subunit of a voltage-dependent calcium channel expressed in pancreatic β cells. Proc. Natl. Acad. Sci. U.S.A. **89,** 584—588

Sen L., Smith T. W. (1994): T-type Ca^{2+} channels are abnormal in genetically determined cardiomyopathic hamster hearts. Circ. Res. **75,** 149—155

Serrano J. R., Perez-Reyes E., Jones S. W. (1999): State-dependent inactivation of the α_{1G} T-type calcium channel. J. Gen. Physiol. **114,** 185—201

Sham J. S. (1997): Ca^{2+} release-induced inactivation of Ca^{2+} current in rat ventricular myocytes: evidence for local Ca^{2+} signalling. J. Physiol. **500,** 285—295

Sham J. S., Cleemann L., Morad M. (1995): Functional coupling of Ca^{2+} channels and ryanodine receptors in cardiac myocytes. Proc. Natl. Acad. Sci. U.S.A. **92,** 121—125

Shirokov R. (1999): Interaction between permeant ions and voltage sensor during inactivation of N-type Ca^{2+} channels. J. Physiol. **518,** 697—703

Shirokov R., Levis R., Shirokova N., Rios E. (1992): Two classes of gating current from L-type Ca channels in guinea pig ventricular myocytes. J. Gen. Physiol. **99,** 863—895

Shirokov R., Ferreira G., Yi J., Rios E. (1998): Inactivation of gating currents of L-type calcium channels. Specific role of the $\alpha_2\delta$ subunit. J. Gen. Physiol. **111,** 807—823

Shistik E., Ivanina T., Puri T., Hosey M., Dascal N. (1995): Ca^{2+} current enhancement by α_2/δ and β subunits in Xenopus oocytes: contribution of changes in channel gating and α_1 protein level. J. Physiol. **489,** 55—62

Sieber M., Nastainczyk W., Zubor V., Wernet W., Hofmann F. (1987): The 165-kDa peptide of the purified skeletal muscle dihydropyridine receptor contains the known regulatory sites of the calcium channel. Eur. J. Biochem. **167,** 117—122

Singer D., Biel M., Lotan I., Flockerzi V., Hofmann F., Dascal N. (1991): The roles of the subunits in the function of the calcium channel. Science **253,** 1553—1557

Sinnegger M. J., Wang Z., Grabner M., Hering S., Striessnig J., Glossmann H., Mitterdorfer J. (1997): Nine L-type amino acid residues confer full 1,4-dihydropyridine sensitivity to the neuronal calcium channel α_{1A} subunit. Role of L-type Met1188. J. Biol. Chem. **272,** 27686—27693

Snutch T. P., Leonard J. P., Gilbert M. M., Lester H. A., Davidson N. (1990): Rat brain expresses a heterogeneous family of calcium channels. Proc. Natl. Acad. Sci. U.S.A. **87,** 3391—3395

Sokolov S., Timin E., Hering S. (2001): On the role of Ca^{2+}- and voltage-dependent inactivation in $Ca_v1.2$ sensitivity for the phenylalkylamine (–)gallopamil. Circ. Res. **89,** 700—708

Soong T. W., Stea A., Hodson C. D., Dubel S. J., Vincent S. R., Snutch T. P. (1993): Structure and functional expression of a member of the low voltage-activated calcium channel family. Science **260,** 1133—1136

Staes M., Talavera K., Klugbauer N., Prenen J., Lacinova L., Droogmans G., Hofmann F., Nilius B. (2001): The amino side of the C-terminus determines fast inactivation of the T-type calcium channel α_{1G}. J. Physiol. **530,** 35—45

Starr T. V., Prystay W., Snutch T. P. (1991): Primary structure of a calcium channel that is highly expressed in the rat cerebellum. Proc. Natl. Acad. Sci. U.S.A. **88,** 5621—5625

Stea A., Dubel S. J., Pragnell M., Leonard J. P., Campbell K. P., Snutch T. P. (1993): A β-subunit normalizes the electrophysiological properties of a cloned N-type Ca^{2+} channel α_1-subunit. Neuropharmacology **32,** 1103—1116

Stea A., Tomlinson W. J., Soong T. W., Bourinet E., Dubel S. J., Vincent S. R., Snutch T. P. (1994): Localization and functional properties of a rat brain α_{1A} calcium channel reflect similarities to neuronal Q- and P-type channels. Proc. Natl. Acad. Sci. U.S.A. **91,** 10576—10580

Stefani A., Spadoni F., Bernardi G. (1998): Gabapentin inhibits calcium currents in isolated rat brain neurons. Neuropharmacology **37,** 83—91

Stephens G. J., Page K. M., Bogdanov Y., Dolphin A. C. (2000): The α_{1B} Ca^{2+} channel amino terminus contributes determinants for β subunit-mediated voltage-dependent inactivation properties. J. Physiol. **525,** 377—390

Stotz S. C., Barr W., McRory J. E., Chen L., Jarvis S. E., Zamponi G. W. (2004): Several structural domains contribute to the regulation of N-type calcium channel inactivation by the β_3 subunit. J. Biol. Chem. **279,** 3793—3800

Strom T. M., Nyakatura G., Apfelstedt-Sylla E., Hellebrand H., Lorenz B., Weber B. H., Wutz K., Gutwillinger N., Ruther K., Drescher B., Sauer C., Zrenner E., Meitinger T., Rosenthal A., Meindl A. (1998): An L-type calcium-channel gene mutated in incomplete X-linked congenital stationary night blindness. Nat. Genet. **19,** 260—263

Suh-Kim H., Wei X., Birnbaumer L. (1996a): Subunit composition is a major determinant in high affinity binding of a Ca^{2+} channel blocker. Mol. Pharmacol. **50,** 1330—1337

Suh-Kim H., Wei X., Klos A., Pan S., Ruth P., Flockerzi V., Hofmann F., Perez-Reyes E., Birnbaumer L. (1996b): Reconstitution of the skeletal muscle dihydropyridine receptor. Functional interaction among α_1, β, γ and $\alpha_2\delta$ subunits. Recept. Channels **4,** 217—225

Takahashi M., Seagar M. J., Jones J. F., Reber B. F., Catterall W. A. (1987): Subunit structure of dihydropyridine-sensitive calcium channels from skeletal muscle. Proc. Natl. Acad. Sci. U.S.A. **84,** 5478—5482

Talavera K., Janssens A., Klugbauer N., Droogmans G., Nilius B. (2003): Extracellular Ca^{2+} modulates the effects of protons on gating and conduction properties of the T-type Ca^{2+} channel α_{1G} ($Ca_v3.1$). J. Gen. Physiol. **121,** 511—528

Talavera K., Staes M., Janssens A., Droogmans G., Nilius B. (2004): Mechanism of arachidonic acid modulation of the T-type Ca^{2+} channel α_{1G}. J. Gen. Physiol. **124,** 225—238

Talley E. M., Cribbs L. L., Lee J. H., Daud A., Perez-Reyes E., Bayliss D. A. (1999): Differential distribution of three members of a gene family encoding low voltage-activated (T-type) calcium channels. J. Neurosci. **19,** 1895—1911

Talley E. M., Solorzano G., Depaulis A., Perez-Reyes E., Bayliss D. A. (2000): Low-voltage-activated calcium channel subunit expression in a genetic model of absence epilepsy in the rat. Brain Res., Mol. Brain Res. **75,** 159—165

Tanabe T., Takeshima H., Mikami A., Flockerzi V., Takahashi H., Kangawa K., Kojima M., Matsuo H., Hirose T., Numa S. (1987): Primary structure of the receptor for calcium channel blockers from skeletal muscle. Nature **328,** 313—318

Tareilus E., Roux M., Qin N., Olcese R., Zhou J., Stefani E., Birnbaumer L. (1997): A *Xenopus* oocyte β subunit: evidence for a role in the assembly/expression of voltage-gated calcium channels that is separate from its role as a regulatory subunit. Proc. Natl. Acad. Sci. U.S.A. **94,** 1703—1708

Todorovic S. M., Perez-Reyes E., Lingle C. J. (2000): Anticonvulsants but not general anesthetics have differential blocking effects on different T-type current variants. Mol Pharmacol. **58,** 98—108

Todorovic S. M., Jevtovic-Todorovic V., Mennerick S., Perez-Reyes E., Zorumski C. F. (2001): $Ca_v3.2$ channel is a molecular substrate for inhibition of T-type calcium currents in rat sensory neurons by nitrous oxide. Mol. Pharmacol. **60,** 603—610

Tsakiridou E., Bertollini L., de Curtis M., Avanzini G., Pape H. C. (1995): Selective increase in T-type calcium conductance of reticular thalamic neurons in a rat model of absence epilepsy. J. Neurosci. **15,** 3110—3117

Tsien R. W., Lipscombe D., Madison D. V., Bley K. R., Fox A. P. (1988): Multiple types of neuronal calcium channels and their selective modulation. Trends Neurosci. **11,** 431—438

Vaghy P. L., Striessnig J., Miwa K., Knaus H. G., Itagaki K., McKenna E., Glossmann H., Schwartz A. (1987): Identification of a novel 1,4-dihydropyridine- and phenylalkylamine-binding polypeptide in calcium channel preparations. J. Biol. Chem. **262,** 14337—14342

Van Petegem F., Clark K. A., Chatelain F. C., Minor D. L. Jr. (2004): Structure of a complex between a voltage-gated calcium channel β-subunit and an α-subunit domain. Nature **429,** 671—675

Varadi G., Lory P., Schultz D., Varadi M., Schwartz A. (1991): Acceleration of activation and inactivation by the β subunit of the skeletal muscle calcium channel. Nature **352,** 159—162

Volsen S. G., Day N. C., McCormack A. L., Smith W., Craig P. J., Beattie R. E., Smith D., Ince P. G., Shaw P. J., Ellis S. B., Mayne N., Burnett J. P., Gillespie A., Harpold M. M. (1997): The expression of voltage-dependent calcium channel β subunits in human cerebellum. Neuroscience **80,** 161—174

Walker D., Bichet D., Campbell K. P., De Waard M. (1998): A β_4 isoform-specific interaction site in the carboxyl-terminal region of the voltage-dependent Ca^{2+} channel α_{1A} subunit. J. Biol. Chem. **273,** 2361—2367

Walker D., Bichet D., Geib S., Mori E., Cornet V., Snutch T. P., Mori Y., De Waard M. (1999): A new β subtype-specific interaction in α_{1A} subunit controls P/Q-type Ca^{2+} channel activation. J. Biol. Chem. **274,** 12383—12390

Watanabe T., Kalasz H., Yabana H., Kuniyasu A., Mershon J., Itagaki K., Vaghy P. L., Naito K., Nakayama H., Schwartz A. (1993): Azidobutyryl clentiazem a new photoactivatable diltiazem analog, labels benzothiazepine binding sites in the α_1 subunit of the skeletal muscle calcium channel. FEBS Lett. **334,** 261—264

Wei X. Y., Perez-Reyes E., Lacerda A. E., Schuster G., Brown A. M., Birnbaumer L. (1991): Heterologous regulation of the cardiac Ca^{2+} channel α_1 subunit by skeletal muscle β and γ subunits. Implications for the structure of cardiac L-type Ca^{2+} channels. J. Biol. Chem. **266,** 21943—21947

Wei X., Pan S., Lang W., Kim H., Schneider T., Perez-Reyes E., Birnbaumer L. (1995): Molecular determinants of cardiac Ca^{2+} channel pharmacology. Subunit requirement for the high affinity and allosteric regulation of dihydropyridine binding. J. Biol. Chem. **270,** 27106—27111

Welling A., Bosse E., Cavalie A., Bottlender R., Ludwig A., Nastainczyk W., Flockerzi V., Hofmann F. (1993a): Stable co-expression of calcium channel α_1, β and α_2/δ subunits in a somatic cell line. J. Physiol. **471,** 749—765

Welling A., Kwan Y. W., Bosse E., Flockerzi V., Hofmann F., Kass R. S. (1993b): Subunit-dependent modulation of recombinant L-type calcium channels. Molecular basis for dihydropyridine tissue selectivity. Circ. Res. **73,** 974—980

Welling A., Lacinova L., Donatin K., Ludwig A., Bosse E., Flockerzi V., Hofmann F. (1995): Expression of the L-type calcium channel with two different β subunits and its modulation by Ro 40-5967. Pflügers Arch. **429,** 400—411

Welling A., Ludwig A., Zimmer S., Klugbauer N., Flockerzi V., Hofmann F. (1997): Alternatively spliced IS6 segments of the α_{1C} gene determine the tissue-specific dihydropyridine sensitivity of cardiac and vascular smooth muscle L-type Ca^{2+} channels. Circ. Res. **81,** 526—532

Welsby P. J., Wang H., Wolfe J. T., Colbran R. J., Johnson M. L., Barrett P. Q. (2003): A mechanism for the direct regulation of T-type calcium channels by Ca^{2+}/calmodulin-dependent kinase II. J. Neurosci. **23,** 10116—10121

Welty D. F., Schielke G. P., Vartanian M. G., Taylor C. P. (1993): Gabapentin anticonvulsant action in rats: disequilibrium with peak drug concentrations in plasma and brain microdialysate. Epilepsy Res. **16,** 175—181

Williams M. E., Feldman D. H., McCue A. F., Brenner R., Velicelebi G., Ellis S. B., Harpold M. M. (1992a): Structure and functional expression of α_1, α_2, and β subunits of a novel human neuronal calcium channel subtype. Neuron **8,** 71—84

Williams M. E., Brust P. F., Feldman D. H., Patthi S., Simerson S., Maroufi A., McCue A. F., Velicelebi G., Ellis S. B., Harpold M. M. (1992b): Structure and functional expression of an ω-conotoxin-sensitive human N-type calcium channel. Science **257,** 389—395

Williams M. E., Marubio L. M., Deal C. R., Hans M., Brust P. F., Philipson L. H., Miller R. J., Johnson E. C., Harpold M. M., Ellis S. B. (1994): Structure and functional characterization of neuronal α_{1E} calcium channel subtypes. J. Biol. Chem. **269,** 22347—22357

Williams M. E., Washburn M. S., Hans M., Urrutia A., Brust P. F., Prodanovich P., Harpold M. M., Stauderman K. A. (1999): Structure and functional characterization of a novel human low-voltage activated calcium channel. J. Neurochem. **72,** 791—799

Wiser O., Trus M., Tobi D., Halevi S., Giladi E., Atlas D. (1996): The α_2/δ subunit of voltage sensitive Ca^{2+} channels is a single transmembrane extracellular protein which is involved in regulated secretion. FEBS Lett. **379,** 15—20

Wolfe J. T., Wang H., Perez-Reyes E., Barrett P. Q. (2002): Stimulation of recombinant $Ca_v3.2$, T-type, Ca^{2+} channel currents by CaMKIIγ(C). J. Physiol. **538,** 343—355

Wyatt C. N., Page K. M., Berrow N. S., Brice N. L., Dolphin A. C. (1998): The effect of overexpression of auxiliary Ca^{2+} channel subunits on native Ca^{2+} channel currents in undifferentiated mammalian NG108-15 cells. J. Physiol. **510,** 347—360

Yamaguchi S., Zhorov B. S., Yoshioka K., Nagao T., Ichijo H., Adachi-Akahane S. (2003): Key roles of Phe1112 and Ser1115 in the pore-forming IIIS5-S6 linker of L-type Ca^{2+} channel α_{1C} subunit ($Ca_v1.2$) in binding of dihydropyridines and action of Ca^{2+} channel agonists. Mol. Pharmacol. **64,** 235—248

Zamponi G. W., Soong T. W., Bourinet E., Snutch T. P. (1996): β subunit coexpression

and the α_1 subunit domain I-II linker affect piperidine block of neuronal calcium channels. J. Neurosci. **16,** 2430—2443

Zhang Y., Cribbs L. L., Satin J. (2000): Arachidonic acid modulation of α_{1H}, a cloned human T-type calcium channel. Am. J. Physiol. **278,** H184—193

Zhou J., Olcese R., Qin N., Noceti F., Birnbaumer L., Stefani E. (1997): Feedback inhibition of Ca^{2+} channels by Ca^{2+} depends on a short sequence of the C terminus that does not include the Ca^{2+}-binding function of a motif with similarity to Ca^{2+}-binding domains. Proc. Natl. Acad. Sci. U.S.A. **94,** 2301—2305

Zong X., Hofmann F. (1996): Ca^{2+}-dependent inactivation of the class C L-type Ca^{2+} channel is a property of the α_1 subunit. FEBS Lett. **378,** 121—125

Zühlke R. D., Reuter H. (1998): Ca^{2+}-sensitive inactivation of L-type Ca^{2+} channels depends on multiple cytoplasmic amino acid sequences of the α_{1C} subunit. Proc. Natl. Acad. Sci. U.S.A. **95,** 3287—3294

Zühlke R. D., Bouron A., Soldatov N. M., Reuter H. (1998): Ca^{2+} channel sensitivity towards the blocker isradipine is affected by alternative splicing of the human α_{1C} subunit gene. FEBS Lett. **427,** 220—224

Zühlke R. D., Pitt G. S., Deisseroth K., Tsien R. W., Reuter H. (1999): Calmodulin supports both inactivation and facilitation of L-type calcium channels. Nature **399,** 159—162